SANDIA REPORT
SAND2006-4154
Unlimited Release
Printed August 2006

An Evaluation of the Spring Finger Solder Joints on SA1358-10 and SA2052-4 Connector Assemblies (MC3617, W87)

Paul T. Vianco, Alice C. Kilgo, Gary L. Zender, and Paul F. Hlava

Prepared by
Sandia National Laboratories
Albuquerque, New Mexico 87185 and Livermore, California 94550

Sandia is a multiprogram laboratory operated by Sandia Corporation,
a Lockheed Martin Company, for the United States Department of Energy's
National Nuclear Security Administration under Contract DE-AC04-94AL85000.

Issued by Sandia National Laboratories, operated for the United States Department of Energy by Sandia Corporation.

Available to DOE and DOE contractors from
U.S. Department of Energy
Office of Scientific and Technical Information
P.O. Box 62
Oak Ridge, TN 37831

Telephone: (865) 576-8401
Facsimile: (865) 576-5728
E-Mail: reports@adonis.osti.gov
Online ordering: http://www.osti.gov/bridge

Available to the public from
U.S. Department of Commerce
National Technical Information Service
5285 Port Royal Rd.
Springfield, VA 22161

Telephone: (800) 553-6847
Facsimile: (703) 605-6900
E-Mail: orders@ntis.fedworld.gov
Online order: http://www.ntis.gov/help/ordermethods.asp?loc=7-4-0#online

SAND2006-4154
Unlimited Release
Printed August 2006

An Evaluation of the Spring Finger Solder Joints on SA1358-10 and SA2052-4 Connector Assemblies (MC3617, W87)

Paul T. Vianco
Microsystem Materials and Mechanical Behavior Department
Alice C. Kilgo, Gary L. Zender, Paul F. Hlava
Materials Characterization Department

Sandia National Laboratories
P.O. Box 5800
Albuquerque, NM 87185

Abstract

The SA1358-10 and SA2052-4 circular JT Type plug connectors are used on a number of nuclear weapons and Joint Test Assembly (JTA) systems. Prototype units were evaluated for the following specific defects associated with the 95Sn-5Sb (Sn-Sb, wt.%) solder joint used to attach the beryllium-copper (BeCu) spring fingers to the aluminum (Al) connector shell: (1) extended cracking within the fillet; (2) remelting of the solder joint during the follow-on, soldering step that attached the EMR adapter ring to the connector shell (and/or soldering the EMR shell to the adapter ring) that used the lower melting temperature 63Sn-37Pb (Sn-Pb) alloy; and (3) spalling of the Cd (Cr) layer overplating layer from the fillet surface. Several pedigrees of connectors were evaluated, which represented older fielded units as well as those assemblies that were recently constructed at Kansas City Plant. The solder joints were evaluated that were in place on connectors made with the current soldering process as well as an alternative induction soldering process for attaching the EMR adapter ring to the shell. Very similar observations were made, which crossed the different pedigrees of parts and processes. The extent of cracking in the top side fillets varied between the different connector samples and likely

the EMR adapter ring to the shell. Very similar observations were made, which crossed the different pedigrees of parts and processes. The extent of cracking in the top side fillets varied between the different connector samples and likely reflected the different extents to which the connector was mated to its counterpart assembly. In all cases, the spring finger solder joints on the SA1358-10 connectors were remelted as a result of the subsequent EMR adapter ring attachment process. Spalling of the Cd (Cr) overplating layer was also observed for these connectors, which was a consequence of the remelting activity. On the other hand, the SA2052-4 connector did not exhibit evidence of remelting of the spring finger solder joint. The Cd (Cr) layer did not show signs of spalling. These results suggested that, due to the size of the SA1358-10 connector, any of the former or current soldering processes used to attach the EMR adapter ring and/or EMR shell to the connector shell, requires a level of heat energy that will always result in the remelting of the spring finger solder joint attached with either the Sn-Ag or the Sn-Sb alloy. Lastly, it was construed that the induction soldering process, which is used to attach the EMR adapter ring onto the shell, was more likely to have caused the remelting event rather than the more localized heat source of the hand soldering iron used to attach the EMR shell to the adapter ring.

Acknowledgements

The authors wish to thank L. Andrews for his thorough review of the manuscript.

(This page was intentionally left blank)

Contents

(This page was intentionally left blank)

1. Introduction

1.1 Background information

The SA1358-10 (non-hermetic, circular JT06-14-18P) and SA2052-4 (non-hermetic, circular JT06-10-5S) plug connectors are used on a wide variety of nuclear weapons and Joint Test Assembly (JTA) systems. The current emphasis on these connectors stems from their use in the MC3617 Interconnection Unit (ICU) of the W87 system. Stereo photographs of the SA1358-10 connector type are provided in Fig. 1, which also included the EMR adapter ring and shell components that were assembled to the back side of the shell. Similar photographs of the SA2052-4 connector were shown in Fig. 2. Besides the reduced number of contacts, the SA2052-4 connector (shell size 10) is physically smaller than the SA1358-10 connector (shell size 14). Otherwise, the two connectors have similar design aspects, materials, and manufacturing processes. Both connectors are built at Amphenol (Sydney, NY)

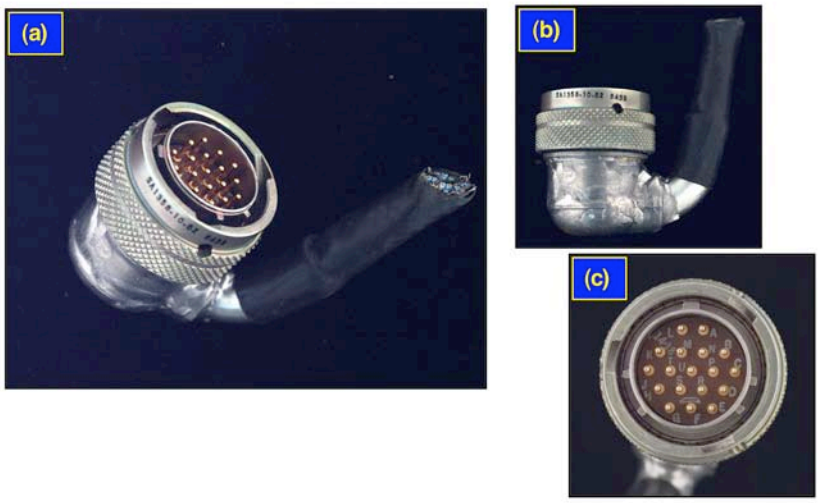

(a)

Fig. 1 Stereo photographs showing the SA1358-10 connector: (a) the mating end of the connector. *(con't)*

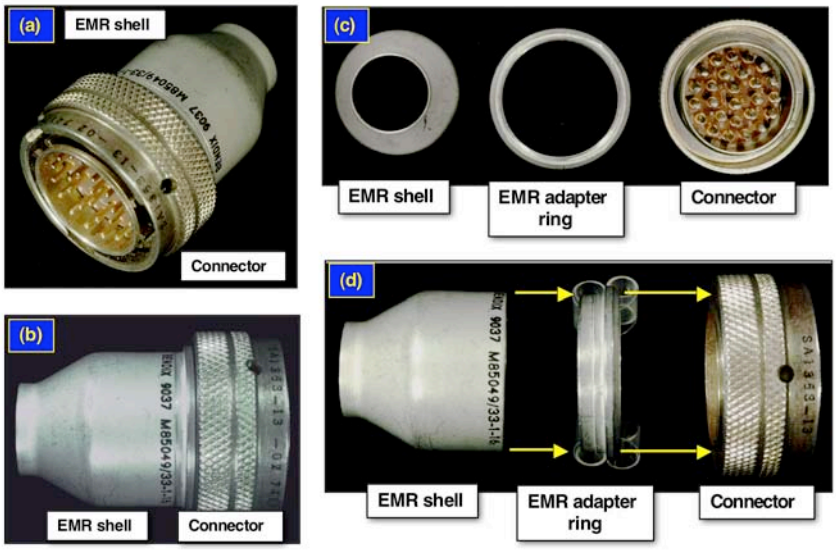

(b)

Fig. 1 Stereo photographs showing the SA1358-10 connector: (b) the back side of the shell showing the location of the EMR adapter ring and shell assemblies.

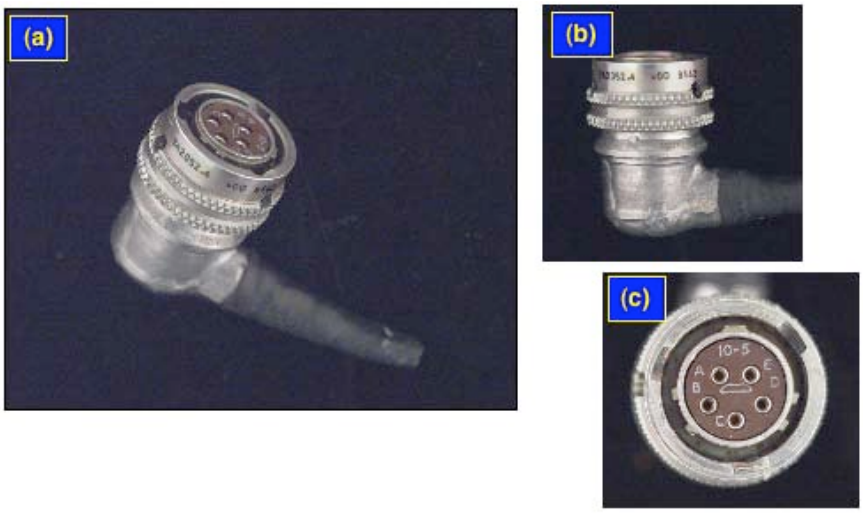

Fig. 2 Stereo photographs showing the SA2052-4 connector.

The current investigation stemmed from a failure analysis study of SA1358-10 units that were constructed during the middle 1980s to early 1990s [1]. The specific structures of interest in that prior study were the beryllium-copper (BeCu) spring fingers that are soldered to the connector shell and provide electrical contact between the shell and the mating connector (shell). The spring fingers on the SA1358-10 connector are shown in Fig.

3 by view (a) that was directed towards the contacts and view (b) that is a side view that was generated by removing the coupling ring and outer skirt of the connector shell.

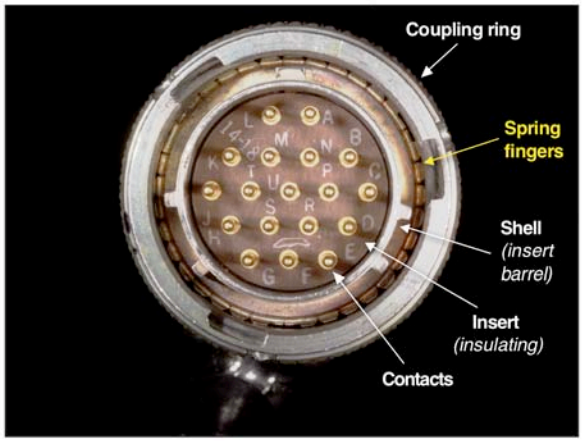

(a)

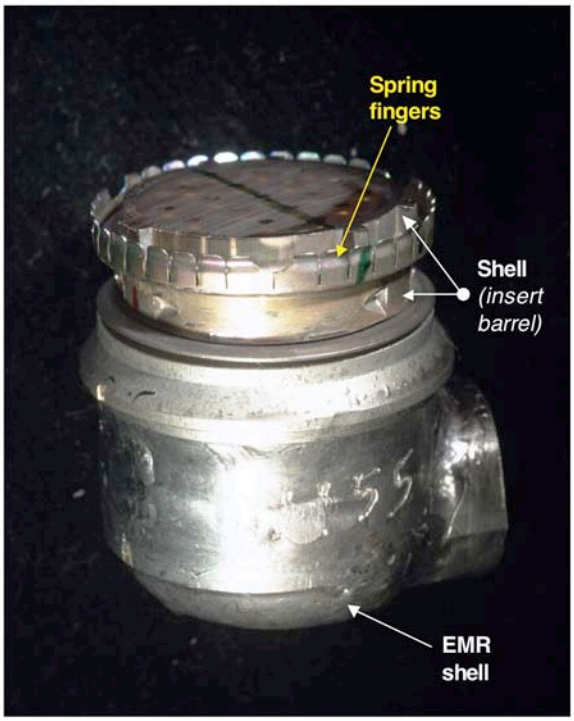

(b)

Fig. 3 Stereo photographs showing the spring finger structure in the SA1358-10 connector: (a) view looking down to the contacts and (b) a side view resulting from the removal of the coupling ring and outer skirt of the connector shell.

The following concerns were addressed in that earlier study and resulting report. *(1) Cracks were observed in the fillets of the solder joint that attached the spring fingers to the connector shell.* Cracks are illustrated both by optical microscopy and scanning electron microscopy (SEM) in Fig. 4. Although the assembly specification (AY357007) allowed such cracks to be present in the fillet region, it was necessary to confirm that the cracks terminated had not propagated through the entire section of the joint, thereby potentially causing the spring fingers to separate from the connector shell.

(2) The morphology of some of the cracks (locations "A" and "B" in Fig. 4a) indicated that the tin-silver (Sn-Ag) solder used to attach the spring fingers to the shell had remelted during next-assembly processes performed at Honeywell/KCP. The *uncontrolled* remelting of previously formed solder joints is not permitted in WR and JTA components or sub-assemblies[1]. In the absence of a flux, the solder can dewet from the surface, resulting in an unacceptable fillet. The fact that the spring finger solder joints could not be visually inspected for such degradation lent further unacceptability to a remelting occurrence.

(3) Further analysis indicated that areas of cadmium-plus-chromate conversion plating, abbreviated Cd (Cr), were flaking off of the top side solder fillet of the joint. The connector shell and spring finger, received a final overplating finish of Cd and a chromate conversion (Cr) layer after the soldering process. This layer was put into place to provide corrosion protection. The flaking of the Cd (Cr) layer may have resulted from flexing of the finger upon insertion/desertion of the mating connector or, it was caused by remelting of the solder. In either case, separation of the Cd layer posed a reliability concern with respect to compromising the corrosion protection of the part as well as drew scrutiny because of the potential generation of unsecured particles in the connector that could negatively impact electrical performance and/or mechanical fit-up.

Physical evidence was obtained in that study, which confirmed the presence of each of the three listed defects. Shown in Fig. 5 are optical micrographs that identified a crack that propagated from the top side fillet (Fig. 4) through the gap and into the lower fillet, resulting in complete separation of the spring finger from the shell. For this particular connector, the 96.5Sn-3.5Ag (Sn-Ag) solder was used to attach the spring fingers to the connector shell.

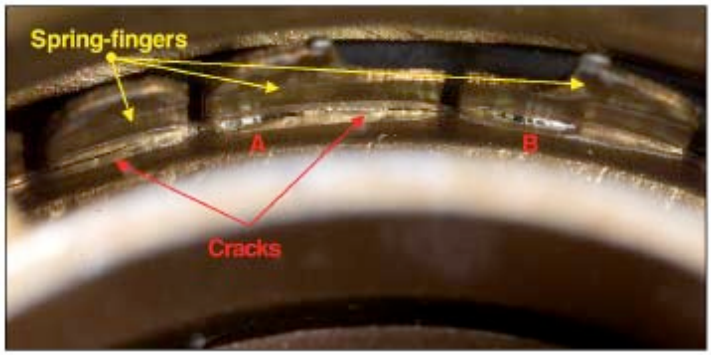

(a)

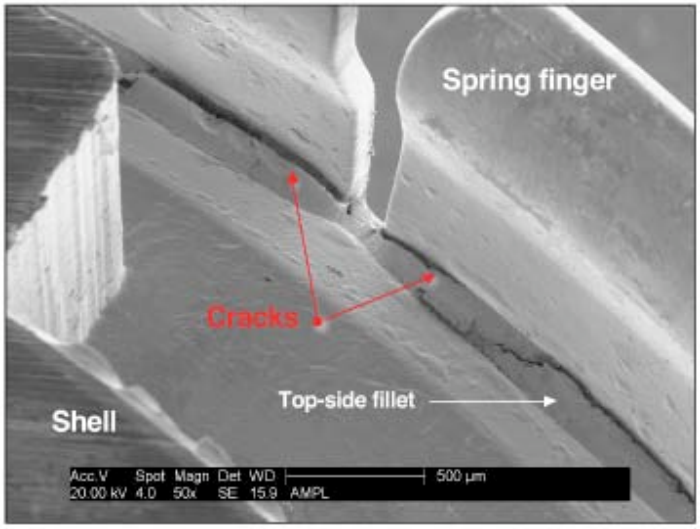

(b)

Fig. 4 Stereo photograph showing cracks in the top side fillet of the spring finger solder joint from an SA1358-10 connector (S/N6000). The locations "A" and "B" suggest remelting of the 96.5Sn-3.5Ag solder had occurred. (b) SEM photograph illustrating the cracking of the spring finger solder joint at higher magnification on a different SA1358-10 connector (S/N1430).

[1] The term "uncontrolled" implies that the solder melting occurs under an uncontrolled thermal profile; without specific instructions established with respect to providing a flux; and in the absence of a specific process for re-inspecting the joint.

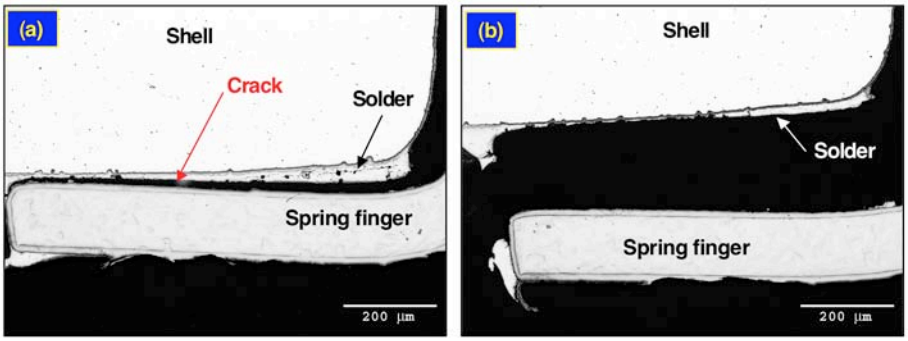

Fig. 5 (a) and (b) Optical micrographs of cross sections of SA1358-10 connectors from S/N1782 that show cracks that had propagated from top side fillet, through the gap. and into the bottom side fillet. In case (b), the spring finger had fully separated from the connector shell.

The second concern was remelting of the spring finger solder joints. The remelting of the Sn-Ag solder joint would have occurred during the attachment of the EMR adapter ring and/or EMR shell, which is performed with the low melting temperature, eutectic 63Sn-37Pb (Sn-Pb) alloy. The eutectic temperature is 183°C. Evidence to this effect is exemplified in Fig. 6.

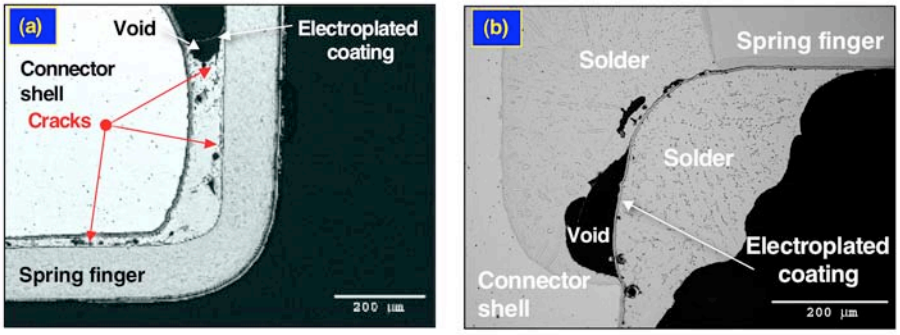

Fig. 6 Optical micrographs of cross sections of SA1358-10 connectors from S/N1782 showing the evidence of remelting of the 96.5Sn-3.5Ag solder: (a) the unsupported electroplated Cd (Cr) layer at the top side fillet and (b) solder breaching through, and void formation underneath, the electroplated Cd (Cr) coating on the bottom side fillet.

The top side fillet in Fig. 6 (a) had remelted and then retreated, leaving the post-soldering electroplated Cd (Cr) layer suspended above the resulting void. In Fig. 6 (b), which depicts the bottom side fillet region, the optical micrographs clearly show that the electroplated Cd layer had been breached, and its external surface wetted, by the molten Sn-Ag solder.

The last phenomenon was that of flaking of the Cd layer from the connectors and, in particular, from the spring finger solder joint fillet. The prevalence for Cd flaking in the earlier connectors is illustrated by the SEM photographs in Fig. 7. Lifting of the Cd coating is observed.

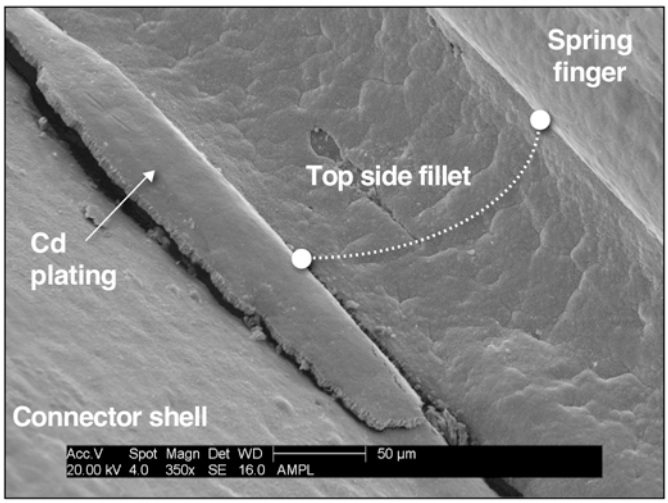

Fig. 7 SEM photograph showing flaking or spalling of the Cd coating from the top side fillet of the spring finger solder joint. The SA1358-10 connector was S/N 1430.

In summary, a prior study of SA1358-10 connectors illustrated that the defects, which included *extended* solder joint cracking, solder remelting, and Cd (Cr) layer spalling in the spring finger solder joints, could occur in these assemblies. Therefore, a follow-on study was developed, the objective of which was to further confirm the extent to which these defects occurred in built and/or built-and-fielded SA1358-10 connectors as well as in the "sister" connector family designated as SA2052-4.

1.2 Present study of SA1358-10 and SA2052-4 connectors.

The present study evaluated the SA1358-10 and SA2052-4 connector types. Both connectors are fabricated at Amphenol (Sydney, NY). The connector shells (and coupling

rings) were fabricated from aluminum (Al). The specified electroplated layers are listed below for the SA1358-10 (PS357007) and SA2052 (313562) connectors:

SA1358-10

Connector shell

Electroless nickel (Ni) flash: No thickness designated
(A (Cu) copper layer may substitute for the Ni flash.)
Electroplated Ni layer: 200 microinches minimum
Electroplated Cd layer: 100 microinches minimum
(The Cd layer included a chromate conversion coating.)

Spring fingers

Cu flash: No thickness designated
Electroplated Ni layer: 200 microinches minimum
Electroplated Cd layer: 100 microinches minimum

SA2052-4

Connector shell

Electroless nickel (Ni) flash: 5 – 10 microinches
(A copper layer may substitute for the Ni flash.)
Electroplated Ni layer: 100 – 200 microinches
Electroplated copper (Cu) layer: 100 – 200 microinches
Electroplated Cd layer: 300 – 500 microinches
(The Cd layer included a chromate conversion coating.)

Spring fingers

Electroless Ni flash: 5 – 10 microinches
Electroplated Cd layer: 300 – 500 microinches

In the case of the connector shell, the electroless Ni layer, actually designated as Ni (P) to indicated the phosphorous (P) component of the layer, substituted for the zincate treatment as a means to assure adhesion of the Ni layer to the Al shell. The Ni layer served primarily as a corrosion inhibitor, but could also provide a “back-up” solderability finish to the Cu layer, which was deposited expressly for that function, initially on the SA2052-4 and later on the SA1358-10 (which is the reason that the Cu layer is not listed above).

The Cd (Cr) layer served as the overall corrosion inhibitor for the connector assembly. Therefore, the Cd (Cr) layer was plated onto the connector after the spring fingers had been soldered to the shell so that the entire surface, including the solder fillets, was coated with the protective finish. Cadmium layers are particularly effective against salt spray environments.

The electron probe microanalysis (EPMA) technique was used to confirm the composition of the plated layers that were present in the connector structures. An effort was not made to measure the thicknesses of those layers at this time.

The three spring finger segments were *specified* to have been soldered to the shell using a donut-shaped perform of the Sn-Ag solder. The Sn-Ag solder was located between the spring finger segment and the shell. Soldering was performed in a hot oil bath, using the Alpha™ 816-35 flux. The connector received a Cd electroplated protective finish. Then, the contacts are added to the shell.

The second family of connectors was the SA2052-4. The latter connectors were a smaller version (fewer pins) of the SA1358-10. But, the SA2052-4 connectors were fabricated using the same steps as were used with the SA1358-10; therefore, the same concerns were raised that were described above. The only difference between the specifications of the two connectors was that the SA2052-4 document established plating thickness ranges rather than minimum values and made the provision for a Cu layer as the solderable finish on the connector shell.

In the case of each connector type, after installation of the electrical contacts, the connectors were then shipped to Honeywell Kansas City Plant (KCP) to complete their assembly. At KCP, the cable leads were soldered to the contacts at the back of the connector shell. Then, the EMR (adapter) ring was screwed into the back side of the connector and induction soldered into place with the 63Sn-37Pb (Sn-Pb) alloy; see Fig. 1b that exemplifies the SA1358-10 case. Finally, the EMR shell was located over the ring and, likewise, soldered in to place with the Sn-Pb filler metal. *It was either or both of these latter two processes – the induction soldering of the EMR adaptor ring or the hand soldering of the EMR shell – that were suspected of having caused the remelting of the spring finger solder joint.*

The connector parts used in the present study and their pedigrees are listed below according to item #. The “item #” designation will be used throughout this report in order to

correlate the findings with the nomenclature used to distinguish the various histories of the connectors. A brief description of each connector set will follow the list. The terms “old connector” and “new connector” refer to units that have an earlier or current date code, respectively. The terms “old process” and “new process” indicated the time that the spring fingers were attached to the connector, either at the time of the earlier manufacturing date code (“old”) or at the time of the recent date code (“new”).

Item #1: OLD CONNECTORS, OLD PROCESS
SA1358-10, DC 1984-25 from MC3617 S/N 1460
SA2052-4, DC 1984-42 from MC3617 S/N 1460

Item #2: OLD CONNECTORS, NEW PROCESS
SA1358-10, DC 1990-25 from MC3617 S/N X706 (PPI)
SA2052-4, DC 1986-34, from MC3617 S/N X706 (PPI)

Item #3: NEW CONNECTORS, NEW PROCESS
SA1358-10, DC 2001-03 from MC3617 S/N 5326
SA2052-4, DC 2001-52 from MC3617 S/N 5422

Item #4: NEW CONNECTORS, NO PROCESSING *(Baseline)*
SA1358-10, DC 2002-26
SA2052-4, DC 2001-52

Item #5: NEW CONNECTORS, INDUCTION SOLDERING OF EMR RING
SA1358-10, DC 2001-52 (210°C, 3s)
SA2052-4, DC 2001-52 (191°C, 1.5s)

The “OLD CONNECTORS” represent fielded hardware that were manufactured with the older date codes (DCs), which were from the middle 1980s to early 1990s. The “NEW CONNECTORS” refers to units having the recent date codes with years 2001 or 2002. The “OLD PROCESS” refers to the soldering process that used to assemble the connector during the middle 1980s to early 1990s. The “NEW PROCESS” is the current procedure used to make the connector. That is, the new process has not been altered from the OLD PROCESS; it is merely the fact that it has been performed over the past one – to – two years. The “NEW CONNECTORS” are from recent builds at Amphenol (2001 and 2002) and would incorporate recent design changes, if any.

The purpose for Item #1 was to determine the prevalence of the cracking and remelting defects in heritage connectors. Item #2 looked at the old connector design assembled with the new (present day) cable attachment procedure. Item #3 examined the new connectors assembled with the new assembly processes. The data obtained from Items #1, #2, and #3 were used to determine whether remelting of the spring finger joints was a result of the process or the connector design. Item #4 provided a baseline for the new connector designs.

Lastly, Item #5 was used to determine whether the induction heating process used to solder the EMR adapter ring to the connector shell was responsible for remelting of the spring finger solder joints. The hand soldering of the EMR shell was not performed on these units. The soldering process exposed the SA1358-10 connector to a peak temperature of 210°C for 3 s. The SA2052-4 connector was exposed to less harsh conditions due to its smaller size; the peak temperature was 191°C and the hold time at that temperature was 1.5 s.

2. Analysis procedures

The study of the Item #1 through Item #5 connectors was performed with the following steps:

(1) Each of the connectors was photographed using a stereo microscope. Side views as well as views into the pin cavity were completed. The resulting photographs were used primarily to develop maps and locators for the subsequent analysis steps that are described below. A limited number of photographs were taken of the top side fillet of the spring finger solder joints; however, the reduced depth-of-focus of the stereo microscope limited the extent of detail that could be observed by this means.

(2) The coupling ring was slit with a diamond saw and removed, thereby providing a better view of both the top side and bottom side fillets of the spring finger solder joints. In addition, the pin contact cavity was filled with epoxy and the pins were then cut off just above the skirt. Both of these procedures provide for a closer approach of the microscope and camera to the above-board solder fillet. Additional stereo photographs were taken of the top side fillet regions.

(3) The spring finger solder joints were examined using the scanning electron microscope (SEM). Although this examination concentrated on the top side fillet, the bottom side fillet was also surveyed. The SEM photographs were then

used to determine those locations around the spring finger solder joint that would be targeted for metallographic cross sections.

(4) The connectors were cross-sectioned at the desired locations. Defective as well as sound fillet configurations were subjected to cross sectioning, the latter providing baseline data. (The pin cavity had been filled with epoxy and the lengths of the pins cut off earlier; this procedure also facilitated the cross section analysis.) The microstructures of the spring finger solder joints were carefully evaluated by optical microscopy.

(5) Electron probe microanalysis (EPMA) was performed on selected solder joint cross sections in order to identify the chemical composition of the structures comprising those sections. In general, the needed information was adequately provided through X-ray dot maps. Quantitative line scans were reserved for those circumstances for which such exacting analyses would be required.

3. Results and Discussion

3.1 Item #1: OLD CONNECTORS, OLD PROCESS

SA1358-10, DC 1984-25 from MC3617 S/N 1460

An inspection was performed of the spring fingers and the solder joints after removal of the coupling ring and the cutting-off of the pin contacts. The SA1358-10 connector exhibited isolated blisters of the plating on the top side fillet as shown in Fig. 8 (a).

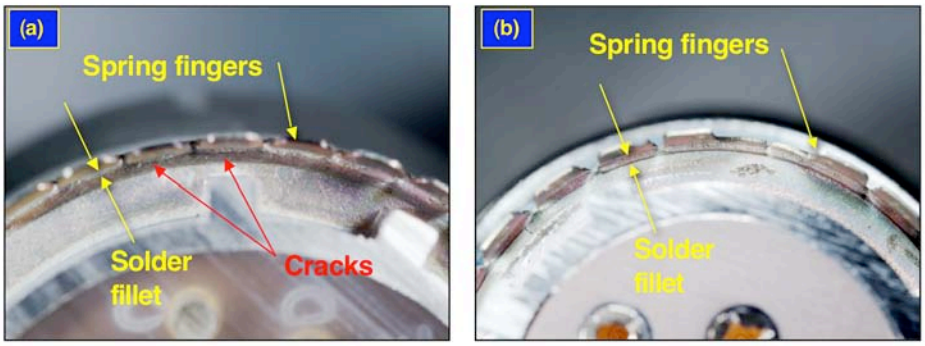

Fig. 8 Stereo photographs showing the top side fillet on the spring finger solder joints of (a) the SA1358-10 connector and (b) the SA2052-4 connector. Isolated cracks were observed in the solder fillet of the SA1358-10 unit; there were no obvious defects to the SA2052-4 solder joint.

There appeared to be some isolated cracking in the same fillets, as well. There was no damage to the spring fingers, themselves, nor was there degradation to the bottom side fillet. There were no obvious defects to the fillet of the SA2052-4 connector solder joint as shown in Fig. 8 (b). The solder surface had a more frosty appearance as compared to the SA1358-10 solder fillets. The spring fingers exhibited no indications of damage to them.

Scanning electron microscope photographs were taken of the spring finger solder joints. Shown in Fig. 9 are representative SEM photographs from the SA1358-10 unit. Cracks appear in the top side solder fillet at a number of locations around the spring fingers as shown in (a), (b), and (c). It could not be determined from the SEM photographs whether the cracks represented through-cracks into the solder fillet or were the result of fissures in the plated Cd (Cr) layer. The surface morphology of the Cd (Cr) coating is shown in Fig. 9 (d).

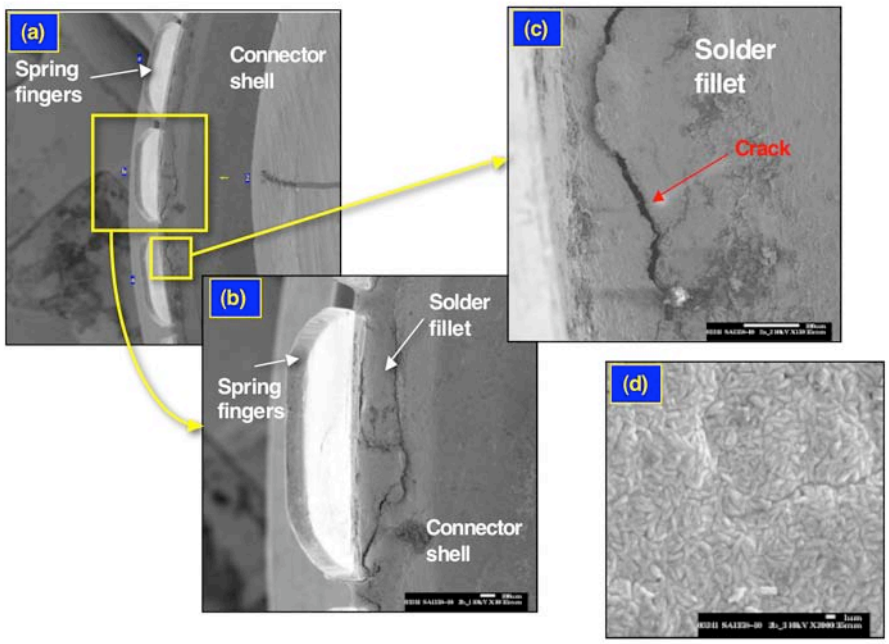

Fig. 9 SEM photographs showing the top side fillet on the spring finger solder joints of the Item #1 SA1358-10 connector: (a) low-magnification view showing several spring finger tines; (b) and (c) medium magnification views showing the extent of cracking on the fillet surface; and (d) high magnification view showing the surface morphology of the Cd (Cr) plating.

The top side fillet region of the spring finger solder joints from the SA2052-4 connector were shown in Fig. 10. Flaking of the Cd (Cr) plating was observed on the connector shell *near* to the solder fillet (Fig 10 (a)). Large-scale cracks were absent from the fillets; rather, smaller cracks were present as is illustrated in Fig. 10 (b). At this surface view, crack propagation occurred between the Cd (Cr) nodules. The surface morphology of the Cd (Cr) plating on the SA2052-4 connectors was further illustrated in Fig. 10 (c). It is clear that the Cd (Cr) plating on these connectors had a coarser structure than that on the SA1358-10 connector.

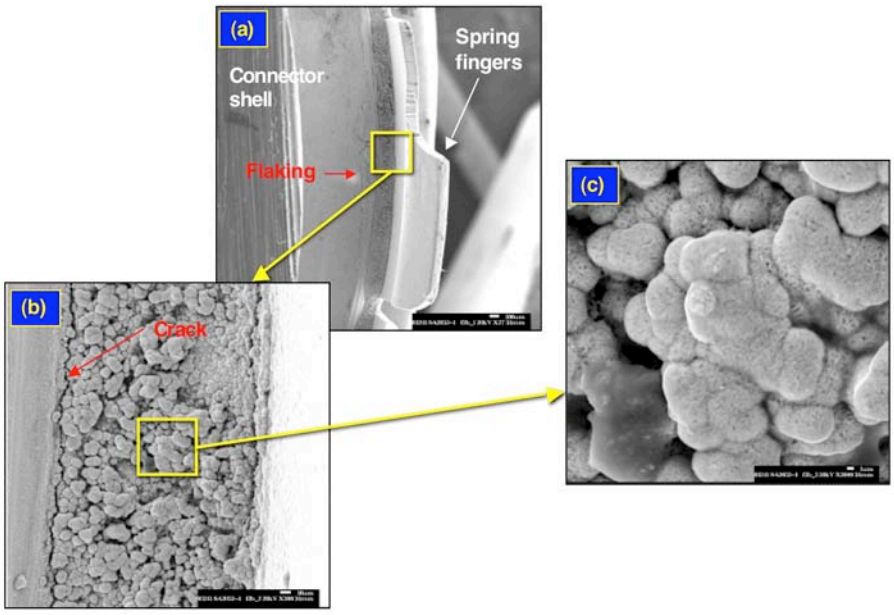

Fig. 10 SEM photographs showing the top side fillet on the spring finger solder joints of the Item #1 SA2052-4 connector: (a) low-magnification view showing several spring finger tines; (b) medium magnification views showing minor cracking at fillet/connector shell interface; and (c) high magnification view showing the surface morphology of the Cd (Cr) plating.

The SEM analyses (Figs. 9 and 10) confirmed the presence of cracking in the top side fillets of both the SA1358-10 and SA2052-4 connector, spring finger solder joints. As was noted above, it was not possible to discern the extent to which, those cracks extended into the solder fillets. A determination of crack depths required metallographic cross sections. Shown in Fig. 11 is the manner in which, the cross sections were made of the spring finger

solder joints. The SA1358-10 connector was used in this particular illustration; the procedure was similar for the SA2052-4 connector. In one of the cuts, it was possible to intersect a row of pins as well as the spring finger solder joints on the diametrically opposing sides of the connector. An examination of the pin solder joints was included to document their integrity.

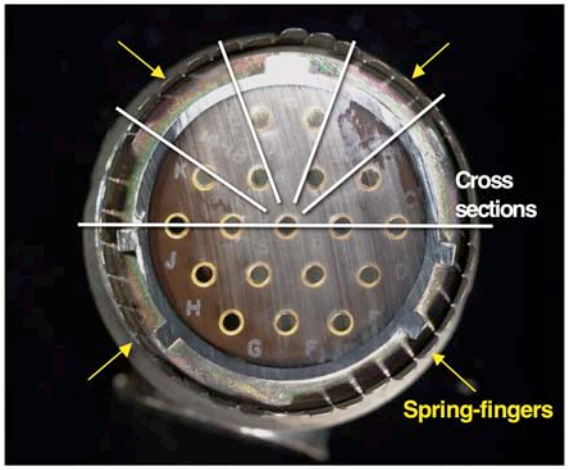

Fig. 11 Stereo photograph showing the configuration of the cross sections made to the SA1358-10 connector. The same procedure was used on the smaller SA2052-4 connector. One cut passed through a row of pins, thereby allowing for an examination of the solder joints on the termination end of the contacts.

Shown in Fig. 12 is an SEM photograph and two optical micrographs that were taken of one of the two spring finger solder joints on the SA1358-10 connector. The SEM image in (a) shows the topography of the solder joint where the cross section was taken. The low magnification view (b) illustrates the connector shell, spring finger, and solder joint geometries. The view in (c) is of the top side fillet (that is exposed to visual inspection). The EPMA technique was used to determine the compositions of the electroplated layers put on the connector structures as well as that of the solder used in the attachment process. Those results are listed in Table 1, which lists all of the layer compositions used on the connectors that were studied throughout this study. For the item #1 SA1258-10 connector, both the connector shell and BeCu spring fingers were electroplated with a Cu solderable layer. Instead of the Sn-Ag solder, it appeared that a Sn-Sb solder, most likely the 95Sn-5Sb (wt.%) alloy (T_s = 232°C, T_l = 240°C), was used to make the joints. Upon completion of the soldering process, the entire assembly was electroplated with a Ni layer followed by a

Cd layer. Lastly, a chromate conversion coating (labeled Cr) was added to provide corrosion and abrasion resistance to the Cd layer. These coatings were identified in Fig. 13, which is a high-magnification view of the top side solder fillet. Several artifacts in Fig. 13 are discussed in greater detail below.

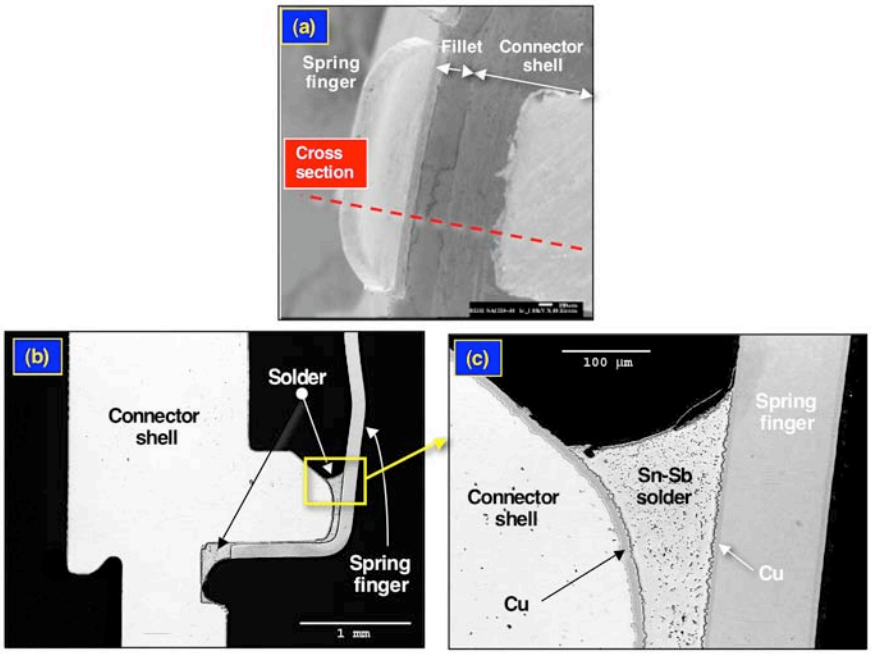

Fig. 12 (a) SEM photograph showing the location of the cross section on the connector. Optical micrograph (b) showing one of two spring finger solder joints that were obtained by a diametrical section through the Item 1, SA1358-10 connector. The higher magnification view in (c) shows the top side fillet and identifies the Cu coating used on the connector shell and spring finger.

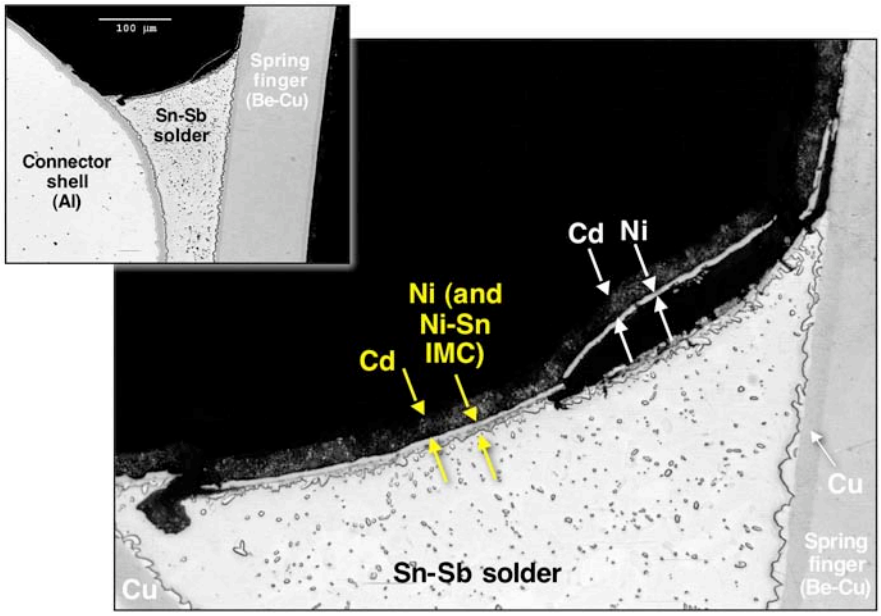

Fig. 13 Optical micrographs showing a high magnification view of the top side fillet shown in Fig. 12b. Spalling of the combined Ni and Cd layers was evident over a part of the fillet. A Ni-Sn intermetallic compound (IMC) layer had developed between the Ni coating and the Sn-Sb solder.

Item Description	Connector Type	Spring Finger Plating	Connector Shell Plating	Post-Solder Overplating
#1 OLD Process, OLD Design	SA1358-10	Cu	Cu	Ni, Cd, Cr
	SA2052-4	Cu	Cu	Ni, Cd, Cr
#2 NEW Process, OLD Design	SA1358-10	Cu	Ni (P), Cu	Cd, Cr
	SA2052-4	Cu	Cu	Ni, Cd, Cr
#3 NEW Process, NEW Design	SA1358-10	Cu	Ni (P), Cu	Cu, Cd, Cr
	SA2052-4	Cu	Ni (P), Cu	Cu, Cd, Cr
#4 NO Process, NEW Design ****Baseline****	SA1358-10	Cu	Ni (P), Cu	Cu, Cd, Cr
	SA2052-4	Cu	Ni (P), Cu	Cu, Cd, Cr
#5 Induction soldering of EMR coupling ring, NEW Design	SA1358-10	Cu	Ni (P), Cu	Cu, Cd, Cr
	SA2052-4	Cu	Ni (P), Cu	Cu, Cd, Cr

Table 1

Compositions of the Electroplated Layers on the SA1358-10 and SA2052-4 Connectors

The Cu, Ni, and Cd (with Cr) layers had excellent adhesion to the connector shell and spring finger structures. However, as was evident in Fig. 13, the combined Ni and Cd (Cr) layers had locally spalled away from the solder fillet surface. Specifically, the separation occurred at the interface between the Ni layer and the Ni_3Sn_4 intermetallic compound (IMC) layer that developed between the Ni coating and the solder. The blocky morphology of the Ni_3Sn_4

layer, together with relatively large thickness of the IMC layer, itself, indicate that the latter was formed by contact with *molten* solder rather than having resulted from a solid-state reaction. Additional evidence that the solder had melted after application of the Ni and Cd (plus chromate) coatings was the void located on the left-hand side of the fillet. The absence of the Ni and/or Cd coatings on the interior surface of the void implied that the latter was generated after the electroplated deposition of the Ni and Cd finishes.

The analysis turned to the gap between the horizontal leg of the spring finger and the similar surface of the SA1358-10 connector shell (Fig. 14). A Cu-Sn IMC layer having the Cu_6Sn_5 stoichiometry (as determined by EPMA) was located between the Sn-Sb solder and the Cu plating layers of the respective structures. There were no indications of crack development within any feature of the gap structure.

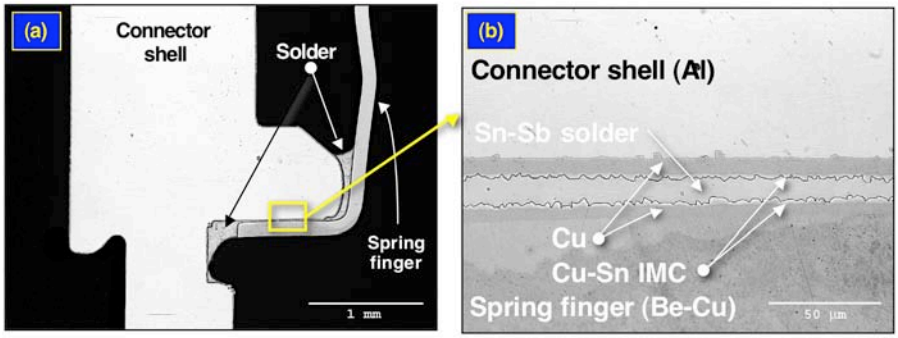

Fig. 14 Optical micrograph showing the gap region between the horizontal sections of the connector shell and the spring finger of the Item #1 SA1358-10 connector. The Cu plating layers and Cu-Sn IMC layers were identified.

The Cu-Sn IMC layer appeared to be thicker that would be expected from the typical soldering process with the Sn-Sb alloy. Therefore, the Cu-Sn IMC thickness was measured in the gap regions of the joints observed using the diametric cross sections (e.g., Fig. 11). The thicknesses were measured at 13 locations on each of the aluminum shell and BeCu spring finger sides of the joint. Those data are listed in Table 2, together with the results of measurements pertaining to the other "items" as will be described below. In the case of the SA1358-10 Item #1 unit, the three locations F1, F2, and F3 were evaluated. Those values, together with results discussed later on in this report, were listed in Table 2. The IMC layer thicknesses reported in Table 2 for these connectors were compared to 1.09±0.34 μm, which was measured from the exposure of Cu to molten 95Sn-5Sb solder (280°C) for 5 s

[2]. The IMC layers were considerably thicker on the connectors, an effect that would be expected from an extended time of exposure between Cu and the molten Sn-Sb solder. Solid-state, IMC layer growth between 95Sn-5Sb solder and Cu over the 20 year component life would not account for the larger thicknesses on the connector. Such growth would require a sustained exposure to temperatures in excess of 60°C during that period. On the other hand, the observed degree of IMC layer growth could have occurred by exposing the joint to temperatures of approximately 230°C, just below the solder solidus temperature, for time periods of about 15 min. Such conditions are certainly possible during follow-on processing of the connector, such as the attachment of the EMR shield. On the other hand, this IMC morphology could have developed from the molten solder and Cu dissolved into the confined geometry of the gap. Therefore, it was not possible to determine for certain, the source of the thick IMC layers in the horizontal gap. Nevertheless, the IMC layers did not appear to pose a reliability concern for the solder joint.

Item Description	Connector Type	Location	Mean IMC Thickness - Spring Finger (µm)	SD IMC Thickness - Spring Finger (µm)	Mean IMC Thickness - Connector Shell (µm)
#1 OLD Process, OLD Design	SA1358-10	F1	1.64	0.57	1.89
	SA1358-10	F2	2.22	0.68	1.53
	SA1358-10	F3	2.21	0.56	1.96
	SA2052-4	F1	1.79	0.68	1.28
	SA2052-4	F2	1.65	0.55	1.69
	SA2052-4	F3	1.45	0.58	2.12
#2 NEW Process, OLD Design	SA1358-10	F1	1.68	0.80	1.30
	SA2052-4	F2	2.11	0.73	1.97
	SA2052-4	F3	1.64	0.59	1.58
#4 NO Process, NEW Design ****Baseline****	SA1358-10	F1	1.93	0.63	2.02
	SA2052-4	F1	1.84	0.63	1.82
#3 NEW Process, NEW Design	SA1358-10	F1	1.82	0.81	1.79
	SA1358-10	F2	1.43	0.74	2.61
	SA1358-10	F3	2.01	1.03	1.39
	SA2052-4	F1	1.59	0.87	1.67
	SA2052-4	F2	1.64	0.59	1.65
	SA2052-4	F3	1.65	0.54	1.39
#5 NEW Design, Induc Soldering of EMR Coupling Ring	SA1358-10	F1	1.80	0.66	2.16
	SA1358-10	F2	1.97	0.58	1.89
	SA2052-4	F4a	2.08	0.88	1.64

Table 2

Intermetallic Compound (IMC) Layer Thicknesses Measured at the Horizontal Gap Between the Connector Shell and the Spring Fingers

Next, the lower solder fillet was examined. The fillet structure is shown by the cross section micrographs in Figs. 15 and 16. The view of the lower fillet provided in Fig. 15 shows good integrity to the solder joint. Except for one location, the Ni and Cd (plus chromate) coatings adhered to the fillet surface. The view in Fig. 16 shows separation of the overplating (Ni + Cd + chromate layers) from the solder fillet, specifically, at the interface between the Ni layer and the Ni_3Sn_4 IMC layer. Similar to the case presented with reference to Fig. 13 above, the relatively large thickness as well as blocky morphology of the Ni_3Sn_4 layer, indicated its source as being contact between Ni and *molten* solder; the IMC layer was not the product of

the very slow solid-state reaction between Sn and Ni. This morphology implies that the solder in the lower fillet likewise remelted during processing.

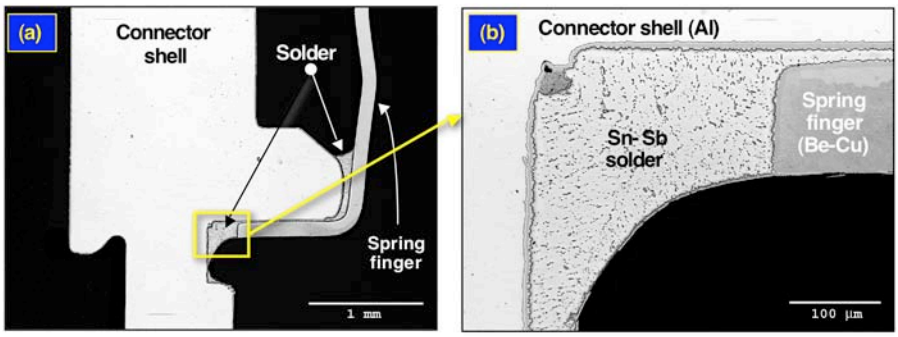

Fig. 15 Optical micrographs showing the lower fillet region of the solder joint between the SA1358-10 connector shell and the spring finger. The Cu plating layers and Cu-Sn IMC layers were identified.

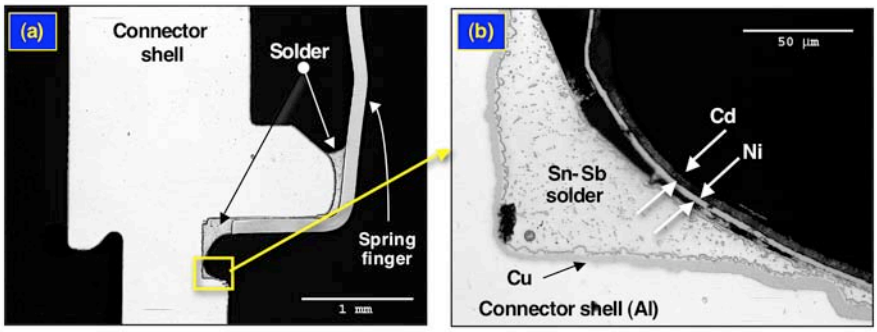

Fig. 16 Second set of optical micrographs showing the lower fillet region of the solder joint between the SA1358-10 connector shell and the spring finger.

The coating layers on the spring finger were also evaluated. Shown in Fig. 17 is a micrograph identifying the Cu, Ni, and Cd electroplated layers on the spring finger. The interfaces between the Be-Cu base material and Cu layer, as well as that between the Cu and Ni layers, have been highlighted in view. Each of the Cu and Ni layers was 4 – 5 μm thick; the Cd layer was approximately 10 μm thick. The layers exhibited excellent adhesion between themselves as well as to the Be-Cu spring finger.

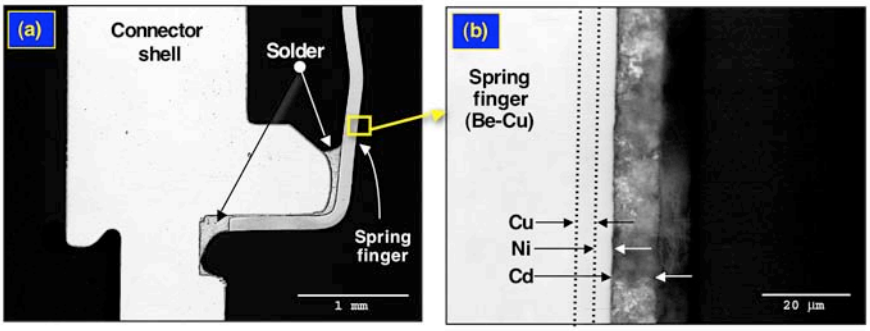

Fig. 17 Optical micrographs showing the Cu, Ni, and Cd layers on the spring finger of the Item #1 SA1358-10 connector at a location away from the solder joint. The chromate conversion coating was not visible on the Cd layer.

Shown in Fig. 18 is the second view of the connector shell/spring finger solder joint (F1b) that was provided by the diametrical cross section. A low magnification view is provided of the entire solder joint in (a); the higher magnification image in (b) revealed the top side fillet structure.

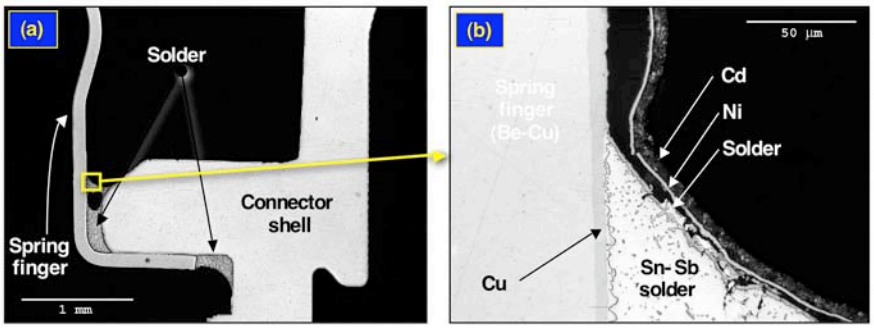

Fig. 18 (a) Optical micrograph showing the second solder joint of the diametrical cross section of the Item #1 SA1358-10 connector (F1b). (b) A high magnification view of the top side fillet). Spalling of the combined Ni and Cd layers was evident, resulting from separation between the Ni and Ni_3Sn_4 IMC layers over the solder and separation of the Ni layer from the Cu layer on the shell. There was also 95Sn-5Sb solder between the Ni_3Sn_4 layer and the Ni layer.

It was evident that a Ni_3Sn_4 layer had grown between the solder (that was molten at the time) and the Ni layer. Moreover, a thin film of solder was observed between the Ni_3Sn_4 layer and the spalled Ni layer. Because the former layer would only be wettable immediately after the disengagement of the Ni layer, the release of the Ni layer occurred while the solder was molten so that a breach in the Ni_3Sn_4 layer would cause the solder to wet its top surface.

The evaluation examined the remaining portions of the top side fillet as well as the horizontal gap and bottom side fillet of this solder joint. The features were very similar to those described above for the first view of the joint.

A third spring finger solder joint was examined primarily for indications of solder reflow after the protective finishes (Ni, Cd, and chromate) had been electroplated to the connector. Shown in Fig. 19 is an SEM photograph of the spring finger joint (F2) and low magnification optical micrograph of the cross section of the top fillet of that solder joint. The location of the cross section (dotted red line) is shown in (a). Features that appear to be cracks (yellow diamonds) in the SEM photograph (a) were confirmed in the optical micrograph (b) to be spalling of the protection finish from the top fillet surface

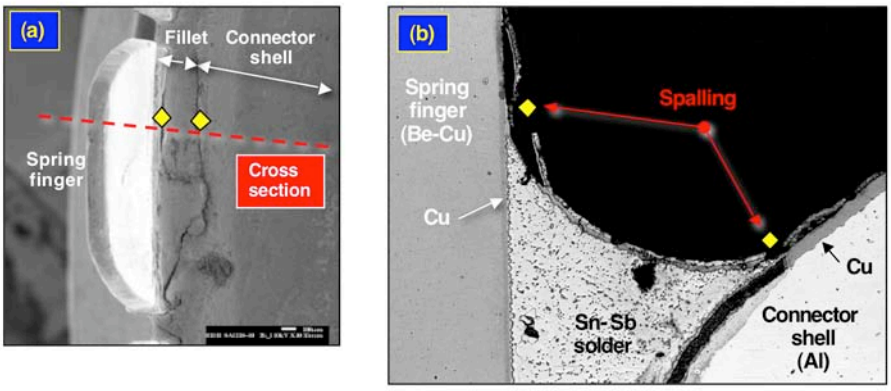

Fig. 19 (a) SEM photograph showing a third spring finger solder joint (F2) on the Item #1 SA1358-10 connector. (b) Optical micrograph of the cross section of the top solder fillet of the joint, along the red dotted line in (a). The yellow diamonds indicate areas of spalling by the plating layer, which appeared as cracks in the SEM image.

A closer examination was made of the spalled plating layers on the top fillet. Shown in Fig. 20 are low and high magnification views of the top fillet, (a), (b), respectively, of the F2 joint. The high-magnification image shows the presence of solder on top of the Ni layer, which is a clear indication of remelting of the joint. The solder had dissolved a significant portion of the Cd plating.

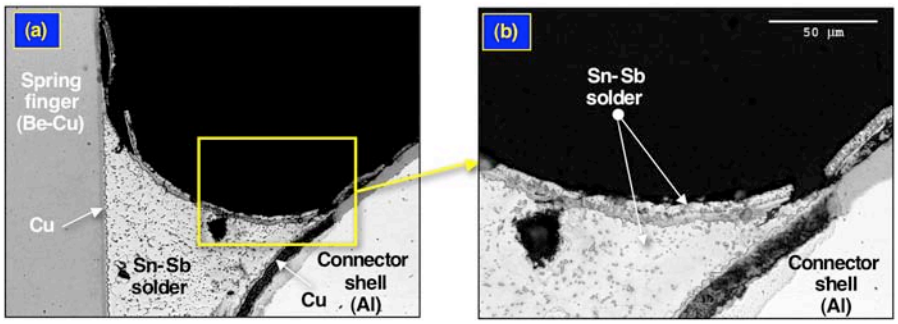

Fig. 20 Low (a) and high magnification (b) optical micrographs of the top fillet of the F2 solder joint on SA1358-10 connector shown in Fig. 19. The presence of solder on the top of the Ni layer provides a clear indication of remelting after the application of the latter and Cd layers.

Evidence of remelting of the solder was also observed in the bottom side fillet of this joint. Low and high magnification optical micrographs are shown in Fig. 21.

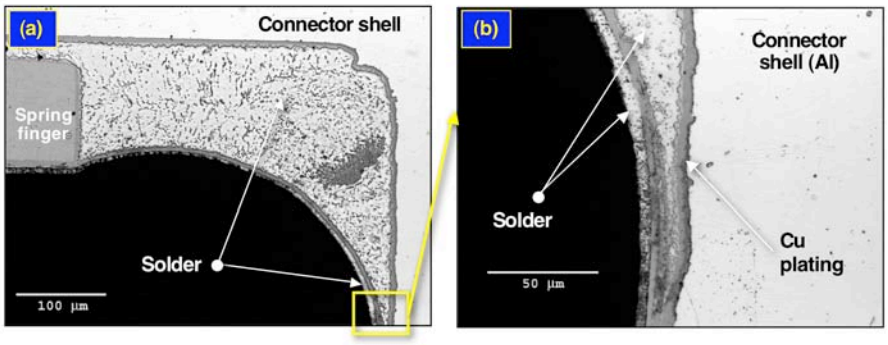

Fig. 21 Low (a) and high magnification (b) optical micrographs of the bottom fillet of the F2 solder joint on SA1358-10 connector. The presence of solder on the top of the Ni layer provides a clear indication of remelting after the application of the latter and Cd layers.

The presence of a solder coating on top of the Ni layer is shown in (b). Again, a large part of the Cd layer thickness had been dissolved into solder.

An examination was made of the horizontal section of the solder joint, which showed significant IMC layer development similar to that shown in Fig. 14. However, the gap region showed no indication of cracking damage.

A fourth spring finger solder joint (F3) was also examined on this connector. In this case, there was no clear evidence of remelting of the solder after the application of the Ni-Cd-chromate protective finish.

It was noted above that the diametric section through the connector also provided for an examination of the pin contact solder joints. Those interconnections were made between the "solder cup" on the termination end of the pin and the stranded Cu wire. Two cross section micrographs are shown in Fig. 22 that represent the excellent quality of those interconnections. The presence of voids was commensurate with historical observations concerning solder joints made to stranded wire. Solderability of the wire and connector pin were excellent. There were not indications of cracking in the joints that would have been caused by fatigue or an overload. There was clearly solder flow down the outside surface of the solder cup. It did not appear that the latter interfered with the overall construction of the connector. Also, there was no evidence of excessive Au contamination in the solder, which would have originated from the pin surface finish.

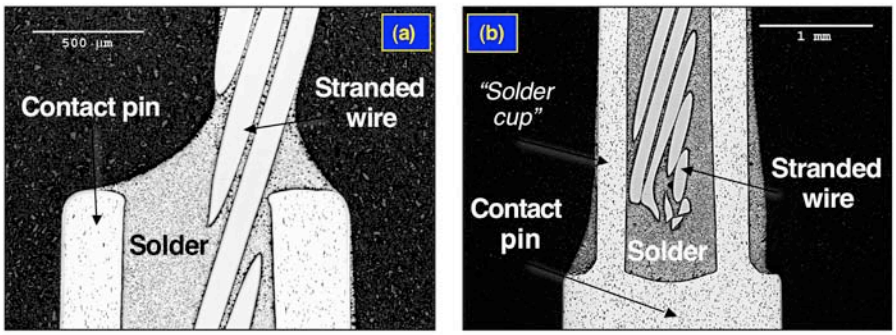

Fig. 22 (a) and (b): Optical micrographs of the pin contact solder joints on the Item #1, SA1358-10 connector (F1). The solder joints exhibited excellent quality.

In summary, the following observations were made of the Item #1 SA1358-10 solder joints. There was evidence to indicate that the 95Sn-5Sb solder had melted *after* application of the Ni, Cd, and chromate conversion protective coatings (Cr). Spalling of the Ni and Cd (Cr) layers was due primarily to separation between the Ni and Ni_3Sn_4 IMC layer, the latter having been formed during the transient melting event by the reaction between the molten Sn-Sb solder and the Ni overplated layer. Spalling of the Ni/Cd layer could present a corrosion concern for the connector structure. An excessively thick IMC layer developed between the Cu plating of the connector shell and the Sn-Sb solder, which suggested an exposure to very high temperature. It could not be determined from the morphology of the IMC layer, whether its source was a prolonged exposure to liquid Sn-Sb solder or solid-state aging resulting from follow-on processing. There was no evidence to suggest that the thick Cu/Sn IMC layer would pose a reliability concern for the solder joint. Lastly, the pin contact solder joints exhibited excellent quality; there were no indications of damage to the solder joints.

SA2052-4, DC 1984-42 from MC3617 S/N 1460

The electroplated layers on the connector shell and spring fingers, as well as the overplating layer, were the same as those shown in Table 1 for the SA1358-10 connector. The spring finger solder joints were examined, which were located on the “old connectors, old process” SA2052-4 connector. It was noted with reference to Fig. 8 that cracks were not observed in the top side fillet regions of the SA2052-4 spring finger solder joints when viewed by (low-magnification) stereo microscopy. However, cracks were detected when the joints were examined by SEM as well as by means of metallographic cross sections, as will be apparent in the discussion to follow. Shown in Fig. 23 is a series of SEM photographs of the F1a section through the SA2052-4 connector. The location of the subsequent metallographic cross section is shown by the photograph in (a). A small crack was detected near the solder/spring finger interface as indicated in (b). The nodular appearance of the electroplated layer that covered the Sn-Sb solder fillet was apparent by the higher magnification view in (c). There were no indications of spalling of the electroplated layer from the surface of the solder fillet.

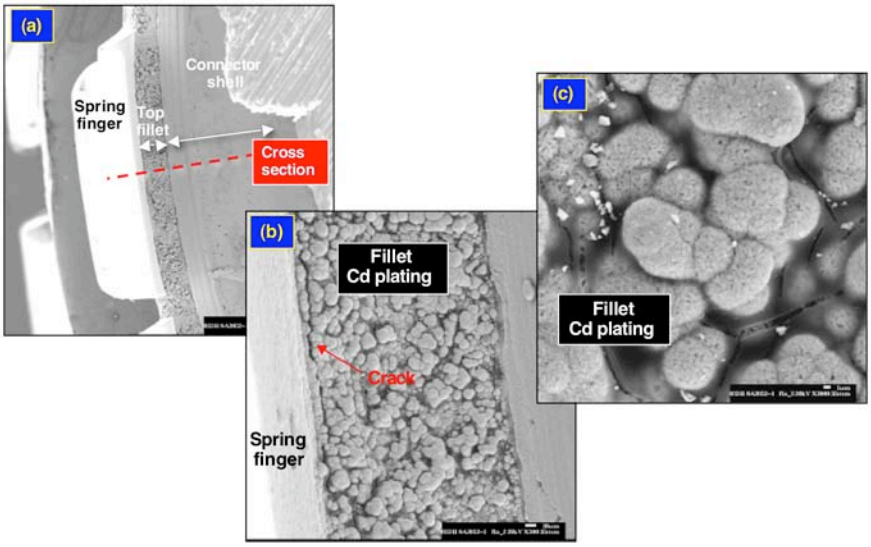

Fig. 23 (a), (b), (c): SEM photographs of the spring finger solder joints on the SA2052-4 connector (at location F1a). A small crack was observed between the solder fillet and the spring finger. The nodular nature of the electroplated coating was clearly evident.

A metallographic cross section was made of the spring finger solder joint at the F1a location. That location was duplicated in Fig. 24 (a).

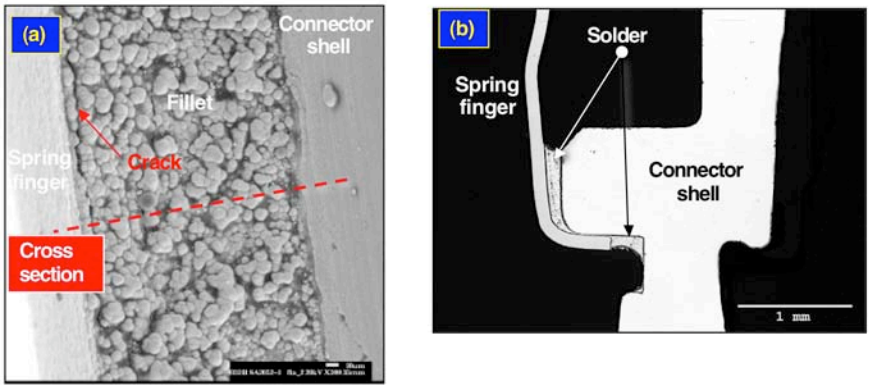

Fig. 24 (a) SEM photograph of the top side spring finger solder joints on the SA2052-4 connector at location F1a showing the location of the cross section. (b) Low-magnification optical micrograph showing the entire solder joint at the F1a location. There were no indications of large scale degradation to the joint or nearby structures.

A low-magnification optical micrograph, which shows the section through the entire solder joint, was provided in Fig. 24 (b). There was no large-scale degradation to the solder or to the connector structures. The optical micrographs in Fig. 25 show the top side fillet microstructure. The crack at the solder/spring finger interface was located, specifically, in the IMC layer that formed between the Sn-Sb solder and the Cu plating on the spring finger. This crack morphology is indicative of an overload failure that would result from the spring finger being bent away from the connector housing, such as would occur when it was mated to its counterpart connector. A resulting peel force placed the top of the solder joint into a tension load, resulting in separation in the IMC layer.

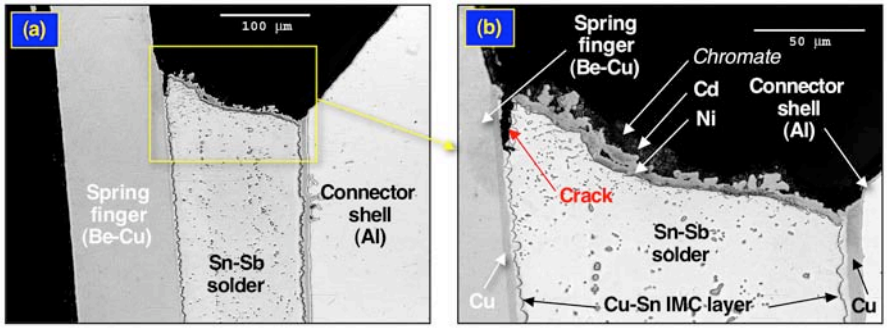

Fig. 25 (a) and (b) Optical micrographs of the cross section performed through the spring finger solder joint of the SA2052-4 connector at location F1a.

A more extensive crack was observed at location F2a. As shown in Fig. 26, the crack was apparent in both the SEM image (a) as well as the metallographic cross section (b). In this latter case, the progression of the crack through the IMC layer was more evident. The extents of cracking that was observed in both Figs. 25 and 26 would not pose a reliability issue with regards to the spring finger detaching from the connector housing. There was no microstructural evidence of TMF having occurred in the solder joint.

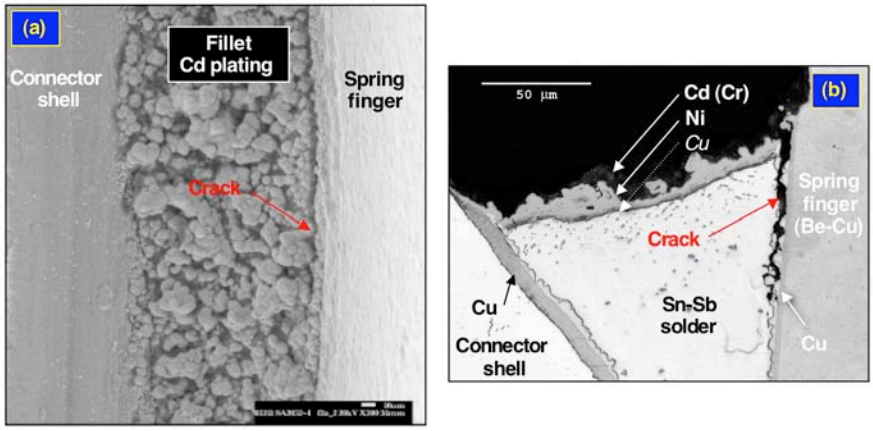

Fig. 26 (a) SEM photograph of the spring finger, top side solder fillet on SA2052-4 at location F2a. (b) Optical micrograph of the cross section performed through the spring finger solder joint of the SA2052-4 connector at location F2a. A significant crack was observed at the spring finger/solder interface. The Cd layer was also covered with a Cr (chromate conversion) coating

The microstructures that were shown in Figs. 25 and 26, were scrutinized for indications that the solder joint had been remelted. No such evidence could be identified in the cross section image. The nodular morphology of the electroplated layer, which was evident in the SEM images, was also apparent in the cross section micrograph. In fact, that nodularity appears to be associated with the Ni layer, and was subsequently amplified by the Cd deposit. Irrespective of the irregular morphology, the coatings were free of any breaches (with the exception of the aforementioned crack) that would jeopardize the corrosion protection.

Electron probe microanalysis (EPMA) x-ray dot maps were used to qualitatively assess the spatial composition of the solder joints. Shown in Fig. 27 are the dot maps of the F2a location shown in Fig. 26, but reversed about a vertical plane. Specifically, there are the dot maps for Cr, Cd, Cu, and Ni in (b), (c), (d) and (e), respectively. The dot maps in Fig. 27 confirmed the structure of the post-soldering electroplated coating. A thin Cu layer was placed over the solder fillet (as well as spring finger and connector housing) followed by the Ni barrier layer. Then, the Cd layer was electroplated over the surfaces followed by the chromate (Cr signal) conversion coating. Not shown in Fig. 27 was the Sb map that confirmed the composition of the solder.

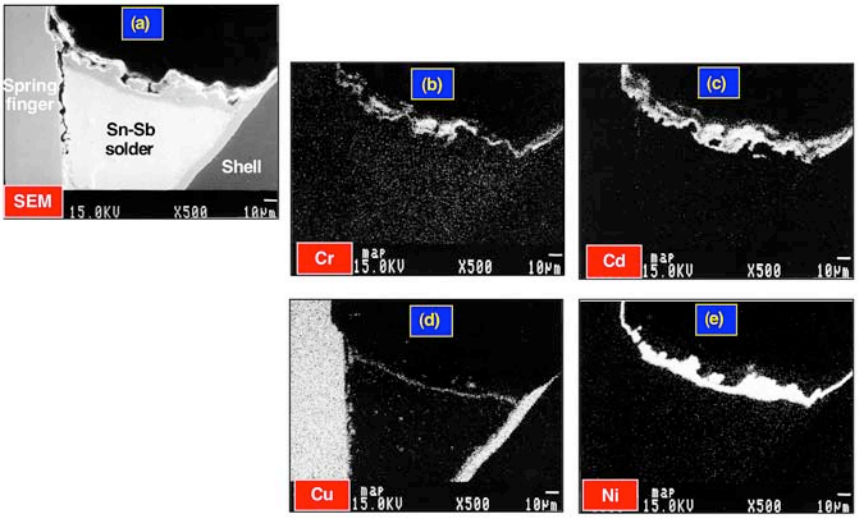

Fig. 27 Electron probe microanalysis x-ray dot maps showing the distribution of elements on the surface of the top fillet (SA2052-4, location F2a): (a) SEM/BSE of the fillet region; (b) Cr; (c) Cd; (d) Cu; and (e) Ni, the Cr layer being the chromate conversion coating.

The next region of the solder joint that was examined was the gap between the horizontal sections of the spring fingers and the connector housing. Representative of this region were the optical micrographs in Fig. 28, which were from location F1a. Grain boundaries were prevalent in the Sn-Sb solder, indicating some grain boundary sliding, the cause of which, was thermal expansion mismatch between the connector housing and spring finger as well as between these structures and the Sn-Sb solder. Cracks were not observed in any of cross sections. An IMC layer was also prevalent in the joint. Both the Cu_6Sn_5 and Cu_3Sn stoichiometries comprised the layer. The total IMC layer thickness was measured on both sides of the gap (N=13 measurements per side); those data were listed in Table 2. Although the morphology of the Cu_6Sn_5 layer could not discern its source as being due to liquid Sn-Sb solder or solid-state aging, the presence of the Cu_3Sn layer was more indicative of solid-state growth rather than having developed by exposure to *molten* solder. However, the latter case could be completely ruled out as a contributing factor, because the confined geometry may have altered the IMC morphology that formed between molten solder and Cu.

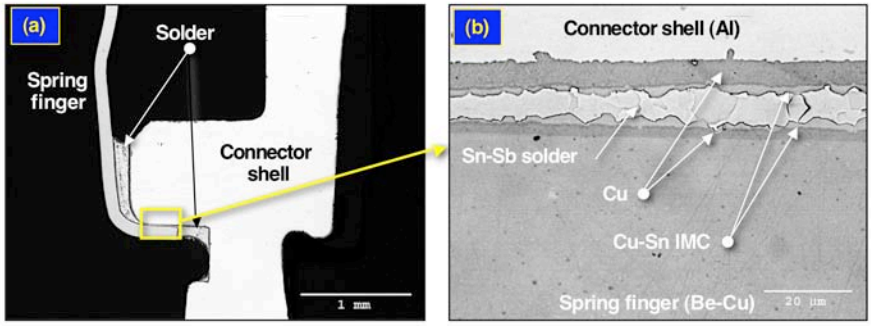

Fig. 28 (a) Low magnification optical micrograph showing the gap region between the horizontal sections of the connector shell and the spring finger of the SA2052-4 connector. The cross section was at location F1a. (b) High magnification optical micrograph of the solder joint in that gap region.

The bottom side fillet of the spring finger solder joint was examined via several cross sections. The F1a cross section was representative of the structures observed in the other locations; low and high magnification optical micrographs are shown in Fig. 29.

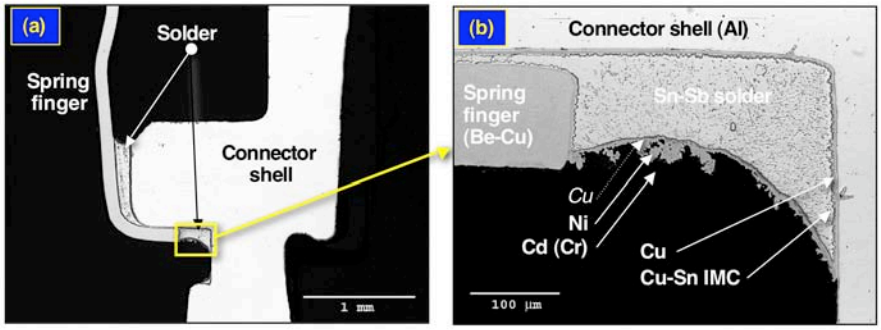

Fig. 29 (a) Low magnification optical micrograph showing the bottom side fillet region of the SA2052-4 connector. The cross section was at location F1a. (b) High magnification optical micrograph of the fillet. The Cd layer was also covered with a Cr (chromate conversion) coating.

All of the electroplated layers exhibited excellent integrity. There were no indications that the solder had been remelted subsequent to the application of the Cu-Ni-Cd-plus-chromate overplated layers. The nodularity of the Ni electroplated layer was replicated by the Cd

layer. It was observed in Fig. 29 (b) that there was a significant number of Cu-based particles in the solder (along with the Sb component). The particles, which were likely Cu_6Sn_5 per the phase diagram and historical data, were generated by the dissolution of Cu from the spring finger as well as from the connector housing. The IMC layer that formed between the Sn-Sb solder and the Cu layers of the connector and spring finger was similar in thickness to that observed in the gap region (Fig. 28).

In summary, the following observations were made of the SA2052-4 solder joints. There was no evidence to indicate that the Sn-Sb solder had melted *after* application of the Cu-Ni-Cd-plus-chromate conversion protective coatings. The nodularity of the surface plating observed in the top side fillet SEM images was caused by the Ni layer deposition. There was no evidence of spalling of the Ni and Cd (with chromate coating) layers from any of the surfaces. Spalling of the Ni/Cd layer could present a corrosion as well as particulate concern for the connector structure and engagement, respectively. A thick IMC layer developed between the Cu plating on the connector shell and spring finger and the Sn-Sb solder. There was no evidence to suggest that the thick Cu/Sn IMC layer would pose a reliability concern for the solder joint. Lastly, the pin contact solder joints exhibited excellent quality; there were no indications of damage to the accompanying solder joints.

3.2 Item #2: OLD CONNECTORS, NEW (RECENT) PROCESS

SA1358-10, DC 1990-25 from MC3617 S/N X706 (PPI)

The electroplating layers used on the connector shell as well as the overplating layer differed from the Item #1 units (Table 1). An electroless Ni (P) layer was added between the Cu and Al connector shell material. Also, the Ni layer was absent from the overplating coating; only a Cu flash was put down prior to the Cd (Cr) finish. The spring finger was still plated with Cu.

Stereo photographs as well as SEM photographs were provided in Figs. 30, 31, and 32 which show the top side solder fillet at three locations around the SA1358-10 connector, which were designated F1, F2, and F5, respectively. At the location F1, a fissure was observed in the overplating layer (Cd and chromate (Cr) coating). It appeared that the plating had separated from the underlying solder fillet surface (Fig. 30). It could not be determined, conclusively, that there was also a crack in the solder fillet. The more prevalent morphology of the top side fillet was the presence of cracks such as shown in Figs. 31 and 32. As in the previous case, it could not be confirmed whether the cracks

remained only in the Cd (Cr) coatings or had progressed into the solder fillet. Such confirmation awaited the metallographic cross sections.

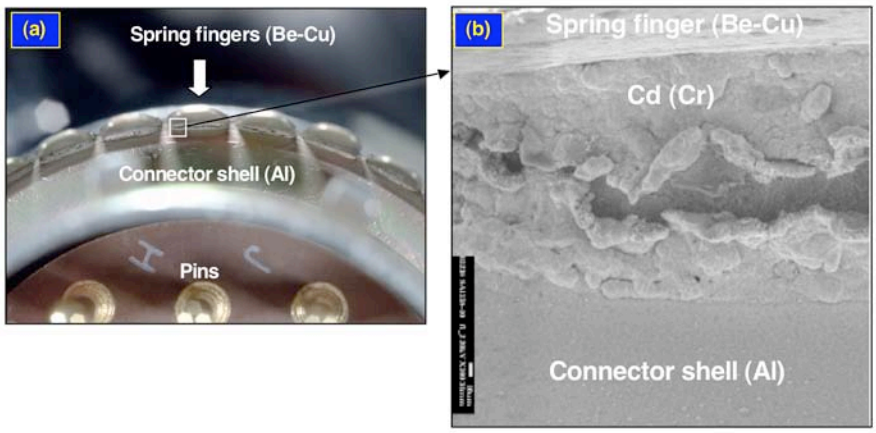

Fig. 30 (a) Stereo photograph showing the location of section F1a on SA1358-10. (b) High magnification SEM photograph of the fillet showing the fissure that formed in the Cd (Cr) electroplated coating on the top side fillet.

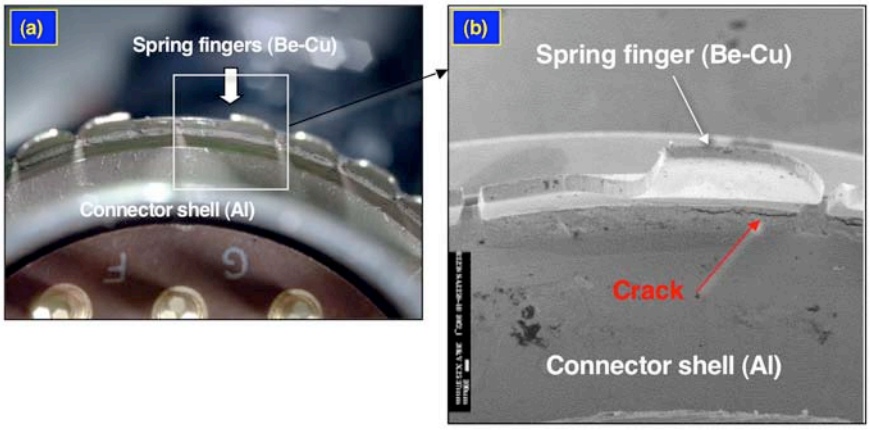

Fig. 31 (a) Stereo photograph showing the location of section F2 on SA1358-10. (b) Low magnification SEM photograph that identifies a crack in the top side fillet.

There was no damage observed to any of the connector structures.

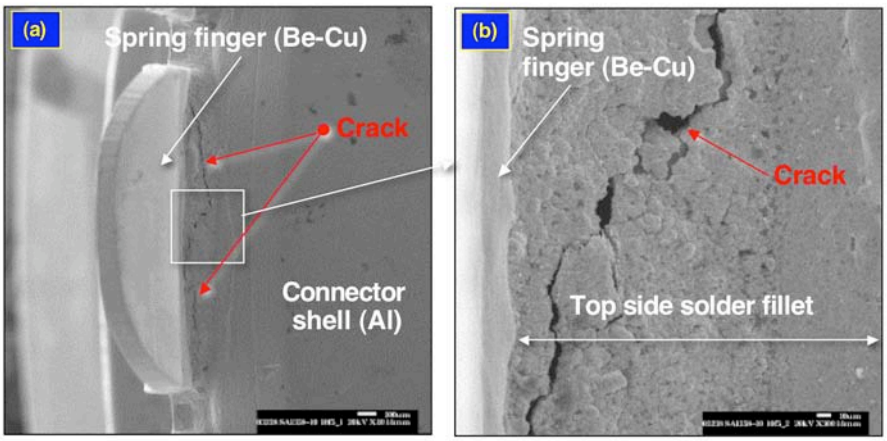

Fig. 32 (a) Stereo photograph showing the location of section F5 on SA1358-10. (b) Low magnification SEM photograph that identifies a crack in the top side fillet.

The connector was subjected to cross sectioning at the three aforementioned locations. Shown in Fig. 33 is an SEM of the surface of the F1a top side fillet location, together with two optical micrographs showing cross sections of the solder joint there.

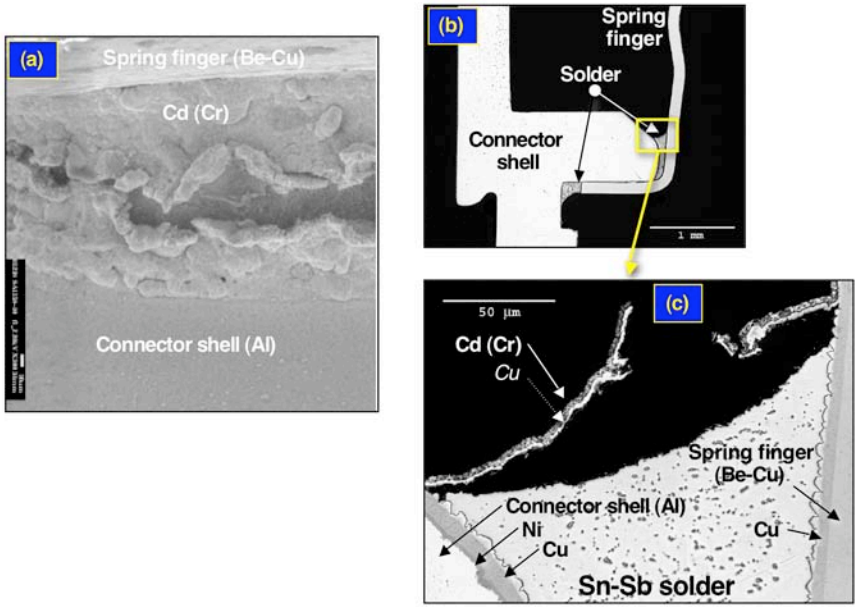

Fig. 33 (a) SEM photograph showing the top side fillet surface of section F1a on SA1358-10. (b) and (c) Low magnification and high magnification optical micrographs showing the cross section of the top side fillet at the same location as the SEM photograph.

It was clear that the Cd (Cr) electroplated layer *plus* the Cu flash layer had together spalled from the solder fillet. The separation had occurred at the Cu/solder interface. There was no evidence of cracking damage to the solder joint.

Next, the gap region between the horizontal sections of the connector shell and the spring finger was examined in metallographic cross section; the micrographs appear in Fig. 34. There was no evidence of the cracking or delamination to the solder joint structures in this location. A significant portion of the joint thickness was composed of the Cu_6Sn_5 IMC layer, albeit, there remained a thickness of Cu at both interfaces that would support joint function and any potential need for rework/repair activities.

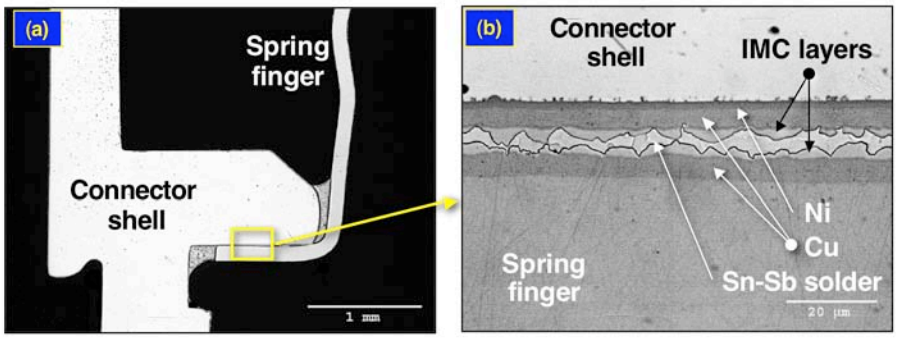

Fig. 34 (a) Low magnification optical micrograph showing the gap region between the horizontal sections of the connector shell and the spring finger of the SA1358-10. The cross section was made at location F1a. (b). High magnification optical micrograph of the solder joint in that gap region.

The IMC layer thickness was measured at both interfaces of (N = 13 data points). At the solder/connector shell interface, the thickness was 1.30±0.98 μm and at the solder/spring finger interface, the thickness was 1.68±0.80 μm as listed in Table 2 (locationF1). Based upon the same discussions above, the IMC layer thicknesses and variable morphology that was observed in Fig. 34, indicated that the layers were created by molten solder, most likely a combination of the solder process and follow-on assembly process.

The bottom side fillet was similarly examined. Cross section micrographs were provided in Fig. 35. The images show that the Cu plus Cd (Cr) plating layers together had separated from the solder fillet as they did at the top side fillet. There was no direct evidence to

suggest that solder melting was responsible for the gap between the fillet and the plated layer(s). The primary exhibit was the fact that the separated, plated layers conformed to the surface shape of the fillet.

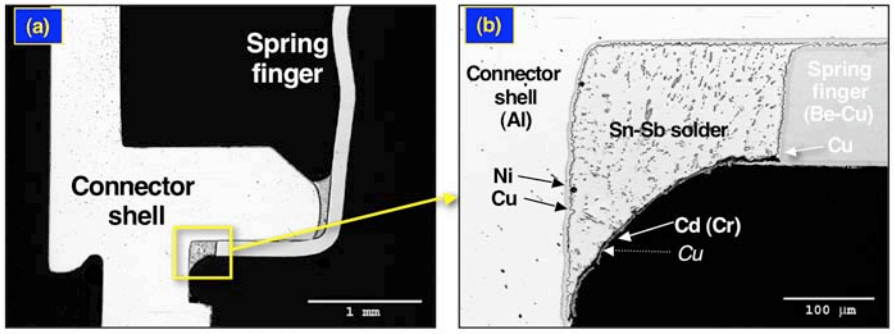

Fig. 35 (a) Low magnification optical micrograph showing the bottom side fillet region of the SA1358-10. The cross section was at location F1a. (b) High magnification optical micrograph of the bottom side fillet.

Two other locations were evaluated on this connector. Each of those locations exhibited evidence that the solder had melted after initial fabrication of the joint and subsequent electroplating operations. Shown in Fig. 36 are low and high magnification optical micrographs of the top side fillet at location F2 of the SA1358-10 connector. Solder was observed on the exposed surface of the plating layer, indicating that the solder had been remelted subsequent to the plating process.

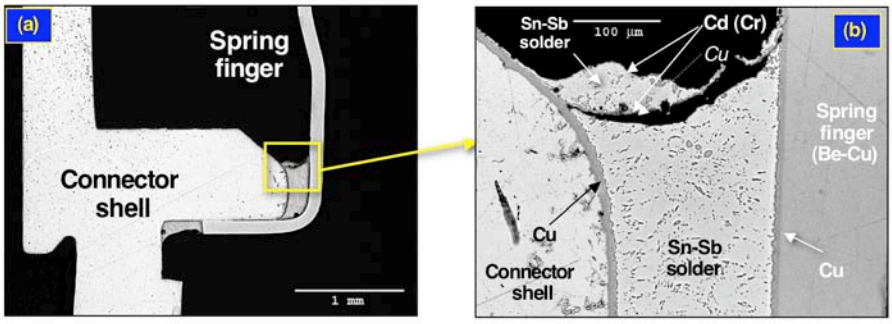

Fig. 36 (a) Low magnification optical micrograph showing the top side fillet region of the SA1358-10. The cross section was at location F2. (b) High magnification optical micrograph of the top side fillet.

Further evidence was obtained to confirm that the Sn-Sb solder had remelted after application of the electroplated coatings. Electron probe microanalysis x-ray dot maps were used to determine the spatial distribution of the materials in the solder joint structure. Shown in Fig. 37a is a high magnification, composite optical micrograph showing the juncture between the top side fillet surface and the connector housing. Two locations were designated by “A” and “B”. First, location “A” was evaluated by the EPMA technique (Fig. 37b). It was confirmed from the maps that the Sn-Sb solder broke through the electroplated layer. The molten solder wet and then dissolved the Cd layer; it was unable to do either to the Cr layer and, as such, the latter remained as a coating “skin” that floated on the solder fillet surface when the latter was molten. Similarly, the Cu was dissolved into the solder, albeit, to a lesser extent than was the Cd, and so remained in its original position underneath the newly extruded solder. The lack of complete Cu layer dissolution suggests that the time that the solder was molten, was not excessively long < 1 – 2 minutes at worst.

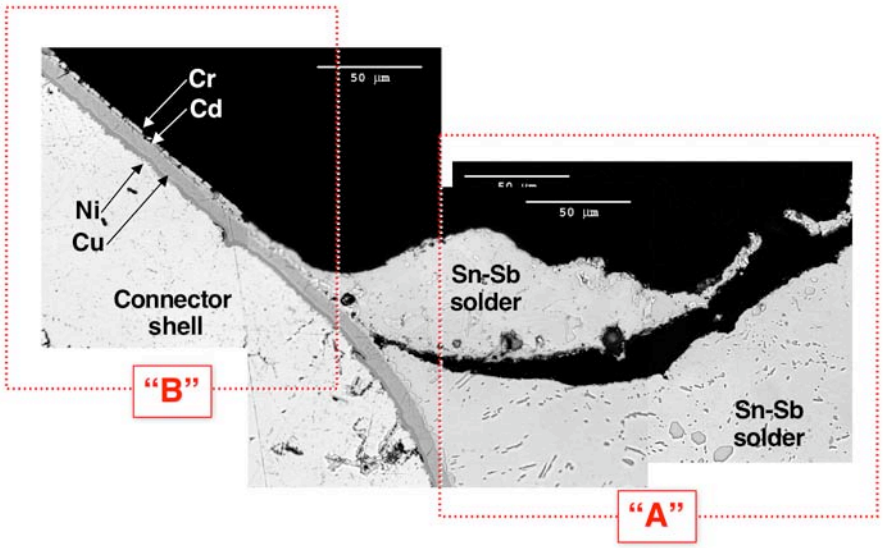

(a)

Fig. 37 (a) High magnification, composite optical micrograph showing the juncture between the top side fillet and SA1358-10 connector housing (location F2). *(con’t)*

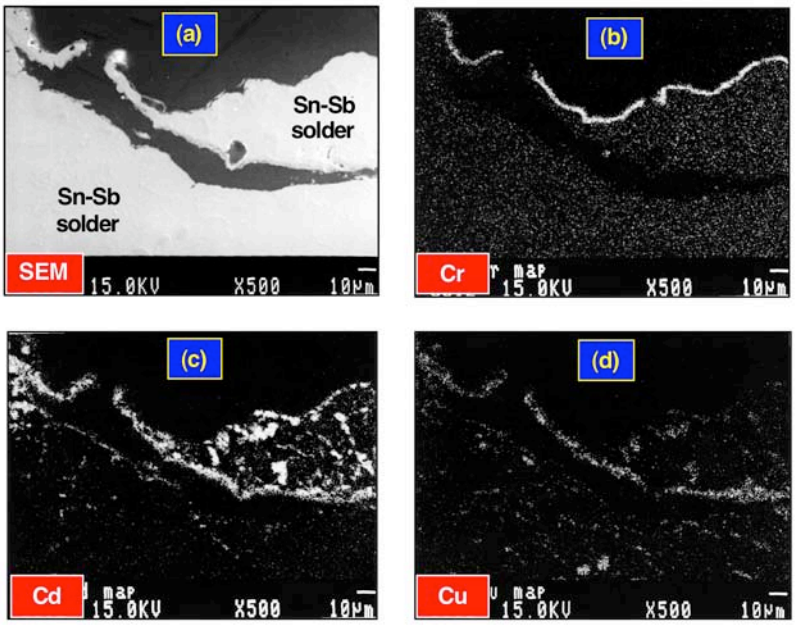

(b)

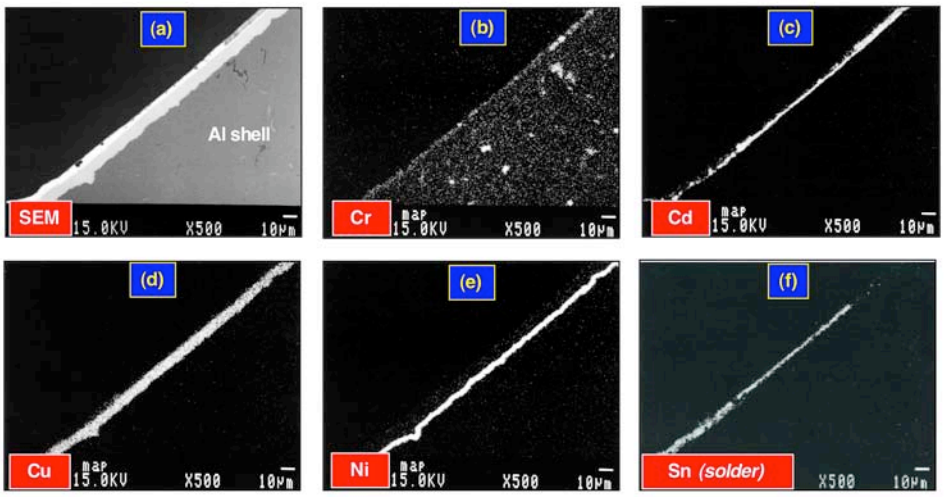

(c)

Fig. 37 ((b) SEM (SE) and EPMA x-ray dot maps of the top side fillet region at location "A" *but reversed about a vertical plane*: (a) SEM/SE image; (b) Cr map; (c) Cd map; (d) Cu map. (c) SEM (SE) and EPMA x-ray dot maps of the top side fillet region at location "B": (a) SEM/SE image; (b) Cr map; (c) Cd map; (d) Cu map; (e) Ni map; and (f) Sn (solder) map.

The location “B” was along the connector shell (Fig. 37c). The molten solder migrated up the connector shell by dissolving away the Cd layer that it had breached in the fillet region. This analysis, along with the optical micrographs shown in Fig. 36, confirmed that the Sn-Sb solder had remelted following the application of the Cr-Cd-Ni-Cu over plated layer.

The spring finger solder joint on the diametrically opposing side of the connector was also examined in the F2 cross section. This microstructure at this location is shown in Fig. 38.

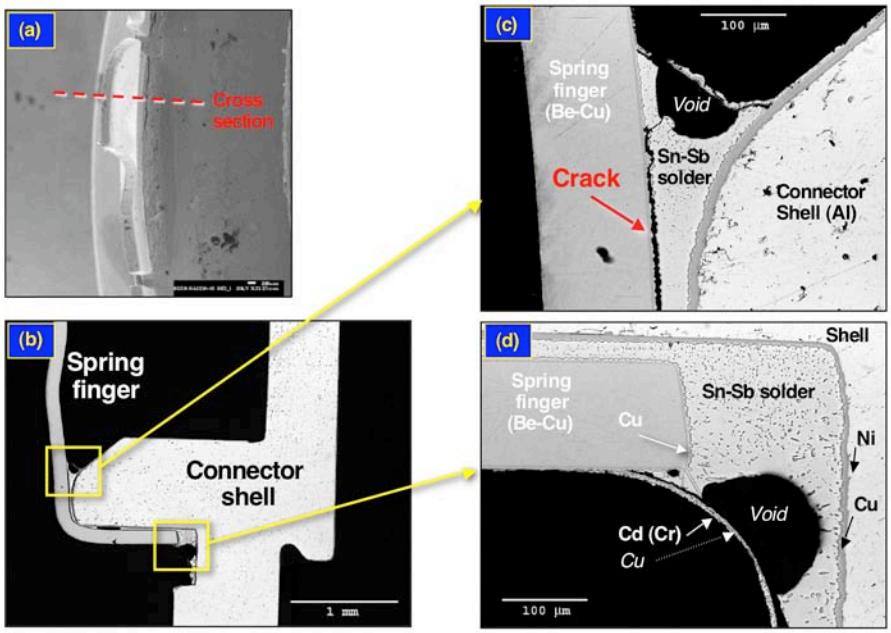

Fig. 38 SEM and optical micrographs showing the juncture between the top side fillet and SA1358-10 connector housing at the *diametrically opposite location* of the F2 as was shown in Fig. 37: (a) SEM photograph showing the location of the cross section through the spring finger solder joints; (b) low magnification optical micrograph of the solder joint cross section, showing the top and bottom fillet locations that were examined at higher magnification in micrographs (c) and (d), respectively.

The optical micrographs in Figs. 38(c) and 38(d) clearly showed the suspension of the electroplated layers over voids in the solder joints, indicating that the latter had remelted after the application of that coating. Therefore, the opening in the top side solder joint fillet observed in the SEM photograph in Fig. 38(a) was, in fact, over a void created in the

solder. In Fig. 38(c), the solder joint had cracked at the Sn-Sb/spring finger interface (after the remelting event). Specifically, the fracture occurred at the solder/IMC layer interface or within the IMC layer, itself, indicating that its source was a subsequent mechanical load applied to the spring finger. Areas of missing Cd plating were the result of the materials ready dissolution into the molten Sn-Sb solder.

The last cross section of this connector, which was designated F5, exhibited features very similar to those depicted in Figs. 37 and 38. That is, there was clear evidence that the Sn-Sb solder had remelted after the final electroplated coatings had been applied to the assembled connector.

In summary, the old style SA1358-10 connector, when subjected to the new assembly process, still experienced remelting of the Sn-Sb solder that attached the spring fingers to the connector shell. Flaws that were observed on the top fillet surface by stereomicroscopic inspection or SEM, were the result of separation and cracking of the Cd (Cr) plating layer due to void formation underneath it when the solder had remelted. Also, there was cracking of the top fillet solder joints; the location of those cracks were at the solder/IMC layer interface of the spring finger. The source of those cracks was a mechanical load placed on the spring finger that occurred after the remelting event. Lastly, the pin contact solder joints exhibited excellent quality; there were no indications of damage to the solder joints. The pins were brass with Cu and Ni barrier layers followed with the Au protective finish.

SA2052-4, DC 1986-34, from MC3617 S/N X706 (PPI)

Three locations were examined about the circumference of the SA2052-4 connector (Item #2), which were designated F2, F3, and F5. Both the spring fingers and the connector shell had only a Cu electroplated layer on them prior to assembly (Table 1). An over plating coating was applied after the Sn-Sb solder process was completed; that coating was composed of a Ni flash layer, followed by the Cd coating, and lastly, the chromate conversion layer. Shown in Fig. 39 are SEM (SE) photographs of the top side fillet at location F2. A crack was observed at the edge of the fillet on the spring finger.

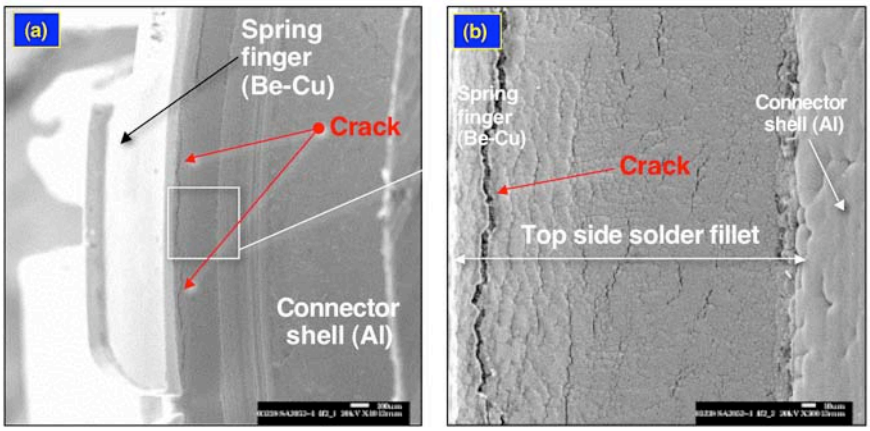

Fig. 39 (a) Low magnification SEM (SE) photograph showing the top side fillet surface of location F2 on SA2052-4. (b) High magnification SEM photograph of the top side fillet surface, showing a crack where the solder fillet joined the spring finger.

Other than the aforementioned crack, the plating exhibited excellent integrity. There was no damage recorded to the spring finger structure.

Metallographic cross section views of the F2 location on the SA2052-4 were provided Fig. 40. The SEM photograph in (a) showed the location of the cross section. Provided in the optical micrograph (b) are the locations of the top side and bottom side views in (c) and (d). The top side and bottom side fillets exhibited excellent integrity. There were no indications of mechanical damage to the solder joints. More importantly, the joint did not exhibit any signs of the Sn-Sb having been remelted after final assembly. It was noted that, when comparing Fig. 39 (b) and Fig. 40 (c), the crack in the former SEM image did not appear in the latter cross section micrograph. This difference indicated that the crack in Fig. 39 (b) was limited to the Ni-Cd (Cr) overplating layer or a minor delamination of the Ni-Cd (Cr) protective finish from the because the crack did not extend into the solder fillet. The fact that the delamination occurred near the spring finger suggested that it was likely caused by flexing of the spring finger during connector mating/unmating activities.

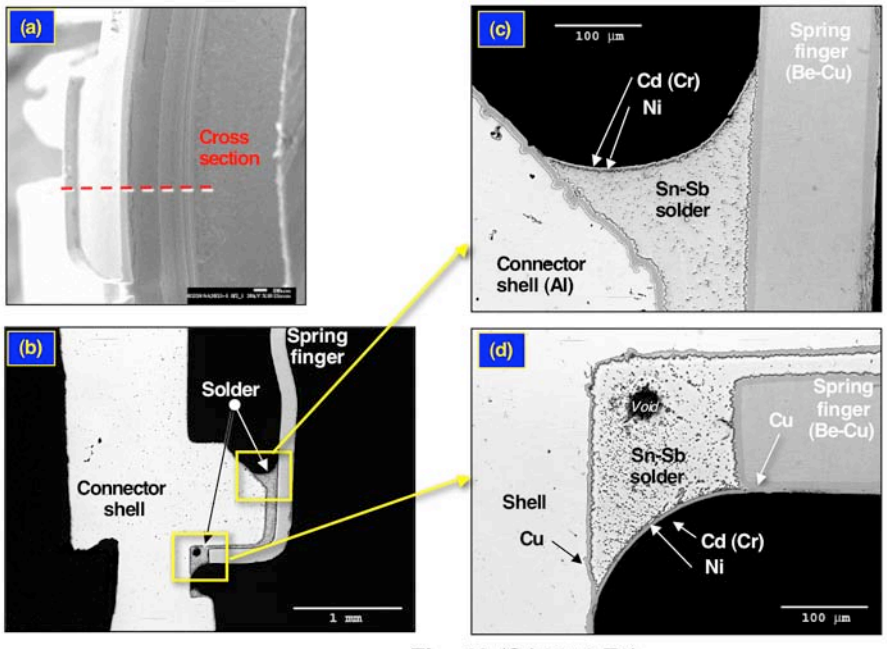

Fig. 40 (a) SEM photograph showing the top side fillet surface of section F2 on SA2052-4 showing the location of the cross section. (b) Optical micrograph showing the spring finger solder joint. (c) High magnification optical micrograph showing the top side fillet. (d) High magnification optical micrograph showing the bottom side fillet.

Shown in Fig. 41 are SEM (SE) photographs of the top side fillet at location F3 on the SA2052-4 connector. The high magnification view in Fig. 41 (b) shows two cracks on either edge of the fillet surface; no other damage was observed. Cross section, optical micrographs were taken of the F3 location on the SA2052-4 connector. Those images were provided in Fig. 42. Overall, the joint exhibited good integrity. The optical micrograph in Fig. 42 (c) showed the top side fillet. The two cracks that were visible in Fig. 41 (b) were observed in Fig. 42 (c). The cracks broke the Ni-Cd (Cr) overplating layer and progressed a short distance into the Sn-Sb solder. No cracks were observed in the bottom side solder fillet in Fig. 42 (d). The cracks in the top side fillet clearly would not have jeopardized the functionality of the interconnection.

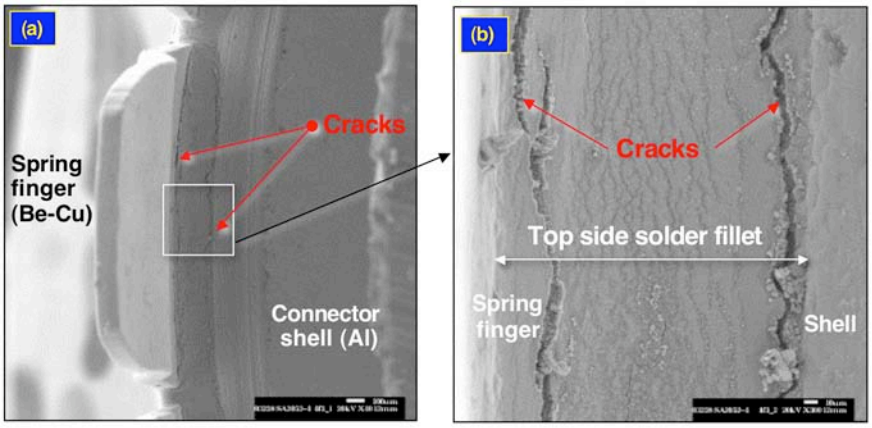

Fig. 41 (a) Low magnification SEM (SE) photograph showing the top side fillet surface of location F3 on SA2052-4. (b) High magnification SEM photograph of the top side fillet surface, showing two cracks where the solder fillet joined the spring finger and connector shell.

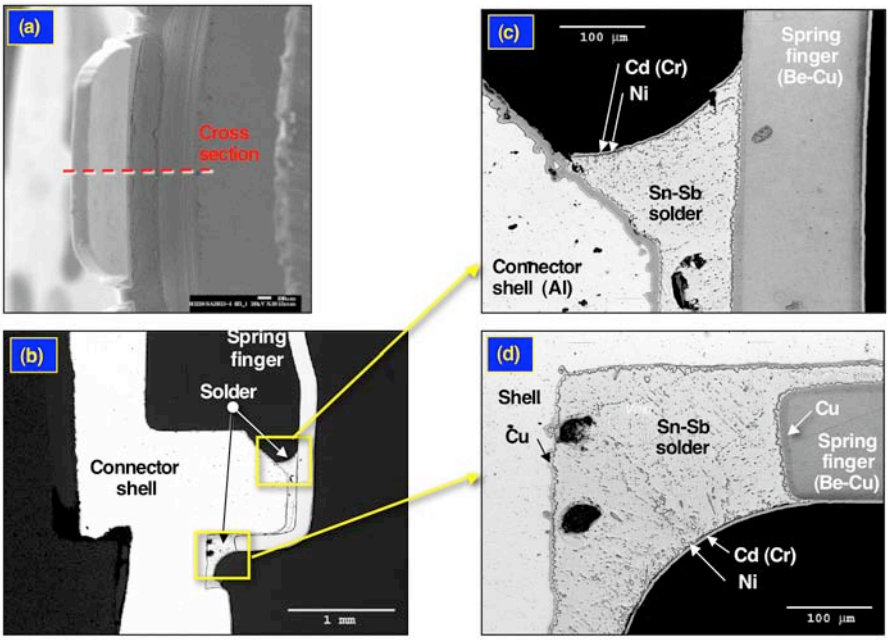

Fig. 42 (a) SEM photograph showing the top side fillet surface of section F3 on SA2052-4 showing the location of the cross section. (b) Optical micrograph showing the spring finger solder joint. (c) High magnification optical micrograph showing the top side fillet. (d) High magnification optical micrograph showing the bottom side fillet.

Although there was some indication of separation between the Ni-Cd (Cr) plating layer and the Sn-Sb solder surface, there were no signs that the latter had remelted after application of the overplating layer.

The same analysis was performed on the location F5 of the SA2052-4 connector. The corroborating SEM images and cross section optical micrographs were provided in Figs. 43 and 44 below. Two cracks were observed in the top side fillet (Fig. 43 (b)), which were then confirmed to have progressed only a small distance into the Sn-Sb solder (Fig. 44 (c)).

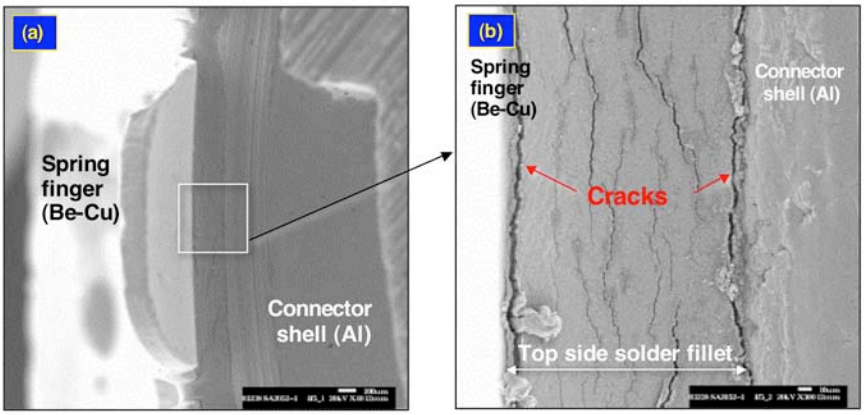

Fig. 43 (a) Low magnification SEM (SE) photograph showing the top side fillet surface of location F5 on SA2052-4. (b) High magnification SEM photograph of the top side fillet surface, showing two cracks where the solder fillet joins the spring finger and connector shell.

The similarity of the microstructures between F3 and F5 would not have warranted significant attention to the latter with the exception of the absence of a bottom side fillet in Fig. 44 (d). Failure of the bottom side fillet to form was caused by an insufficiently large gap between the bottom of the connector shell and spring finger; this situation was illustrated in Fig. 45. Growth of the IMC layer (during the soldering process, while the Sn-Sb alloy was in the molten state) closed the gap further, thereby restricting solder flow to create the bottom side fillet (Fig. 45 (b)). The bottom side fillet did not provide a significant contribution to the strength of the joint and, as such, its lack of development would not impair the reliability of the interconnection.

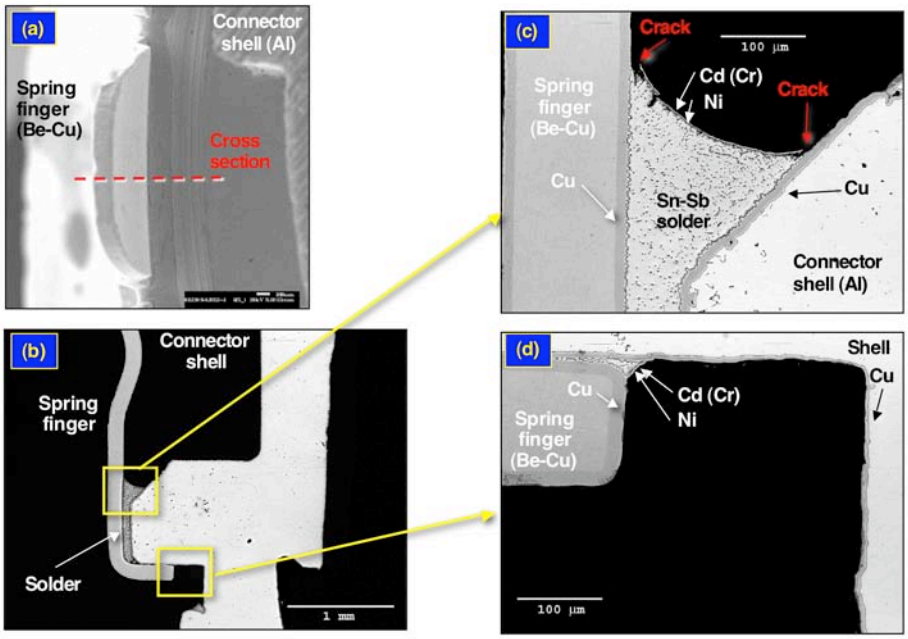

Fig. 44 (a) SEM photograph showing the top side fillet surface of section F5 on SA2052-4 showing the location of the cross section. (b) Optical micrograph showing the spring finger solder joint. (c) High magnification optical micrograph showing the top side fillet. (d) High magnification optical micrograph showing the bottom side fillet.

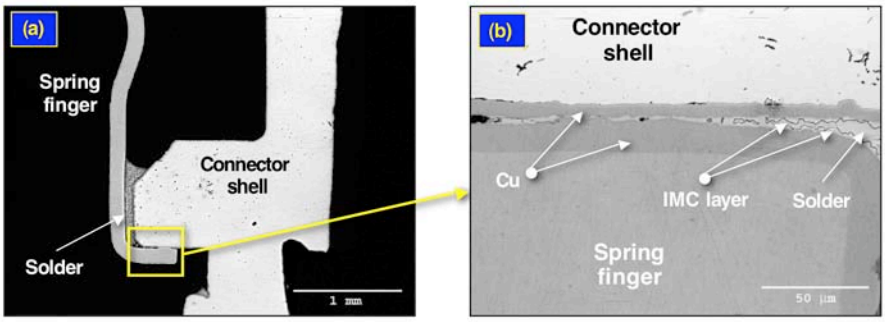

Fig. 45 (a) Optical micrograph showing the location of the gap between the connector shell and the spring finger for section F5 on SA2052-4. (b) High magnification, optical micrograph showing the restricted solder joint gap between the shell and spring finger solder joint.

Lastly, a survey was made of the surfaces of the Ni-Cd (Cr) electroplated layer on the top side fillets at each of the three locations: F2, F3, and F5. High magnification, SEM (SE) images were compiled in Fig. 46. Aside from the larger scale cracks noted in the above discussion, the electroplated layer surface showed surface convolutions (hillococks and valleys) that are common to these types layers when observed at relatively high magnifications. The layer morphology did not indicate a potential for degradation in either the short- or long-term lifetime of the interconnection.

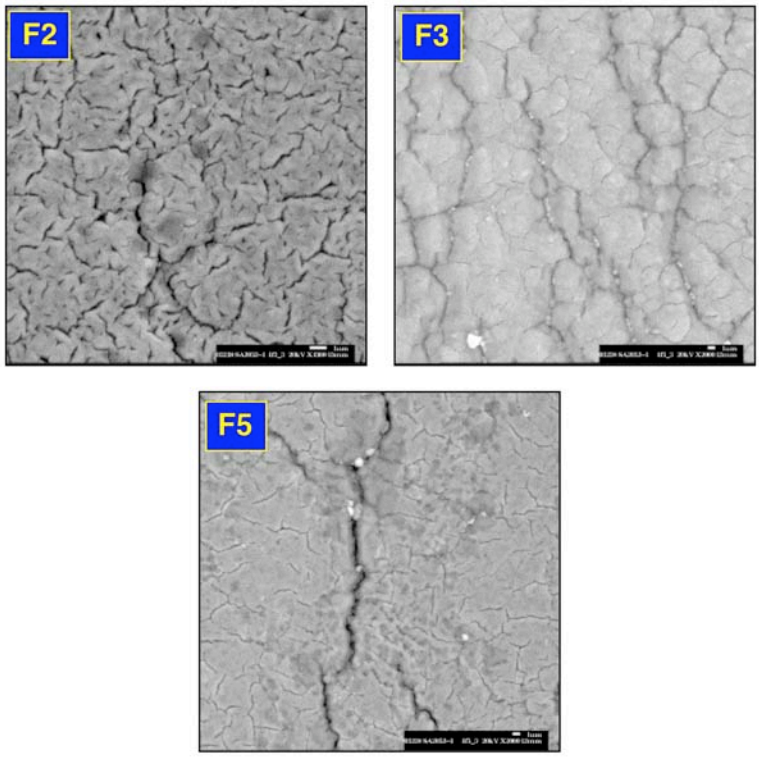

Fig. 46 High magnification, SEM (SE) photographs of the surface of the Ni-Cd (Cr) overplate layer at the three locations, F2, F3, and F5 on the top side fillet of the SA2052-4.

In summary, the old style SA2052-4 connector, when subjected to the new assembly process, exhibited spring finger solder joints having excellent integrity. Minor cracks were observed on the top side fillet that breached the Ni-Cd (Cr) overplate layer and progressed only a short distance into the underlying Sn-Sb solder. Small occurrences were observed in which the overplated layer had separated from the solder surface. The overplating layer exhibited no indications for delamination from the spring finger or connector housing away from the solder joint. Also, there were no indications that the Sn-Sb solder had remelted

as a result of solder process performed after the joint had been completed. Thus, the old style connectors appear to be compatible with the new soldering process without remelting the Sn-Sb solder joint between the spring finger and the shell.

Finally, the cross sections did not include any of the pin contact solder joints. Therefore, their integrity was not assessed for this SA2052-4 unit.

3.3 Item #4: NEW CONNECTORS, NO PROCESS (BASELINE)

SA1358-10, DC 2002-26

In order to assess the performance of a new design of the SA1358-10 connector, it was necessary to examine the connector structure prior to the soldering operation used to attach the cable or EMR structures to the connector. Therefore, an analysis was performed on an SA1358-10 unit in this condition.

Listed in Table 1 are the electroplated layers used on this connector. The spring finger had an electroplated Cu layer to assist solderability. The connector shell (Al alloy) had an *electroless* Ni (P) layer deposited on the Al surface, followed with a Cu electroplated layer for solderability. The OLD SA1358-10 connectors used an electroplated Ni layer whenever, in fact, a Ni layer was present. The overplating layer (post-spring finger soldering process) was Cu, followed by Cd, and then lastly, the chromate conversion (Cr) layer. The solder used to attach the spring fingers to the connector shell was the Sn-Sb alloy.

First, the top side fillets were examined on the SA1358-10 unit, using SEM (SE) imaging. Five views were provided of the top side fillets; those images were provided in Figs. 47 – 50. The SEM photographs illustrated the morphologies of the top side fillet surfaces. Those morphologies were of the Cu, Cd, and chromate (Cr) overplating layers that were deposited after the soldering process. Thus, even on the same connector, the plating layer surface appearance varied considerably between the different locations. A few small “fissure” were observed in the electroplated layer (Figs. 47, 48, and 50). These fissures represented gaps between the nodules as the latter plated up. Cracks were observed on the top side fillets, primarily at the junction between the fillet and the spring finger, which likely resulted from flexing of the spring finger during connector mating/unmating cycles. In Fig. 49, it was apparent that the throwing power of the plating process was locally altered near to the connector shell, resulting in an enlargement of the plating microstructure. No

cracks or other damage was observed in this region. Other than these observations, there did not appear to be any degradation to the connector structures.

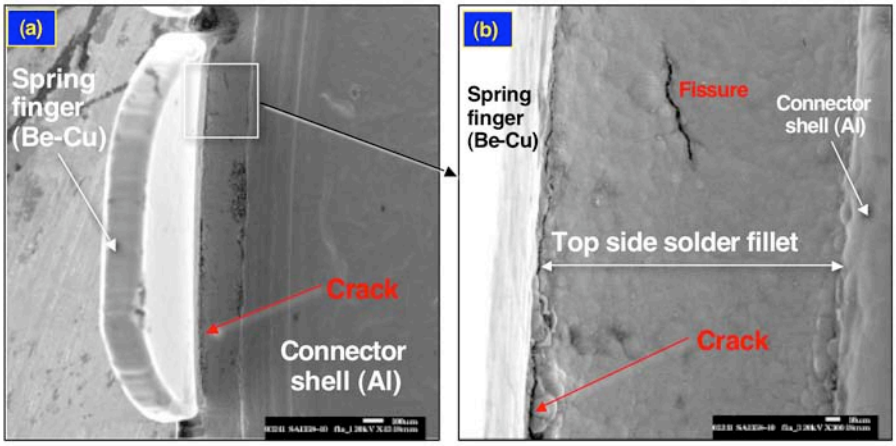

Fig. 47 (a) Low magnification SEM (SE) photograph showing the top side fillet surface of location F1a on the SA1358-10 (item #4). (b) High magnification SEM photograph of the top side fillet surface, showing a crack where the solder fillet joins the spring finger and small fissure in the electroplated layer.

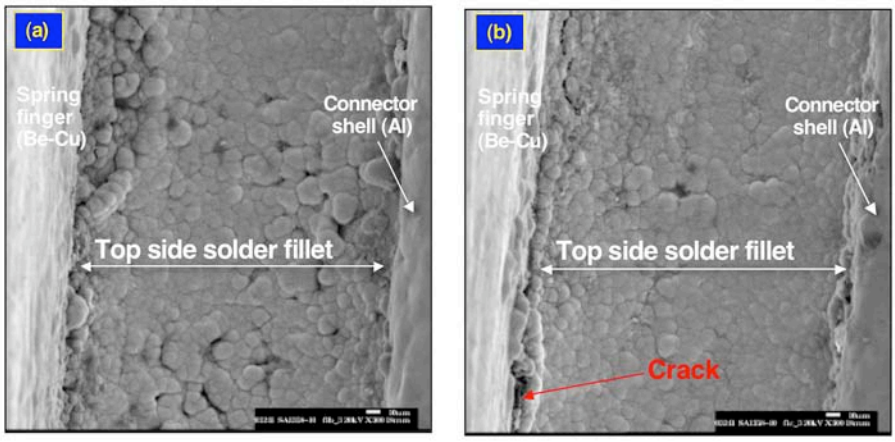

Fig. 48 (a) (b) High magnification SEM photograph of the top side fillet surface at locations F1b and F1c, respectively, on the SA1358-10 connector. A small crack appeared at F1c where the solder fillet joins the spring finger. Numerous, small fissure were observed in the electroplated layer.

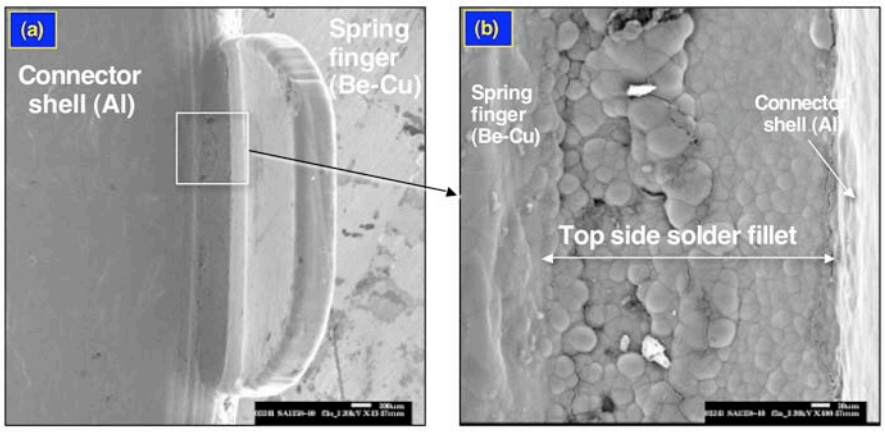

Fig. 49 (a) Low magnification SEM (SE) photograph showing the top side fillet surface of location F3a on the SA1358-10. (b) High magnification SEM photograph of the top side fillet surface, showing a change to the morphology of the overplating layer caused by an alteration of the local throwing power of the plating process.

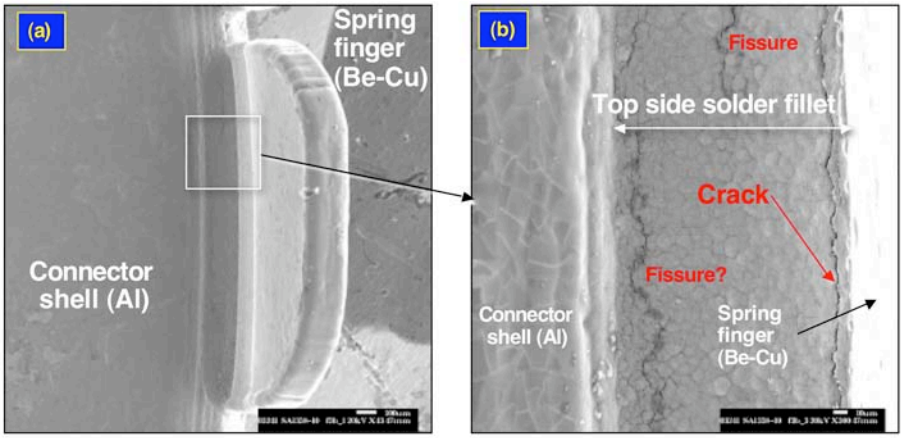

Fig. 50 (a) Low magnification SEM (SE) photograph showing the top side fillet surface of location F3b on the SA1358-10. (b) High magnification SEM photograph of the top side fillet surface showing a crack where the fillet met the spring finger. Fissures were observed in the electroplated coating. One such fissure may have been a crack where the top side fillet joined to the connector shell. It was difficult to decipher the source of the opening.

At location F3b (Fig. 50), the electroplated layer surface morphology was more homogeneous. A small crack was observed at the spring finger side of the fillet. A small fissure was observed in the fillet near the connector shell. Although the morphology suggested that it was a fissure, its consistent position parallel to the shell surface indicates that it may have been a crack. Metallographic cross sections were used to determine its likely source as explained below. Lastly, the SEM survey of the spring finger and associated solder joint did not reveal any unusual features or signs of damage.

Next, metallographic cross sections were made of the solder joints at the selected locations F, the two sites on cross section F2, and F3. Shown in Fig. 51 (a) is the SEM (SE) image of the F1a location. Cross section micrographs show an overall view the spring finger solder joint (b), the horizontal gap region (c), and bottom side fillet (d). The cross section view in (b) showed no damage to the solder joint or substrate structures. The micrograph in (c) showed an excellent solder joint; no cracks were observed. The Cu_6Sn_5 IMC layer thickness was 1.96±0.63 μm on the spring finger side (electroplated Cu) and 2.02±0.46 μm on the connector shell side as measured at the F1 location. These values are similar to those measured on prior units and are indicative of a soldering process that requires a long-than-normal contact between the molten solder and the base material; in this application, the base material is the Cu electroplated layers. Therefore, it appeared that, although next-assembly processes may have reflowed the Sn-Sb solder on the SA1358-10 connectors, that added melting event did not cause a drastic change to the IMC layer thicknesses in the gap. The micrograph in (d) indicated that there was good flow of the Sn-Sb solder during the assembly. The overplating layer – Cu, Cd (Cr) – had excellent adhesion to the solder fillet surface.

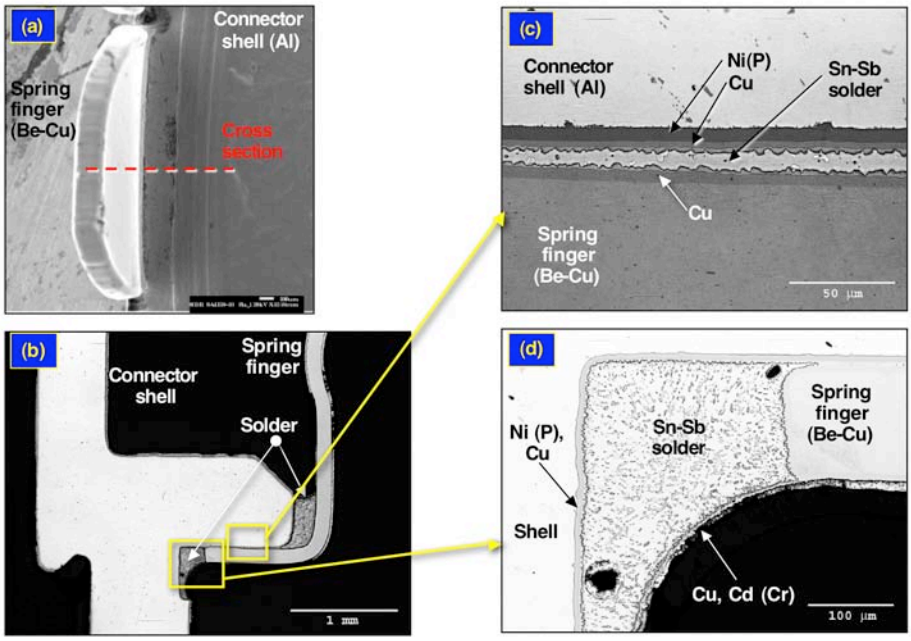

Fig. 51 (a) Low magnification SEM (SE) photograph showing the top side fillet surface of location F1a on the SA1358-10. (b) Low magnification optical micrograph of the spring finger solder joint (F1a). (c) High magnification optical micrograph of the horizontal gap region between the spring finger and the connector shell. (d) High magnification optical micrograph of the bottom side fillet.

The SEM (SE) and optical micrographs in Fig. 52 were used to examine the top side fillet of the F1a location. The location of the section has been shown in (a) and (b). The cross section views in (c) and (d) exemplify the excellent integrity of the solder joint and good adhesion of the overplating layer on the solder, respectively. The adhesion of the Cu, Cd (Cr) layer to the solder is an important factor because in units exposed to subsequent soldering processes, flaking and spalling have been observed with the overplating layer. The small crack in the layer in (d) likely arose from flexure of the spring finger.

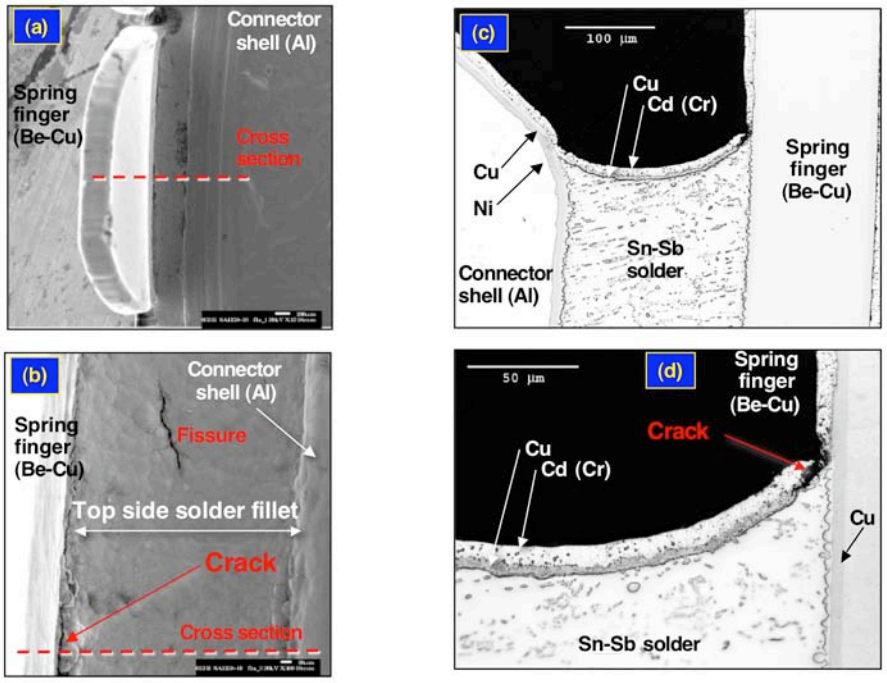

Fig. 52 (a) Low magnification SEM (SE) photograph showing the top side fillet surface of location F1a on the SA1358-10. (b) High magnification SEM (SE) photograph of the top side solder fillet surface. (c) High magnification optical micrograph of the top side fillet. (d) High magnification optical micrograph of the top side fillet showing the integrity of the bond between the overplating layer [Cu, Cd (Cr)] and Sn-Sb solder.

The top side solder fillets were documented for the two diametrically opposed solder joints made available in section F2c. Those micrographs are shown in Fig. 53. Similar observations pertained to these locations as were those made with reference to Fig. 52. Moreover, in general, observation similar to those documented for Fig. 51 that described the horizontal gap and bottom side fillets, were also applicable to the F2 and F3 cross sections.

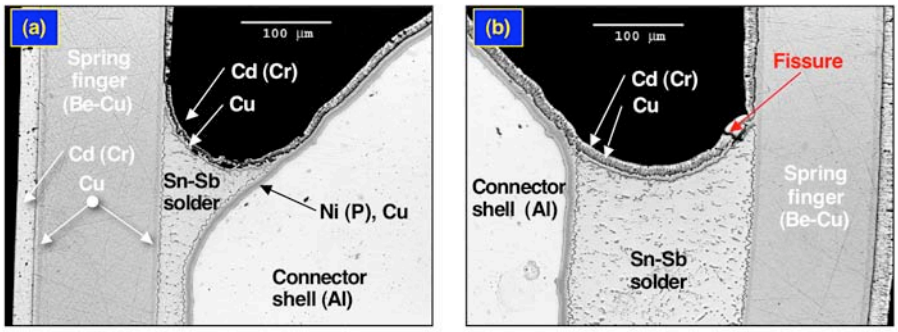

Fig. 53 (a) and (b) High magnification optical micrograph of the top side fillets at the two diametrically opposed locations for cross section F2.

Lastly, the electroplated finishes were examined on the connector shell and spring finger structures. High magnification optical micrographs were provided in Fig. 54 that show the layer stack up for the two parts. It was observed that voids had formed between the Cu and Cd (Cr) layer in the overplating finish. (In the case of (a), it was difficult to distinguish between the Cu finish applied to the spring finger and the Cu layer that was part of the overplating finish.) The voids did not appear to be of an extent that would jeopardize the integrity of the overplating. All finishes exhibited excellent adhesion to the aluminum and Be-Cu substrates.

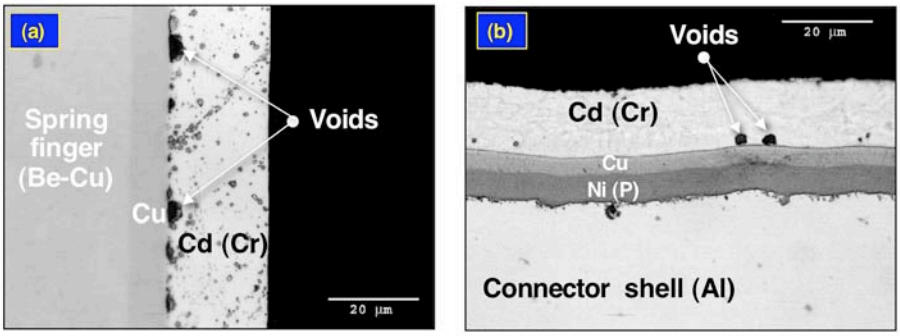

Fig. 54 (a) and (b) High magnification optical micrographs showing the electroplated layers on the spring finger and connector shell, respectively, at location F1a on the baseline SA1358-10 connector. Voids were observed between the Cd (Cr) layer and the Cu layer that was applied as part of the overplating finish.

In summary, the spring finger solder joints exhibited excellent integrity on the new design, SA1358-10 connector. There were no indications of damage to the solder, the interfaces, or to the shell and spring finger structures. All of the electroplated finishes, including the Ni (P), Cu applied to the shell; the Cu layer applied to the spring finger; and the overplating layer of Cu and Cd (Cr) exhibited excellent adhesion to the respective surfaces.

SA2052-4, DC 2001-52

The SA2052-4 DC2001-52 connector represented the new, baseline condition without the EMR assemblies or cable having been soldered into place. Electron probe microanalysis confirmed that the electroplated layers on the connector shell and spring finger were the same as those on the baseline SA1358-10 unit (Table 1). Shown in Fig. 55 are three SEM photographs of the connector. The photograph in Fig. 55 (a) provided a low magnification view of the top side solder fillet at the cross section location F1a.

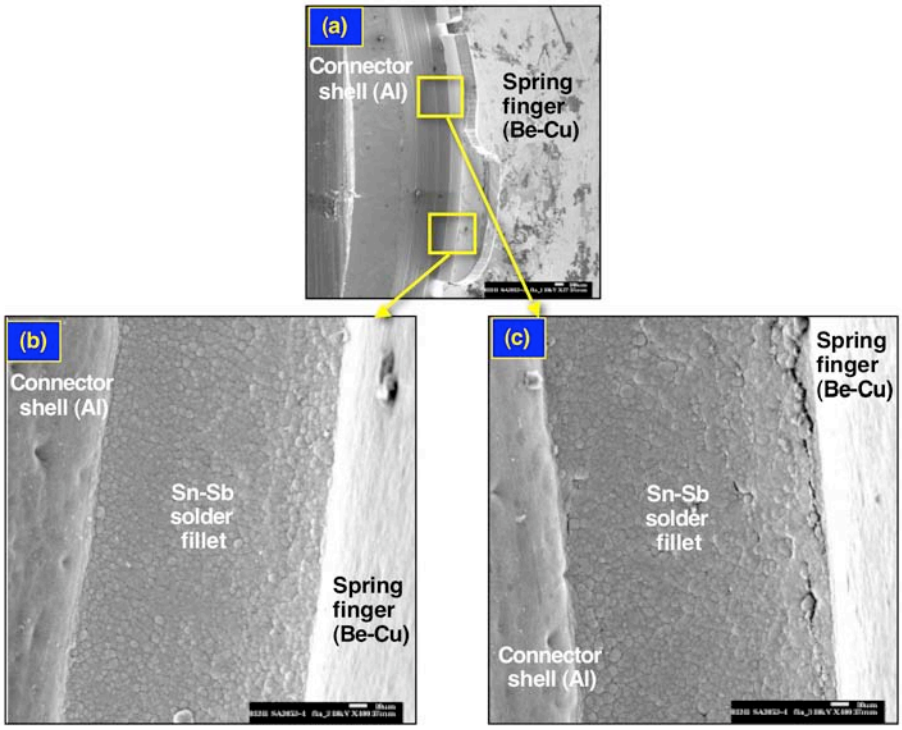

Fig. 55 (a) Low magnification SEM (SE) photograph showing the top side fillet surface of location F1a on the SA2052-4 baseline connector (no EMR shell or cable attachments were performed). (b) and (c) High magnification SEM (SE) images at two locations on the top side fillet.

Higher magnification SEM images, which were provided in Fig. 55 (b) and (c), showed the surface of the solder fillet at two locations. Recall that the electroplated finish was composed of the Cu, Cd (Cr) layers. There were no indications of significant crack formation in the fillet nor spalling of the electroplated coating. Some small fissures were observed on the coating surface; however, the cross section image provided in Fig. 56 (b) confirmed that they were only fissures in the Cu, Cd (Cr) layer and not cracks that reached into the solder joint.

The Cu_6Sn_5 IMC layer thickness was measured in the horizontal gap between the connector shell and the spring finger [see Fig. 56 (d)]. The IMC thickness on the spring finger side (electroplated Cu layer) was 1.84±0.63 μm. On the connector shell (electroplated Cu layer), the IMC layer thickness was 1.82±0.69 μm. These values were very similar to those cited above for the SA2058, as well as for the newly designed, SA1358-10 connector.

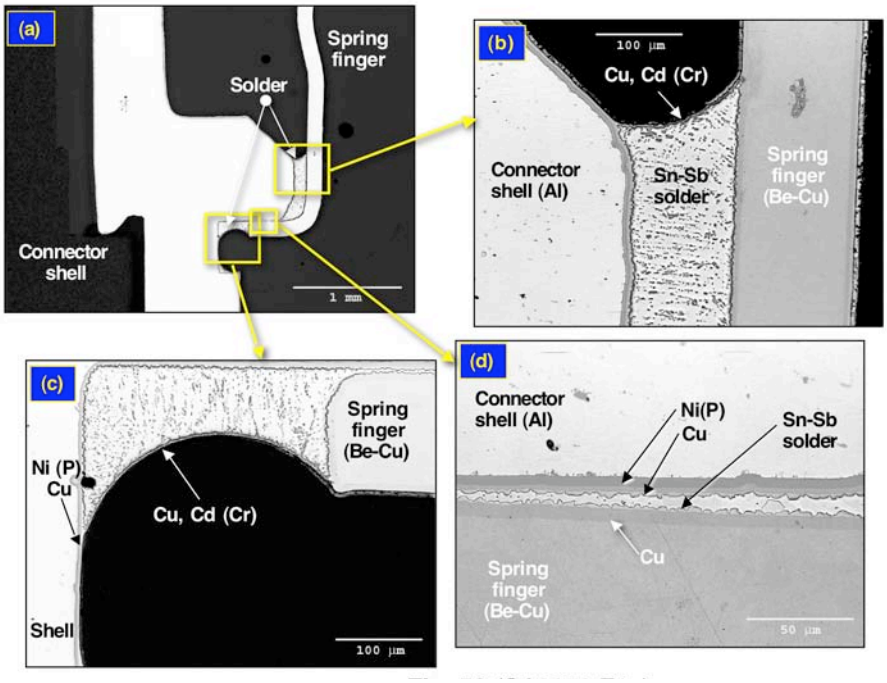

Fig. 56 (a) Low magnification optical micrograph of the spring finger solder joint at location F1a on the SA2052-4 baseline connector. (b) High magnification optical micrograph of the top side solder fillet. (c) High magnification optical micrograph of the bottom side fillet. (d) High magnification optical micrograph of the solder joint horizontal gap between the shell and spring finger.

The optical micrographs showed no indications of significant damage to the solder. Solderability was excellent for all surfaces; void formation was almost non-existent. Similar evaluations were made of the other three cross sections made to this connector and the same observations were documented.

Shown in Fig. 57 are the SEM images and optical micrographs showing cross sections of the top side fillets at two other locations (F2a and F3b) in the spring finger solder joint. The integrity of the solder joints was sound with no indications of defects.

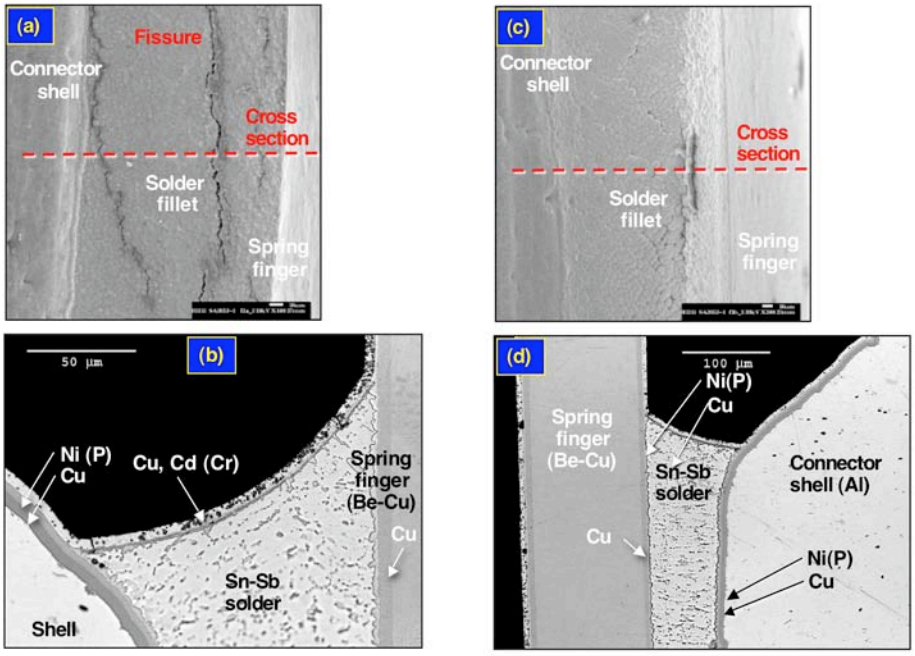

Fig. 57 (a) Low magnification SEM (SE) photograph of the top side fillet at location F2a on the SA2052-4 baseline connector. (b) High magnification optical micrograph of the top side solder fillet. (c) Low magnification SEM (SE) photograph of the top side fillet at location F3b on the SA2052-4 baseline connector. (d) High magnification optical micrograph of the top side solder fillet.

Lastly, the electroplated layers were documented for flaws on the connector shell and spring finger. No such defects were observed. Shown in Fig. 58 are representative optical micrographs of those layers on the two respective structures. Unlike the SA1358-10 baseline unit (Fig. 54), there were no voids observed between the Cu and Cd layers.

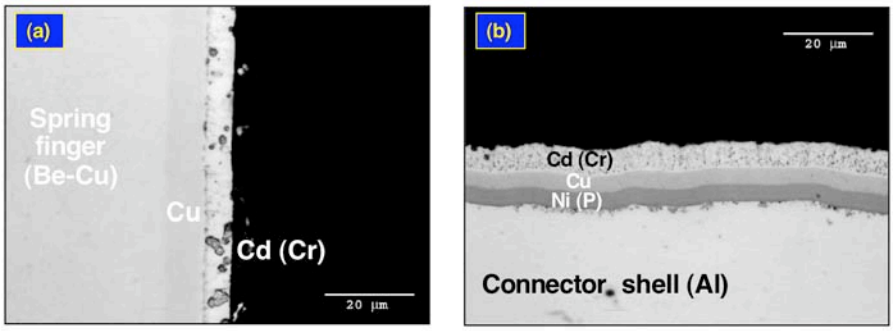

Fig. 58 (a) and (b) High magnification optical micrographs showing the electroplated layers on the spring finger and connector shell, respectively, at location F1a of the SA2052-4 connector.

In summary, the spring finger solder joints exhibited excellent integrity on the new design, SA2052-4 connector. There were no indications of damage to the solder, the interfaces, or to the shell and spring finger structures. All of the electroplated finishes, including the Ni (P), Cu applied to the shell; the Cu layer applied to the spring finger; and the overplating layer of Cu and Cd (Cr) exhibited excellent adhesion to the respective surfaces.

3.4 Item #3: NEW CONNECTORS, NEW (RECENT) PROCESS

SA1358-10, DC 2001-03 from MC3617 S/N 5326

The SA1358-10 connector, having the new connector design, was assembled using the recent cable attachment process, including soldering of the EMR-related structures. The electroplated layers used on the connector shell and spring fingers as well as overplating finishes were the same as those of Item #4, as shown in Table 1. Shown in Fig. 59 are stereo photographs of the connector; that in (a) shows the shell and cable. The image in Fig. 59 (b) shows the two regions of the spring finger solder joint at the male end that were targeted for further analysis. The higher magnification images in (c) and (d) clearly show the presence of voids in the top side fillet of the solder joint at locations designated F1 and F2, respectively.

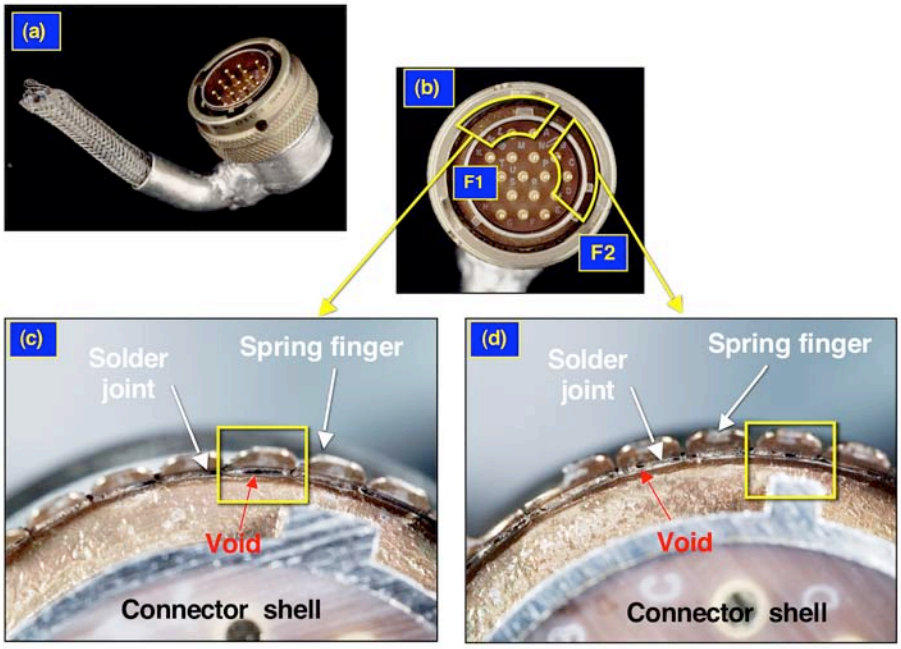

Fig. 59 (a) and (b) Low magnification stereo photographs of the entire connector-plus-cable assembly and male end of the Item #3, SA1358-10 connector, respectively. The stereo images in (c) and (d) clearly show the presence of voids in the top side fillet of the solder joint at locations F1 and F2, respectively.

The extent of the degradation to the top side fillets was further documented via the SEM technique. Shown in Fig. 60 are SEM photographs of the spring finger solder joint at the F1 location, specifically F1c, which were useful to establish the depth of the void. The exact location, with reference to Fig. 59 (c), is indicated by the yellow box.

The SEM analysis was also preformed on the spring finger joint at location F2 (F2c). Those images appear in Fig. 61. The yellow box in Fig. 59 (d) locates the position of the SEM images. The presence of voids was confirmed in the SEM images, as was cracking in the top side fillet surface. The extent of the degradation was further illustrated by the SEM images in Fig. 62. The degradation was far more extensive than would have occurred simply due to flexure of the spring fingers.

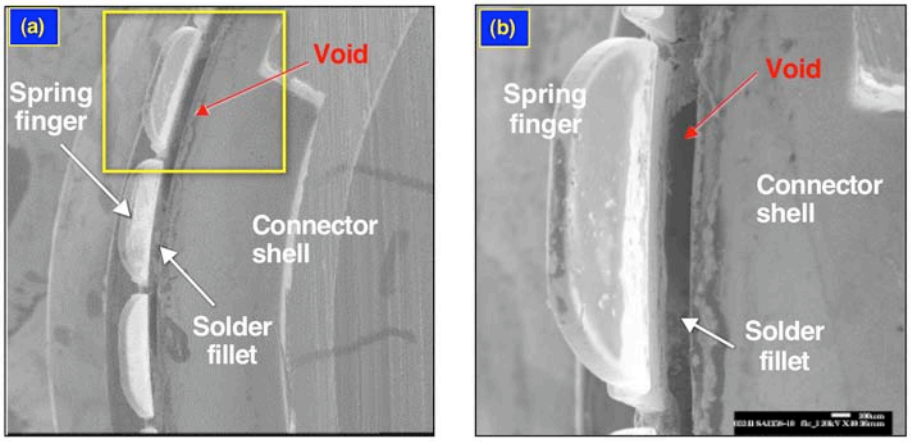

Fig. 60 (a) Low magnification and (b) high magnification SEM photographs showing the void in the top side fillet of the Item #3, SA1358-10 connector at F1c. The exact location can be referenced to the yellow box in Fig. 59 (c).

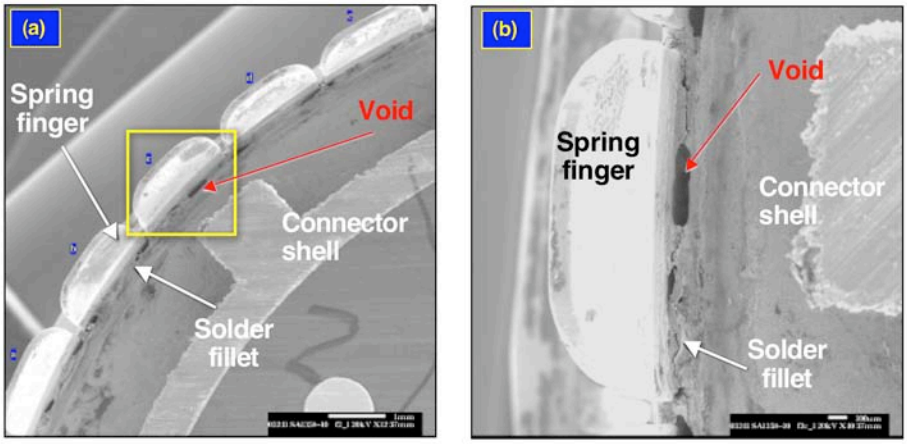

Fig. 61 (a) Low magnification and (b) high magnification SEM photographs showing the void and other degradation to the top side fillet of the Item #3, SA1358-10 connector at F2c. The exact location can be referenced to the yellow box in Fig. 59 (d).

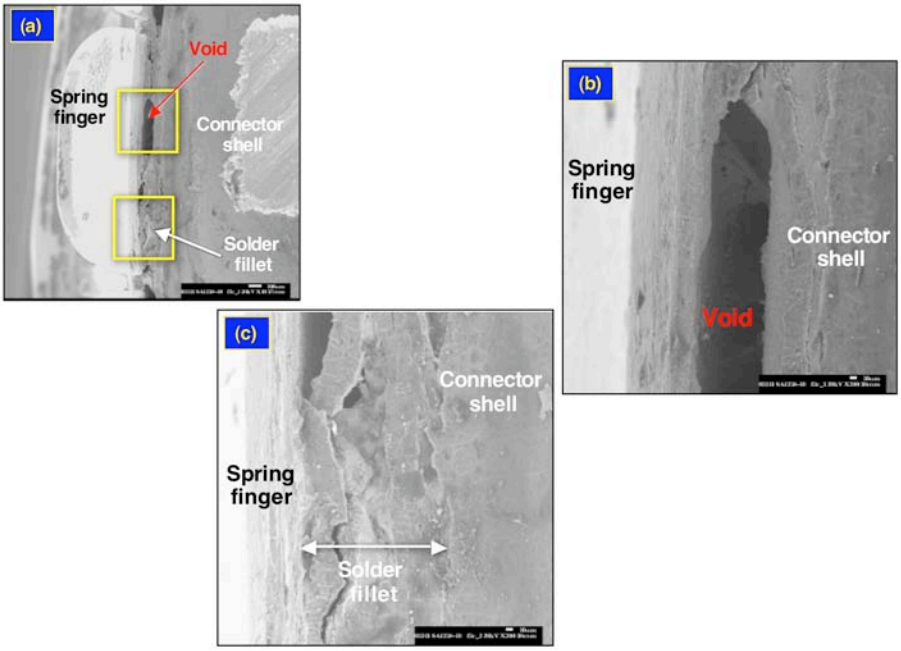

Fig. 62 (a) Low magnification SEM photograph of the top side spring finger solder fillet at location F2c on the Item #3, SA1358-10 connector. High magnification, SEM images appear in (b) and (c) that further illustrated the surface damage.

The two SEM photographs in Fig. 63 showed the extent of fillet surface disruption when voids were not expressly present at location F3b. There was spalling of the Cd (Cr) electroplated layer as well as cracks/voids at the edge of the fillet. The discrimination between voids versus cracks will await metallographic cross sections.

Metallographic cross sections were made of the spring finger solder joints. Shown in Fig. 64 is a cross section through the spring finger solder joint of the Item #3, SA1358-10 connector, and at location F1. This is the same location as that depicted by the SEM images in Fig. 60, but below the large void inside the yellow box. Voids were observed in both the top side and bottom side fillets as shown in Figs. 64 (b) and (c), respectively. The morphologies of those voids were indicative of Sn-Sb solder remelting after the application of the final Cd (Cr), Cu electroplated layer finish.

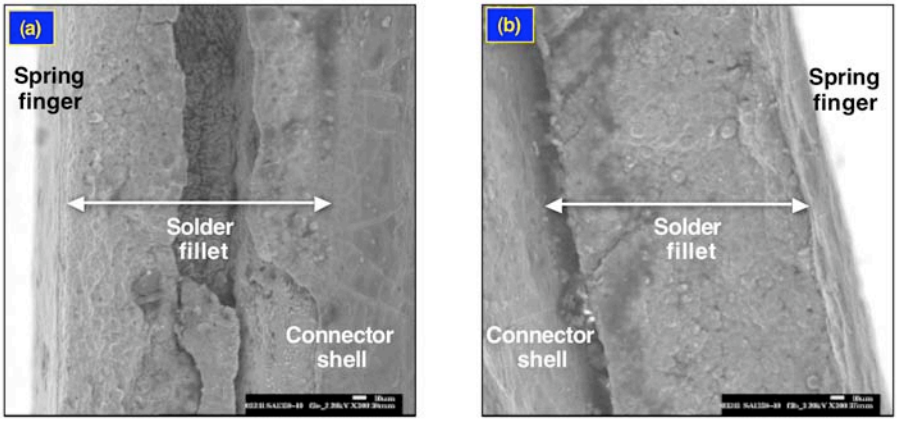

Fig. 63 (a) and (b) SEM photographs at location F2e and F3b, respectively, showing degradation to the top side .

An evaluation of the horizontal gap region, Fig. 64 (d), showed good integrity. The IMC layer thicknesses of the F1 location, as well as those of the F2 and F3 locations, were listed in Table 2. The thickness values were very similar to those observed for other connectors and, in particular, the SA1358-10 unit of Item #4. Recall that the latter connector was not exposed to the EMR process steps. Therefore, it can be surmised that the EMR assembly process did not alter significantly the IMC thickness within the gap, even when remelting of the Sn-Sb solder was clearly in evidence. The insensitivity of the IMC layer to the second exposure to molten solder was likely a result of the confined geometry of the gap and the fact that the solder was already saturated with Cu from the initial assembly process.

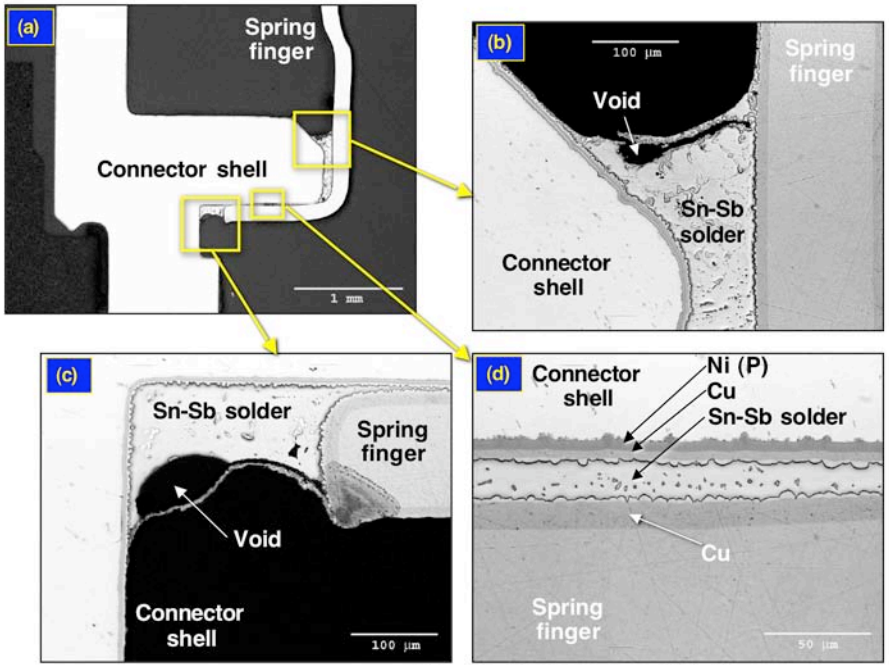

Fig. 64 (a) Low magnification, optical micrograph showing the cross section of the spring finger solder joint at location F1c on the Item #3, SA1358-10 connector. High magnification, optical micrographs of the top side and bottom side fillets appear in (b) and (c), respectively. An optical micrograph of the horizontal gap appears in (d).

Additional evidence was sought that remelting of the Sn-Sb solder had occurred. Shown in Fig. 65 (a) is an SEM (BSE) photograph showing the top side fillet at location F1c. Two locations were targeted for the analysis: the top side fillet that included the void, Fig. 65 (b); and the adjoining surface of the connector shell away from the void, Fig. 65 (c). An EPMA was performed on the two locations, using X-ray dot maps to depict the elemental distributions in those regions. Shown in Fig. 66 are the EPMA results for the top side fillet area presented in 65 (b), that is, the immediate fillet region.

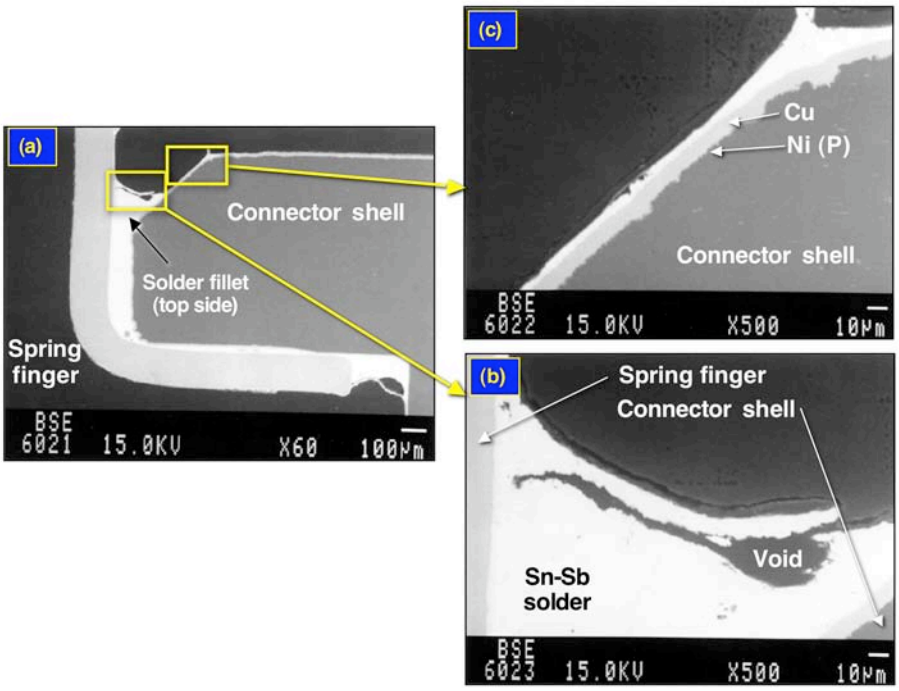

Fig. 65 (a) Low magnification, SEM (BSE) photograph showing the cross section of the spring finger solder joint at location F1c on the Item #3, SA1358-10 connector. (b) High magnification SEM (BSE) photograph showing the top side fillet. (c), High magnification, SEM (BSE) image of the connector shell surface adjoining the top side fillet.

The prevalence of Cd and Cu throughout the solder volume indicated that the solder had remelted and subsequently dissolved these layers into it. The Cr layer was not readily dissolved by the solder; it was sufficiently thick so as to form a “crust” that sat upon the molten solder fillet surface. The void created by the remelting event suggested that there was a loss of solder.

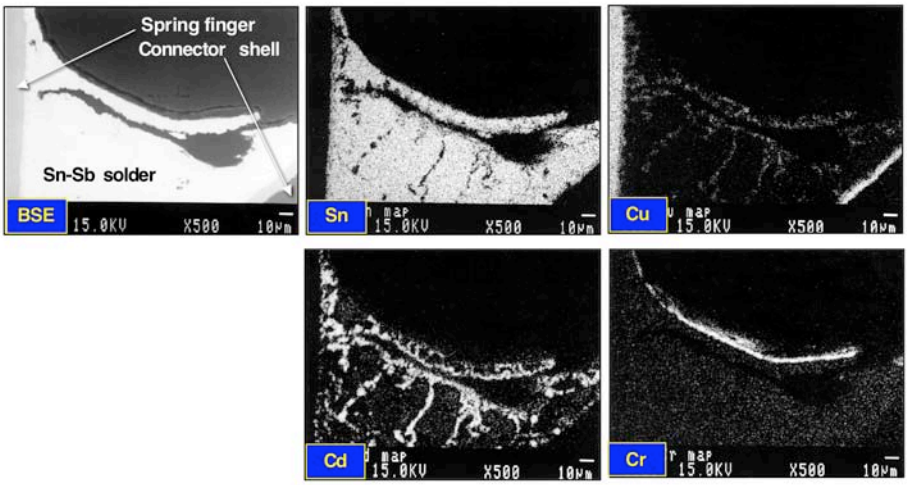

Fig. 66 EPMA of the top side fillet for the spring finger solder joint at location F1c on the Item #3, SA1358-10 connector. The photographs have been labeled with the appropriate imaging mode: BSE, Sn, Cu, Cd, and Cr.

Once the solder had melted, it continued to dissolve away the Cd layer, even up and along the connector shell. This scenario was evidenced in the EPMA analysis of the second region in Fig. 65, now depicted in Fig. 67. The Sn signal was observed all along the surface, having partially dissolved away the Cd coating. The fact that the Cd layer had been partially dissolved away was evidence that the Sn-Sb solder had remelted after the final finish was applied, rather than having been there all along as a result of the initial soldering operation that attached the spring fingers to the shell. The Cr layer remained largely intact, simply resting upon the molten solder film. The Cu electroplated layer on the shell exhibited only minor dissolution that was caused by the molten solder.

The metallographic cross sections revealed the extent of damage to the spring finger solder joints resulting from remelting of the Sn-Sb solder. Shown in Fig. 68 are optical micrographs showing the solder joint at the F2c location of the SA1358-10 connector. This is the same location that was observed by SEM in Fig. 62; those latter images certainly suggested the presence of a large void in the spring finger solder joint.

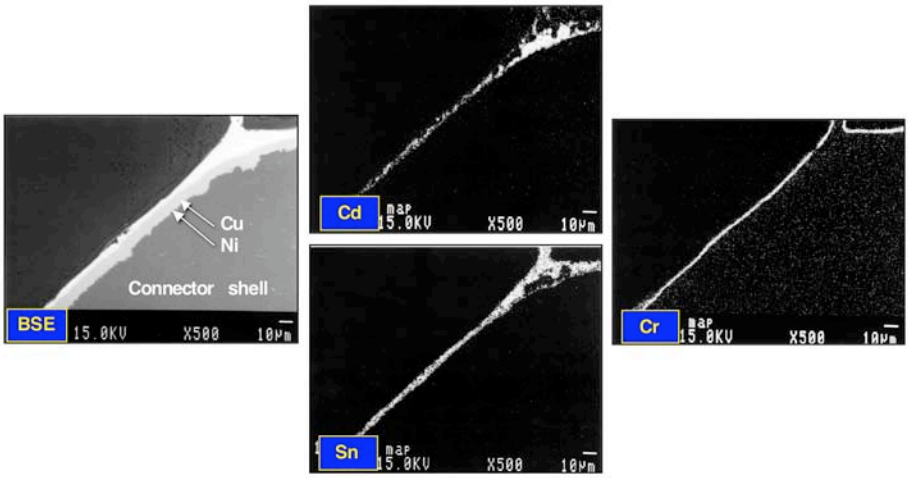

Fig. 67 EPMA of the connector shell surface adjacent to the top side fillet for the spring finger solder joint at location F1c on the Item #3, SA1358-10 connector. The photographs have been labeled with the appropriate imaging mode: BSE, Sn, Cd, and Cr. The Cu layer was unaffected by the solder wetting.

There was a catastrophic loss of solder from the joint at this location; hence, the large void that was observed in Fig. 62. There remained the surface of the top side fillet [Fig. 68 (b)]. A similar microstructure was observed for the bottom side fillet [Fig. 68 (c)]. Solder was absent from the horizontal gap. The observation of the IMC layers on either side of the void [(Fig. 68 (d)] attested to the fact that solder was present, initially.

A similar situation prevailed at location F3a of the SA1358-10 connector. Optical micrographs are shown in Fig. 69, which illustrated the loss of solder from the interconnection. Because of the loss of solder, there was no connecting support between the spring finger and the connector shell. Therefore, upon cross sectioning, the spring finger separated from the shell. This large separation would not have occurred during the connector mating process. It is important to note that location F3b was depicted in Fig. 63 (b) and showed an intact fillet surface. This comparison demonstrates the variation in the extent of solder joint remelting that occurred along the circumference of the spring finger (and hence, the need to examine several locations about the structure).

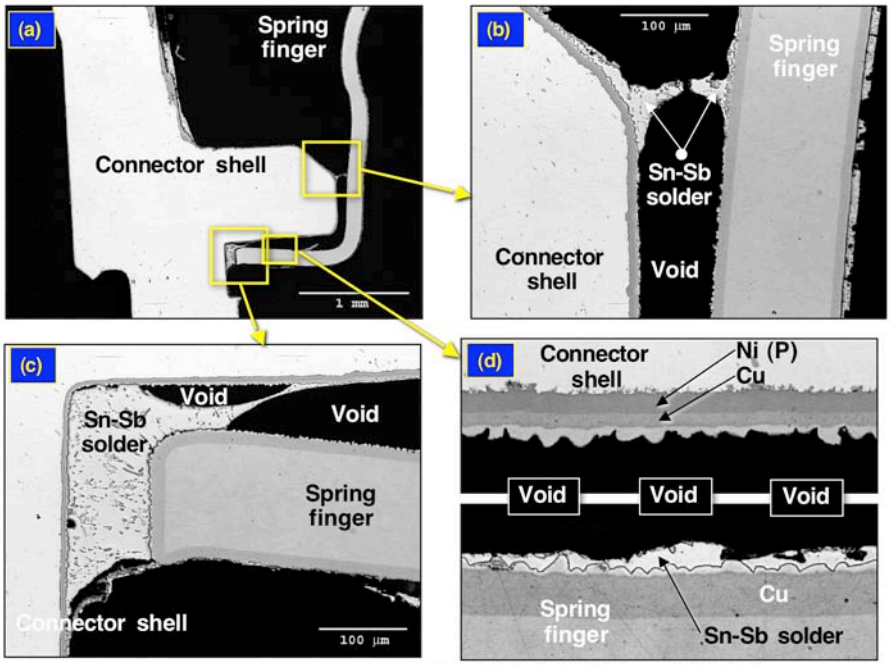

Fig. 68 (a) Low magnification, optical micrograph showing the cross section of the spring finger solder joint at location F2c on the Item #3, SA1358-10 connector. High magnification, optical micrographs of the top side and bottom side fillets appear in (b) and (c), respectively. An optical micrograph of the horizontal gap appears in (d); however, due to the size of the void, the image is a composite of two optical micrographs showing the opposing surfaces of the horizontal gap.

In summary, the SEM, EPMA, and optical microscopy (cross section) analyses confirmed that the spring finger solder joint had remelted after application of the final electroplated finish on the Item #3 SA1358-10 connector. This “item” represented a connector or recent date code and recent assembly. There was no damage detected that occurred to the spring finger, the connector shell, or to the electroplated layers on those structures.

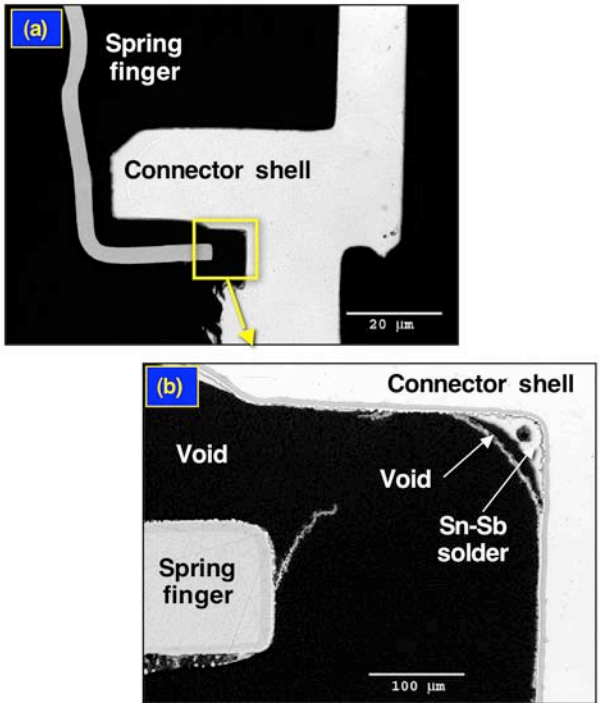

Fig. 69 (a) Low magnification, optical micrograph showing the cross section of the spring finger solder joint at location F3a on the Item #3, SA1358-10 connector. High magnification, optical micrograph of the bottom side fillet appears in (b). A portion of the horizontal gap was also visible.

SA2052-4, DC 2001-52 from MC3617 S/N 5422

The spring finger solder joints on the SA2052-4 connector, Item #3, were evaluated. The electroplated finishes used on the connector shell, the spring finger, and the post-solder overplating were the same as those used on the SA1358-10 connector, as listed in Table 1. Stereo photographs were provided in Fig. 70 that show the top side fillet. The low-magnification view in Fig. 70 (a) shows the connector on-angle. Two sectors were examined as shown in Fig. 70 (b), identified as locations F1 and F2. Higher magnification images were provided in Figs. 70 (c) and (d); even in these images, there is no indication of degradation to the top side fillets.

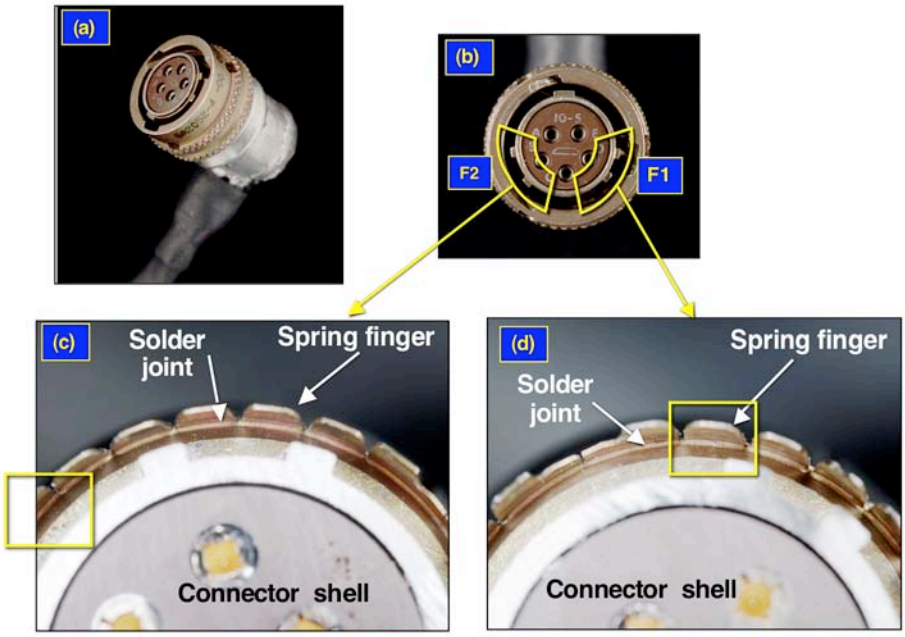

Fig. 70 (a) and (b) Low magnification stereo photographs of the SA2052-4 connector-plus-cable assembly designated Item #3, showing the angled view and a view to the connector contacts, respectively. In the latter image, two sectors were identified as F1 and F2. The high magnification stereo images in (c) and (d) clearly show the absence of noticeable damage to the top side fillet at locations F1 and F2, respectively.

Scanning electron microscopy was used to further examine the top side fillets prior to cross sectioning of the unit. The results of the SEM analysis are exemplified in Figs. 71 and 72, the images of which, came from the locations indicated by the yellow boxes in Figs. 70 (c) and (d), respectively.

In Fig. 71, the top side fillet surface exhibited no significant degradation. A small fissure was observed near the spring finger. A similar observation was made of the images in Fig. 72, with the exception that the surface of the fillet became more nodular near the spring finger. The nodularity was likely a consequence of the electroplating process that administered the protective finish to the connector; metallographic cross sections will confirm this stipulation.

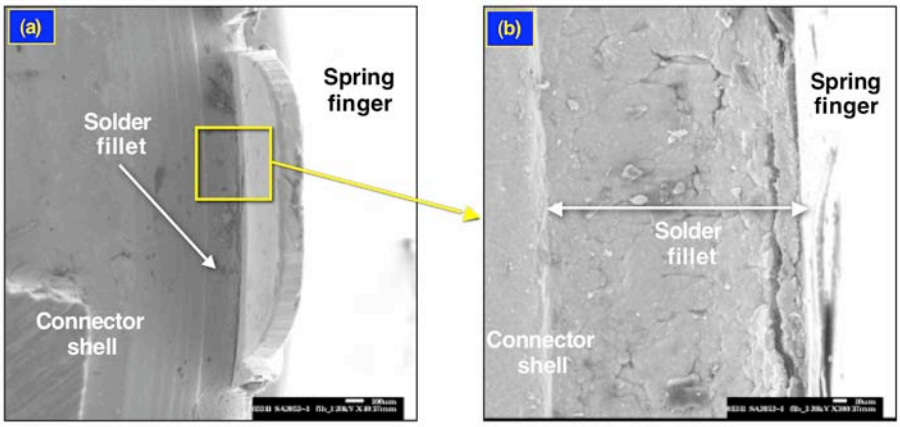

Fig. 71 SEM images of the top side solder fillet at the location F1b on the SA2052-4 connector of Item #3: (a) low magnification and (b) high magnification.

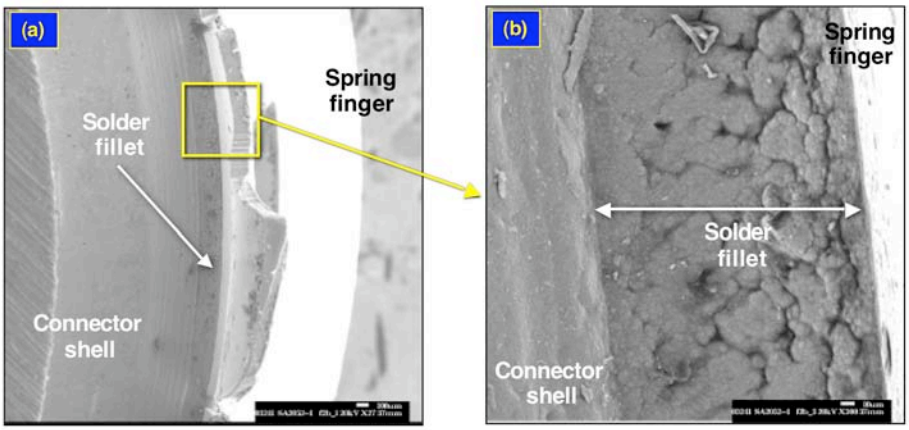

Fig. 72 SEM images of the top side solder fillet at the location F2b on the SA2052-4 connector of Item #3: (a) low magnification and (b) high magnification.

The F1b location of the spring finger solder joint depicted in Figs. 70 (d) and Fig. 71 was metallographically cross sectioned. The resulting optical micrographs were presented in Fig. 73, which besides the overall views in Fig. 73 (a) and (b)(SEM), examined the top side fillet structure. The fissure identified in Fig. 71 was situated over a larger discontinuity in the solder underneath the coating (c) and (d). The red and green arrows indicated that the SEM image and optical micrographs were rotated with respect to one-another about a vertical axis. Although discernable in the micrograph, closer examination of the discontinuity determined that Cd plating was present inside of it. This evidence indicated that the discontinuity was, in fact, a void present in the solder after assembly. The poor

throwing power of the electroplating process did not allow for complete coverage of the void interior with the Cu, Cd (Cr) final finish layers. The geometry of the discontinuity appeared to rule-out its source as having been a crack generated by the flexing of the spring finger. Moreover, nether the morphology of the void nor the remaining fillet microstructure indicated that the Sn-Sb solder joint had be remelted after initial connector fabrication.

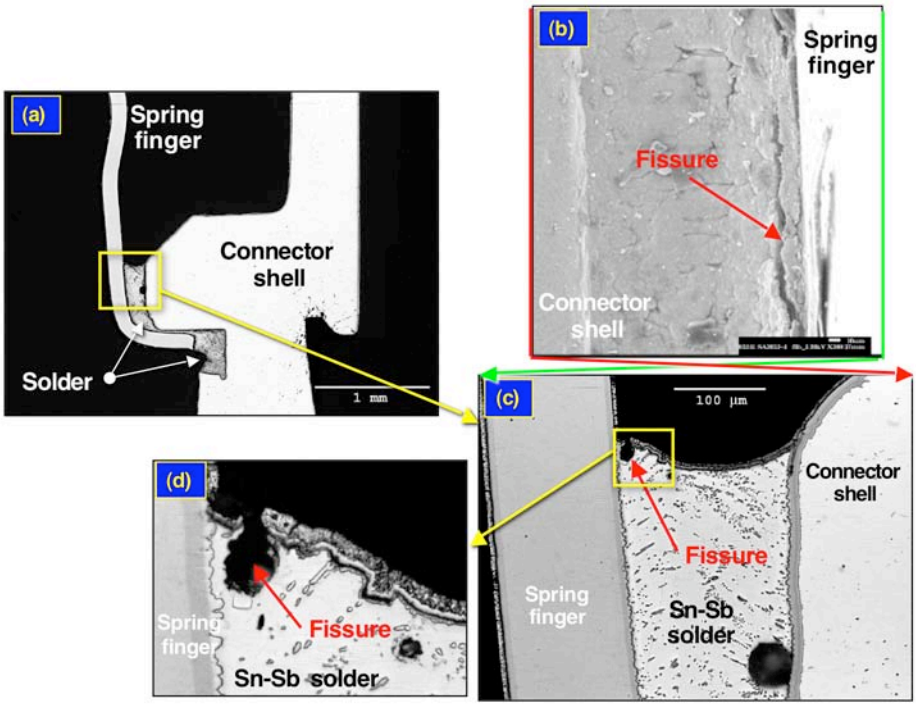

Fig. 73 (a) Low magnification, optical micrograph showing the cross section of the spring finger solder joint a the F1b location for the SA2052-4 connector, Item #3. (b) Reproduction of the SEM image showing the top side fillet surface at the same location. The high magnification optical micrographs in (c) and (d) show the microstructure of the solder joint at the top side fillet. The fissure noted in the SEM image was atop a discontinuity in the Sn-Sb solder, the latter most likely originating as a void at the time of initial assembly. The red and green arrows indicate that the SEM image is rotated 180° about a vertical axis when compared to the optical micrographs.

Electron probe microanalysis provided x-ray maps of the elemental distributions in the solder joint. The top side fillet was examined at location F1b. Shown in Fig. 74 are the SEM/BSE images that corresponded to the locations at which were taken the x-ray maps. The yellow boxes in Fig. 74 (a) indicate connector shell location just above the fillet surface (b) and the top side fillet surface (c), itself, including all of the electroplated finishes.

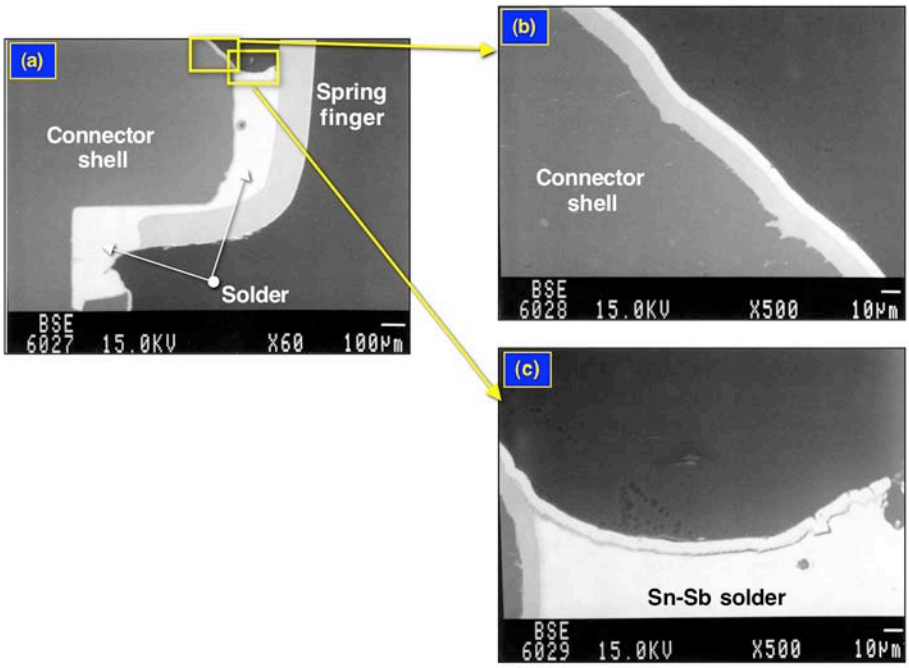

Fig. 74 (a) Low magnification, SEM/BSE image of the cross section of the spring finger solder joint at the F1b location for the SA2052-4 connector, Item #3. The two locations at which were performed the EPMA x-ray maps are delineated by yellow boxes. High magnification, SEM/BSE photographs of the connector shell and top side fillet surface are shown in (b) and (c), respectively.

The x-ray maps of the connector shell at the location in Fig. 74 were shown in Fig. 75. Those maps confirmed the presence of the electroless Ni (P) finish on the Al shell, followed by a thick Cu layer. Although not distinguishable here, the Cu layer was actually composed of two layers: a thick Cu layer to which the soldering was performed elsewhere on the connector, and a second, thinner Cu layer that was deposited as part of the post-soldering, overplating layer. The Cd and Cr layers, which were also part of the overplating finish, were visible on the Cu layer. An important observation was that there was no Sn present along the connector shell surface. This point provided an indication that the solder joint had not been reflowed after the initial soldering process and application of the

overplating layers. This indication arose from the fact that, as has been observed above, when the inadvertent reflow of the Sn-Sb solder occurs, the solder wetted the connector shell above the top side fillet, readily dissolving the Cd layer ahead of it.

The same analysis was performed on the top side solder fillet. The solder was confirmed to be the Sn-Sb composition. The x-ray maps are shown in Fig. 76, which showed the Cu, Cd, and Cr layers that were deposited after the soldering process. An important observation that was made in Fig. 76 was that there was a contiguous Cd layer on the fillet surface. The same observation was made of the bottom side fillet through EPMA exercise, albeit, the data were not shown for brevity. The dissolution of Cd was a prominent artifact when the Sn-Sb solder was reflowed after fabrication of the joint and subsequent application of the overplating layers. This observation, together with the absence of Sn along the connector shell (Fig. 75) confirmed that, at the F1b location, the Sn-Sb solder had not experienced a second (undesirable) reflow step.

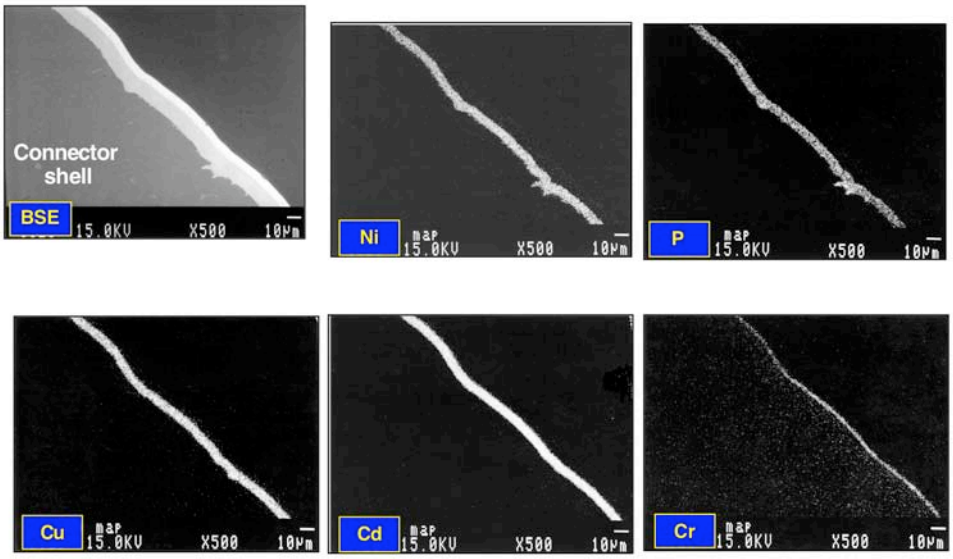

Fig. 75 SEM/BSE image and EPMA x-ray maps of the connector shell just above the top side fillet at the F1b location on the SA2052-4 connector, Item #3. The EPMA x-ray maps examined the elements Ni, P, Cu, Cd, and Cr.

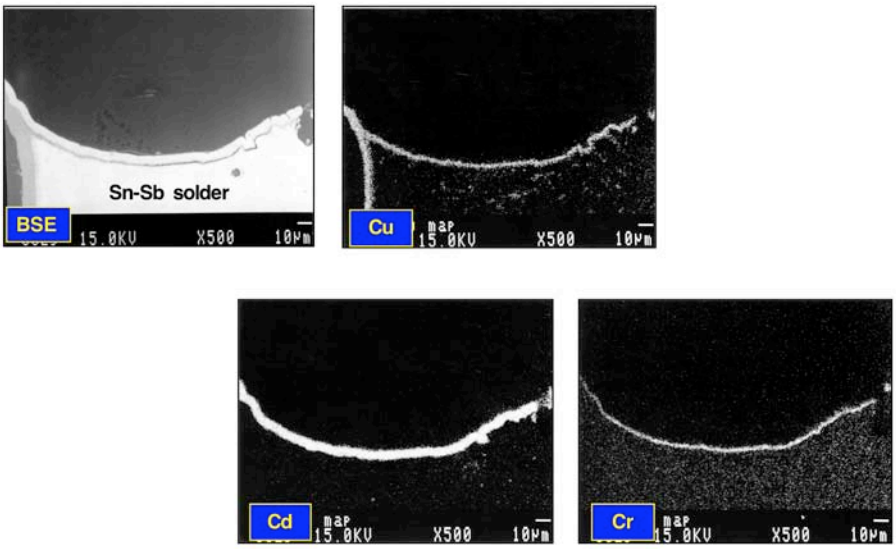

Fig. 76 SEM/BSE image and EPMA x-ray maps of the connector shell just above the top side fillet at the F1b location on the SA2052-4 connector, Item #3. The EPMA x-ray maps examined the elements Cu, Cd, and Cr.

The EPMA was also performed on the BeCu spring finger. That analysis confirmed that only a Cu plating was present along with the Cd and Cr finishes.

The horizontal gap region of the spring finger solder joint was also examined. An optical photograph of the gap at location F1b, SA2052-4, Item #3 was provided in Fig. 77. The gap solder joint appeared very similar at the other two locations, F2b and F3b. The Sn-Pb solder wetted to the Cu plating layers on the spring finger and connector shell structures. The IMC layer thickness was measured on both structures and all three locations designated F1b, F2b, and F3b. Those data were provided in Table 2. The Cu_6Sn_5 stoichiometry predominated; albeit, there appeared to also be a thin Cu_3Sn layer. Only the former was measured. The thicknesses were commensurate with those measured on the other (item) units in this study.

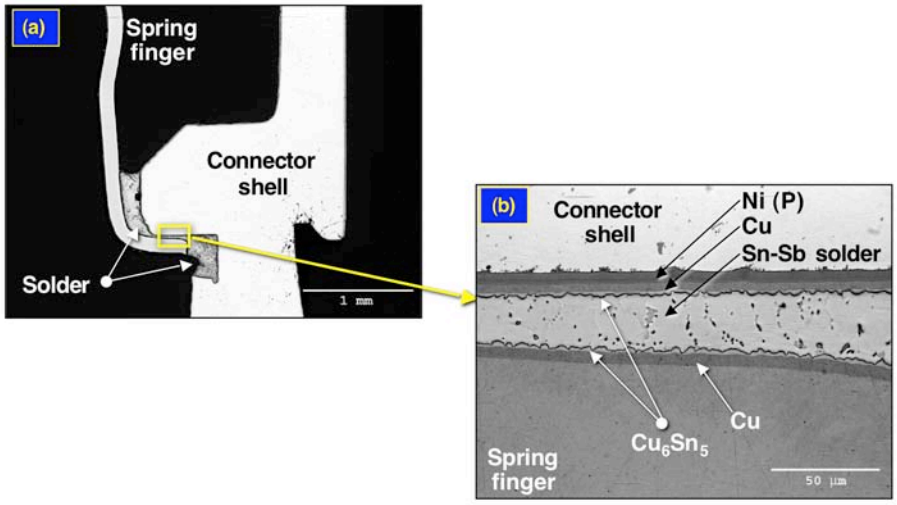

Fig. 77 Optical micrographs depicting the horizontal solder joint gap at the F1b location on the SA2052-4 connector, Item #3: (a) low magnification view and (b) high magnification view showing the electroplated layers as well as IMC layers.

As noted above, metallographic cross sections were also made at the other two locations, F2b and F3b, on the SA2052-4, Item #3. The optical micrographs in Fig. 78 targeted the top side and bottom side solder fillets at location F2b. The horizontal gap region appeared very similar to that at location F1b (Fig. 77).

The SEM/SE photograph in Fig. 78 (b) indicated that the top side fillet surface was rougher than at location F1b. The added roughness was investigated further by metallographic cross section (discussed below). The bottom side fillet (Fig. 78 (c)) was minimally formed. A close examination of the solder fillet surface revealed as gap between the solder and Cd (Cr) layer. The Cd layer was fully intact, indicating that the Sn-Sb solder was unlikely to have reflowed after application of the overplating finish. The separation occurred in the Cd plating was likely a spalling defect related to the latter coating.

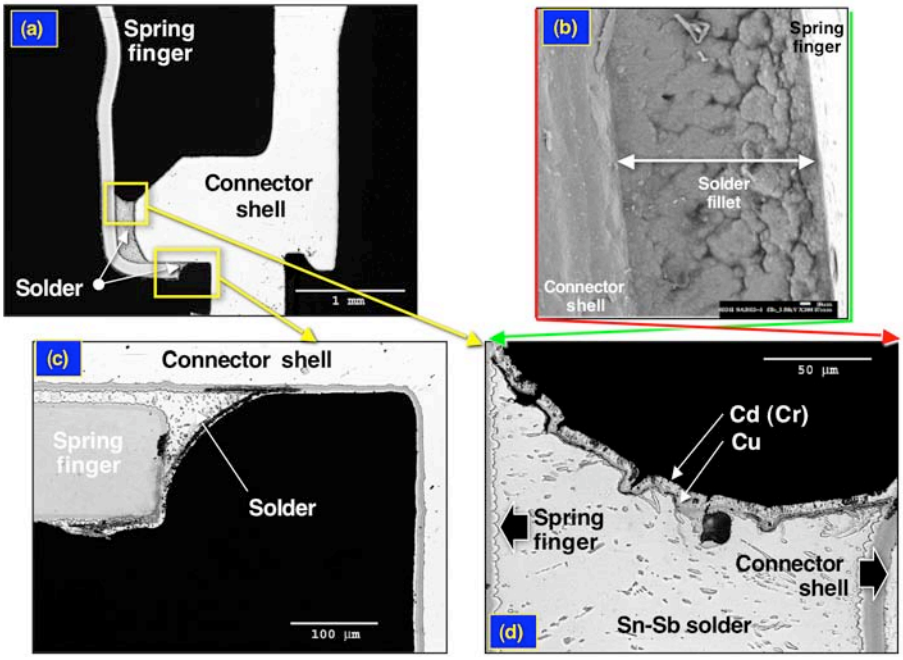

Fig. 78 Optical and SEM micrographs showing the spring finger solder joint at the F2b location on the SA2052-4 connector, Item #3: (a) low magnification view with the yellow boxes indicating the top side and bottom side fillets that were of interest; (b) SEM/SE photograph showing the top side fillet surface morphology; (c) optical micrograph of the bottom side fillet; and (d) optical micrograph of the top side fillet. The red and green arrows indicate that the SEM photograph and cross section micrograph are reversed to one-anther about a vertical (mirror) plane.

The top side fillet shown in Fig. 78 (d) did not reveal a microstructure that was indicative of remelting of the joint. The added roughness observed in Fig. 78 (b) was caused by a combination of solder fillet roughness and the electroplating process used to deposit the Cd layer, not so much the Cu flash or Cr layers. The roughness of the solder fillet surface was surprising, suggesting that it was possible that the solder joint just barely reached the Sn-Sb liquidus temperature (pseudo-cold joint). The fact that the electroplated layers follow the contours of the surface and covered over a small void indicated that the top side fillet did not reflow after the initial connector fabrication.

The third location on the SA2052-4, Item #3 connector, was that designated as F3b. A high magnification optical micrograph provided in Fig. 79 (c) showed a cross section of the

top side fillet. The surface cracks 1 and 2 that were observed on the top side fillet surface in the SEM image (Fig. 79 (d)), extended a short distance into the solder, more so in the former case. The cracks likely originated from flexure of the spring finger; however, the crack 1 was further from the spring finger than has typically been observed for cracks of that origin[2]. Otherwise, no other degradation was observed in the solder joint, including the horizontal gap and bottom side fillet, except for a void at the latter that was attributed to the initial connector assembly process, *not* a remelting of the joint.

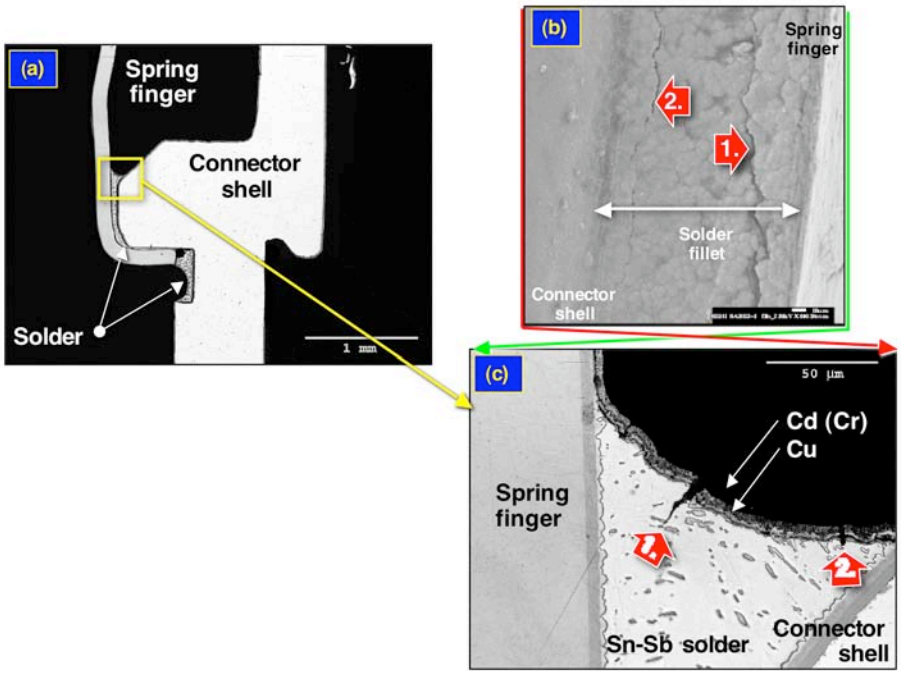

Fig. 79 Optical and SEM micrographs showing the spring finger solder joint at the F3b location on the SA2052-4 connector, Item #3: (a) low magnification view with a yellow box indicating the top side fillet; (b) SEM/SE photograph showing the top side fillet surface morphology; and (c) optical micrograph of the top side fillet. The red arrows indicated cracks observed in the SEM image and optical micrograph.

In summary, the SEM, EPMA, and optical microscopy (cross section) analyses were preformed on the SA2052-4 connector designated Item #3. The solder joints and electroplated layers exhibited excellent integrity. Cross sections of the solder joints were

[2] It would have been interesting if those cracks were caused by solid metal embrittlement resulting from the Cd coating. The Cd atoms would be suspected of embrittling the Sn-based solder.

performed at three locations. In all cases, there was no indication that the Sn-Sb solder joint had remelted following fabrication of the connector. There was no damage detected that occurred to the spring finger, the connector shell, or to the electroplated layers on those structures.

3.5 Item #5: NEW CONNECTORS, INDUCTION SOLDERING OF EMR ADAPTER RING:

SA1358-10, DC 2001-52, soldered 210°C for 3 s

The objective of this prototype was to determine whether the induction heating process used to attach the EMR adapter ring to the connector shell would cause remelting of the spring finger solder joints on these newer versions of the connector. Thermocouple data indicated that the connector shell reached a peak temperature of 210°C for 3 s. Shown in Fig. 80 are stereo photographs of the connector. In Fig. 80 (b) , two locations F1 and F2 were identified, which were observed at higher magnification via Figs. 80 (c) and (d).

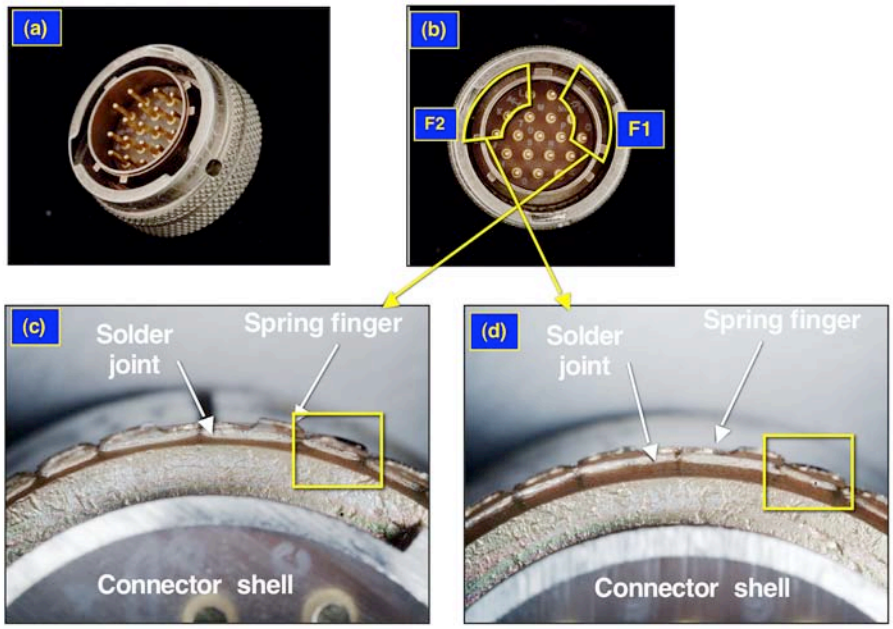

Fig. 80 (a) and (b) Low magnification stereo photographs of the SA1358-10 connector assembly designated Item #5, showing the angled view and a direct view of the connector pins, respectively. In the latter image, two sectors were identified as F1 and F2. The high magnification stereo images in (c) and (d) clearly show noticeable damage to the top side fillet at locations F1 and F2, respectively.

The latter views clearly identified damage to the top fillet of the spring finger solder joints at both locations. The extent of damage was further documented using SEM. The SEM micrographs in Fig. 81 were taken at the F1 location, specifically, the spring finger tine at F1c. The top side fillet at location F2 was shown in Fig. 82.

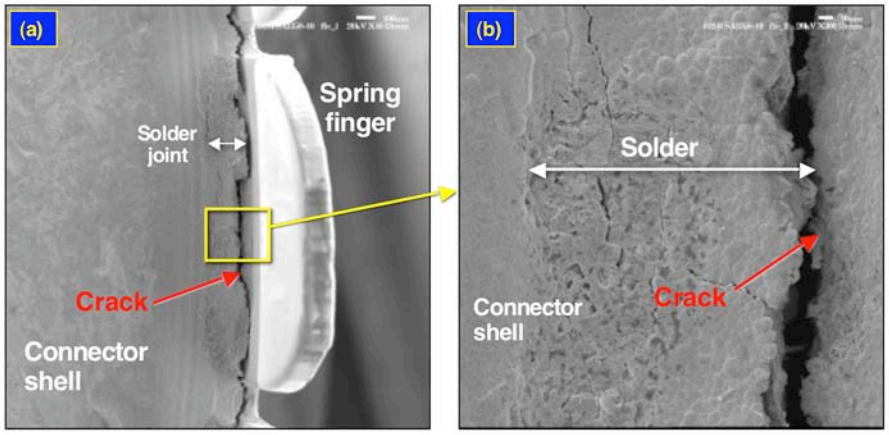

Fig. 81 (a) and (b) are low and high magnification SEM photographs of the SA1358-10 connector (Item #5) showing the extent of degradation to the top side fillets at locations F1c.

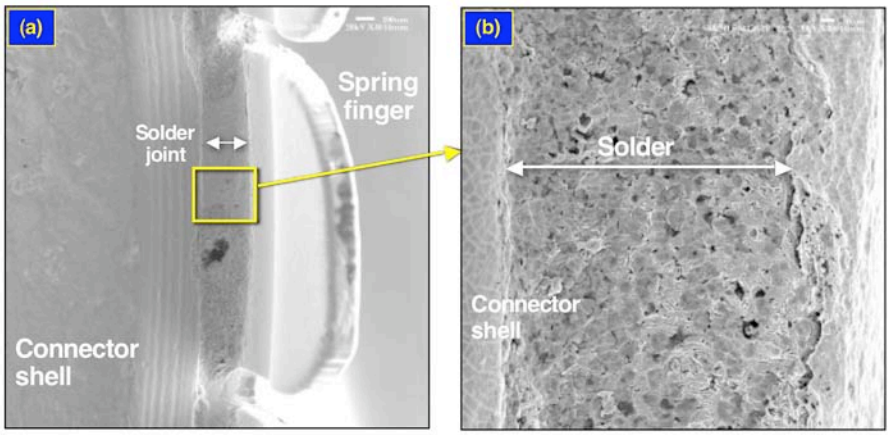

Fig. 82 (a) and (b) are low and high magnification SEM photographs of the SA1358-10 connector (Item #5) showing the extent of degradation to the top side fillets at locations F2.

These two cases – Figs. 81 and 82 – represented the greatest and least cases of degradation, respectively, that were observed on this connector. A third location was also evaluated, F3; it showed degradation that were between the degrees shown in Figs. 81 and 82.

As has previously been the case, metallographic cross sections were required to determine whether the cracks observed by SEM were, in fact, cracks generated by overload stress conditions or were indicative more extensive degradation that underlie the fillet surface, i.e., remelting of the solder. Shown in Fig. 83 (a) is a low magnification, optical micrograph showing the cross section of the spring finger solder joint at location F1a. The SEM photograph corresponding to the location of the metallographic cross section appears in Fig. 83 (b) and shows a significant crack at the spring finger. A lesser crack was observed next to the connector shell.

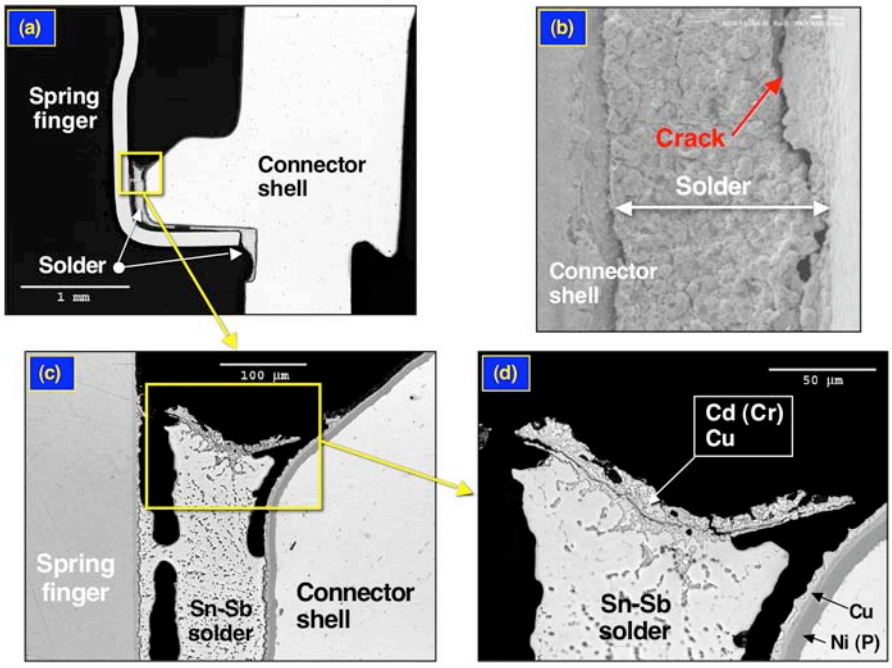

Fig. 83 (a) Low magnification optical micrograph showing the cross section of the spring finger solder joint of the SA1358-10 connector (Item #5) at location F1a. (b) SEM of the F1a location at which the metallographic cross section was taken. (c) and (d) High magnification optical micrographs of the top side fillet.

The high magnification, optical micrographs in Figs. 83 (c) and (d) clearly showed more extensive degradation below the fillet surface. The expanse of voids observed in (c) and

(d) indicated that the solder joints had been reflowed subsequent to their initial fabrication and applications of the overplating layers. The image in (d) showed significant diffusion of Cu and Cd into the Sn-Sb solder that formed the fillet.

Other locations along the spring finger solder joint were evaluated, specifically, at location F2 as noted in Fig. 80. It was observed at these locations that the extent of re-melting of the spring finger (Sn-Sb) solder varied considerably around the circumference of the joint, there by substantiating the need to examine multiple locations in these joints for evidence of defects. Shown in Fig. 84 are micrographs showing a cross section of the solder joint at location F2a.

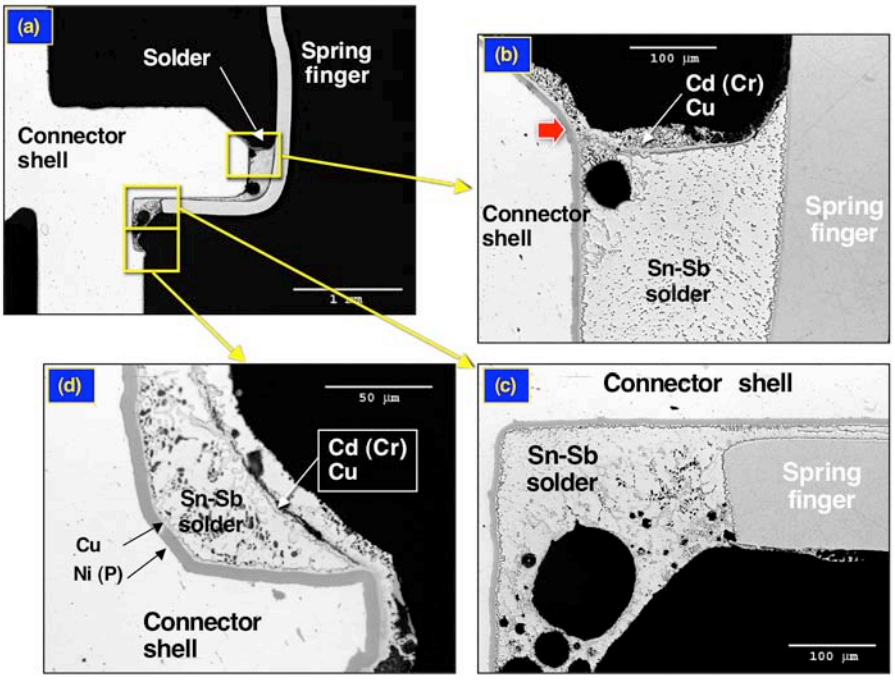

Fig. 84 (a) Low magnification optical micrograph showing the cross section of the spring finger solder joint of the SA1358-10 connector (Item #5) at location F2a. (b) Optical micrograph of the top side fillet. The red arrow indicated a region of flow-out by the Sn-Sb solder. (c) and (d) High magnification optical micrographs of the bottom side fillet.

The view of the top side fillet, which was shown in Fig. 84 (b), indicated a small void, the source of which, was the loss of Sn-Sb solder out of the fillet. The lost solder flowed both on top of the fillet as well as up the connector housing (red arrow). Partial dissolution of

the Cd plating over the top side fillet had also occurred. Confirmation of this scenario was provided in Fig. 85, which shows and SEM/BSE image as well as EPMA x-ray dot maps of the elements: Cr, Cu, Cd, and Sn. The Sn dot map shows the flow of Sn-Sb solder on top of the Cu layer, dissolving the Cd coating into it. The reduced thickness of the Cd layer under the solder was evident, when that thickness was compared to the undissolved Cd layer thickness at the red arrows. The dissolution process also resulted in Cd being dissolved into the top side fillet around the void as indicated by the Cd map. Lastly, it was also interesting to note that the chromate conversion layer (Cr map) remained relatively intact. The Cr layer appeared to float on top of, what was, the molten Sn-Sb solder as the latter readily wetted to the Cd layer, forming a “crust” over the solder.

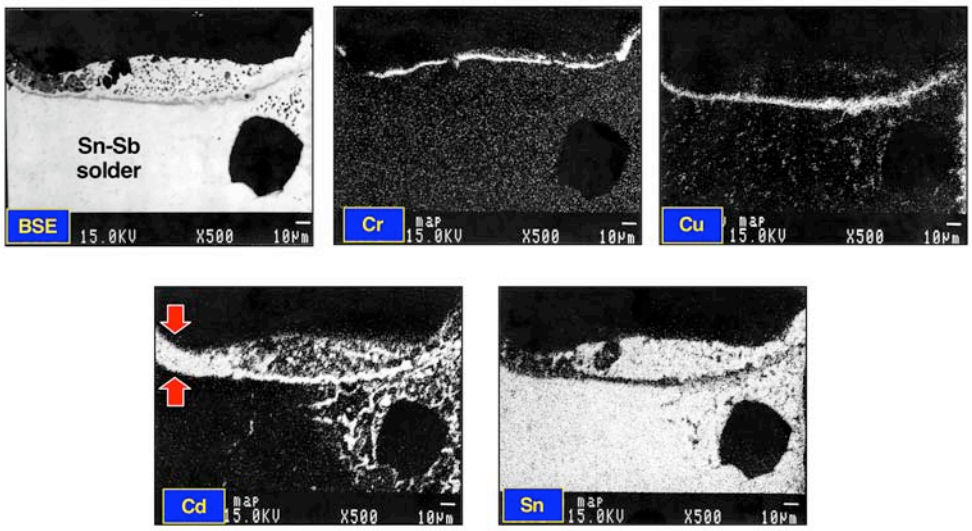

Fig. 85 SEM/BSE image and EPMA x-ray maps of the top side fillet of the SA1358-10 Item #5 connector shell at location F2a. The EPMA x-ray maps were for the elements Cr, Cu, Cd, and Sn.

Referring to Figs. 84 (c) and (d), the large voids and solder covering the Cd plating indicated that the bottom side fillet had also remelted after completion of the connector. Confirmation to this effect was provided by the EPMA x-ray dot maps in Fig. 86 that show, specifically, the presence of Cd in the Sn-Sb solder fillet. That Cd would have dissolved into the fillet when the Sn-Sb solder was molten. Therefore, the Sn-Sb solder had remelted in both the top side and bottom side fillets at this location.

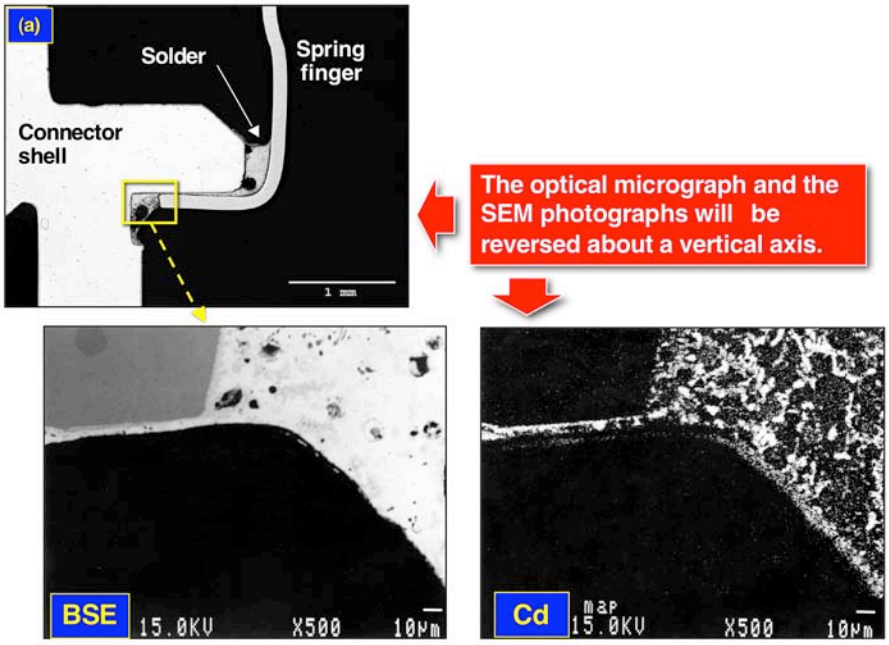

Fig. 86 Electron probe microanalysis of the bottom side fillet of the spring finger solder joint of the SA1358-10 connector (Item #5) at location F2a. Only the BSE image and Cd x-ray dot map were shown for this case.

The distinction that the Sn-Sb spring finger solder joint had remelted was not as obvious in the top side fillet at the third location, F2b. Shown in Fig. 87 (a) is a low magnification optical micrograph of the F2b location on SA1358-10 (item #5). The high magnification image in Fig. 87 (b) showed cracks between the Sn-Sb solder and the connector shell, which may have been caused by an overload condition, as well as between the solder and Cd (Cr) and Cu overplating layers, that appeared to be caused by a delamination. These areas were identified by red boxes. The microstructure of the top side fillet did not indicate reflow of the solder. And, in fact, an EPMA was performed on the top side fillet. Low and high magnification BSE images, as well as Cr, Cd, Cu, and Sn dot maps, were provided in Fig. 88.

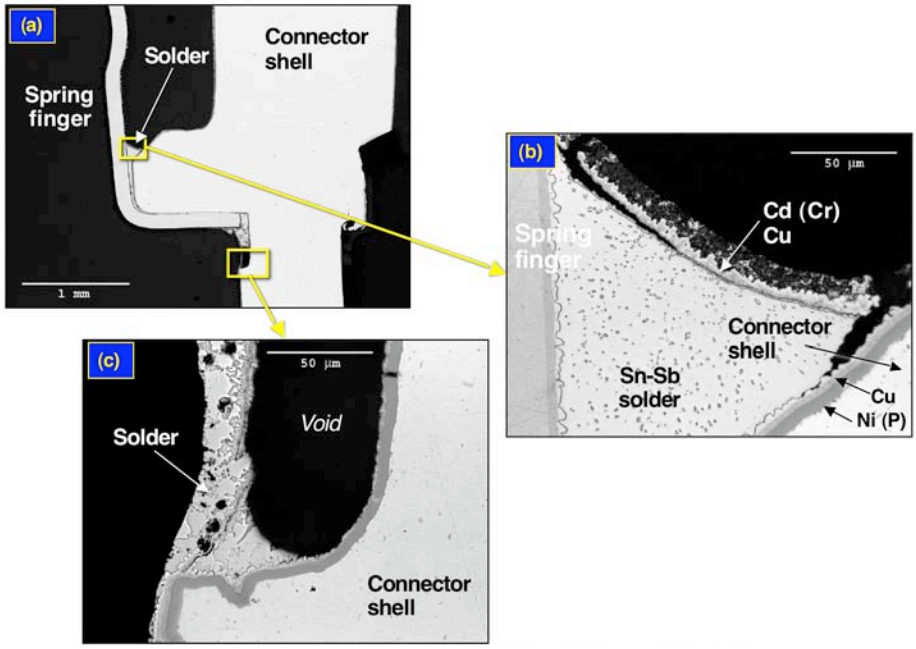

Fig. 87 (a) Low magnification optical micrograph showing the cross section of the spring finger solder joint of the SA1358-10 connector (Item #5) at location F2b. (b) High magnification optical micrograph of the top side fillet. (c) High magnification optical micrograph of the bottom side fillet.

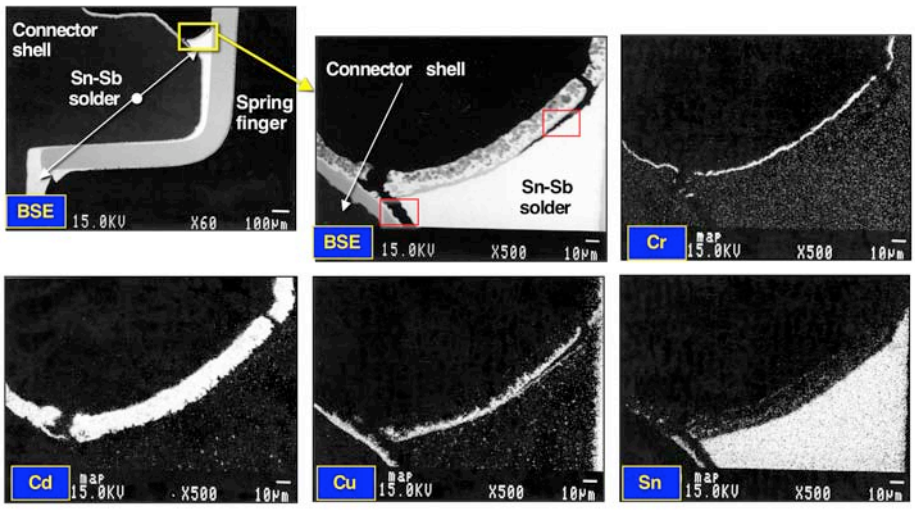

Fig. 88 Electron probe microanalysis of the top side fillet of the spring finger solder joint of the SA1358-10 connector (Item #5) at location F2b. Low and high magnification BSE images as well as dot maps of Cr, Cu, Cd, and Sn were shown.

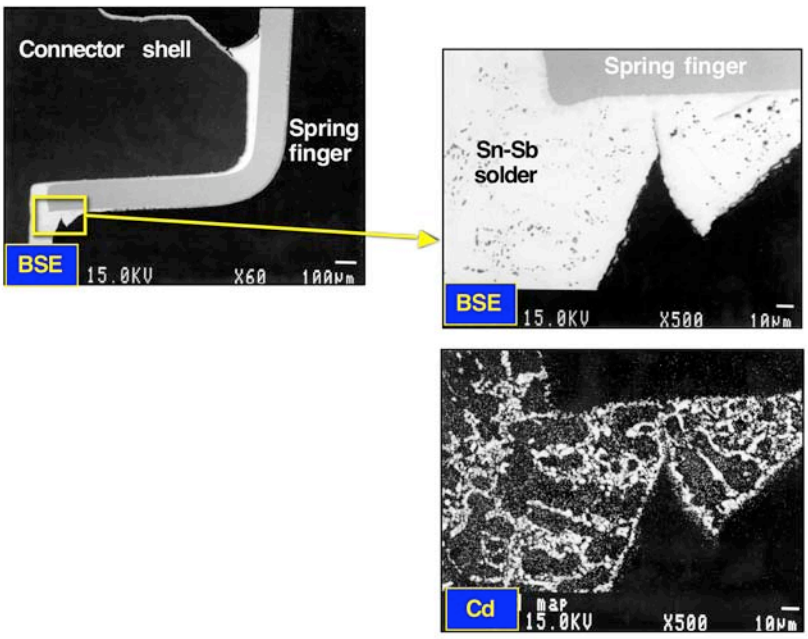

Fig. 89 Electron probe microanalysis of the bottom side fillet of the spring finger solder joint of the SA1358-10 connector (Item #5) at location F2b. Low and high magnification BSE images as well as the dot map of Cd, and Sn were shown.

There was no presence of Cd in the solder, nor solder on top of the Cd layer. The Cr and Cu layers were similarly intact. These observations implied that the Sn-Sb solder had not remelted. In fact, the Cu and Sn signals indicated that the crack at the connector shell wall had occurred between the solder and the Cu-Sn IMC layer there, which is a characteristic of an overload event.

On the other hand, the image in Fig. 87 (c) showed a large void and breaching of the Cd layer by the Sn-Sb solder, which were indicative of remelting of the solder. The remelting event was confirmed by the EPMA results in Fig. 89, which showed the extensive diffusion of Cd into the Sn-Sb solder when the latter had remelted. Therefore, at this location, the bottom side fillet had extensive evidence of Sn-Sb remelting as opposed to the top side fillet that did not exhibit remelting.

The final evaluation of SA1358-10, item #5, was performed at location F3b. A low magnification optical micrograph and SEM photograph of the solder joint were provided in Fig. 90 (a) and (b), respectively.

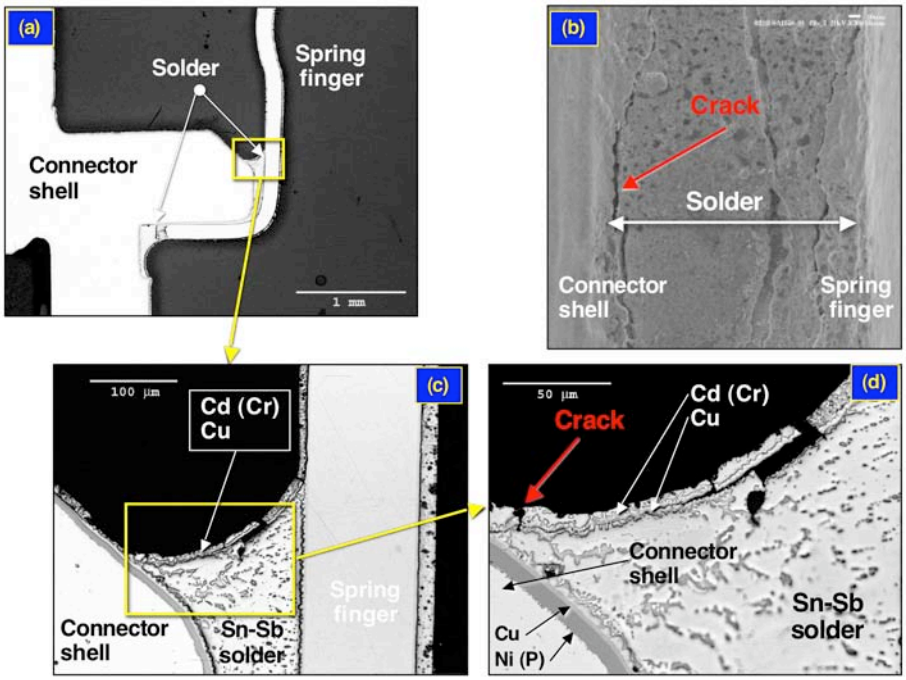

Fig. 90 (a) Low magnification optical micrograph showing the cross section of the spring finger solder joint of the SA1358-10 connector (Item #5) at location F3b. (b) SEM of the F3b location at which the metallographic cross section was taken. (c) and (d) High magnification optical micrographs of the top side fillet.

The damage observed in Fig. 90 (b) was not as extensive as it appeared in that SEM image, and certainly did not indicate remelting of the Sn-Sb solder. The cracks were limited to the Cd (Cr) plating layer and/or only the very-near surface of the solder fillet. A similar observation was made of the bottom side fillet. The EPMA (not shown) also did not indicate the dissolution of Cd into the fillets that was indicative of remelting of the Sn-Sb solder.

In summary, the above analyses clearly showed that the SA1358-10, item #5 spring finger solder joint was susceptible to remelting during the induction soldering process used to attach the EMR coupling ring to the connector shell. However, the extent of Sn-Sb remelting was not uniform around the circumference of the solder joint, and that the

appearance of the top side fillet was not a certain indicator of the extent of remelting because remelting could occur to the bottom side of the joint, but not to the top side Sn-Sb fillet.

SA2052-4, DC 2001-52, soldered at 191°C for 1.5 s

As was the case with the SA1358-10 connector, the objective of this prototype was to determine whether the induction heating process used to attach the EMR adapter ring to the connector shell, would cause remelting of the spring finger solder joints on this newly made SA2052-4 connector. Thermocouple data indicated that the connector shell reached a peak temperature of 191°C for 1.5 s. Because this connector was smaller than its SA1358-10 counterpart, a reduced amount of heat was required to make the joint, hence, the lower soldering temperature and shorter time duration. The electroplated layers for each of the structures: connector shell, spring finger, and solder fillet (overplating) were listed in Table 1.

Stereo photographs of the connector were shown in Fig. 91. Examination of the spring finger solder joint did not reveal indications of significant damage to the top side fillet nor to the Cd plating that would have been indicative of mechanical loading (bending) or remelting of the Sn-Sb solder.

Shown in Figs. 92 and 93 are low and high magnification SEM photographs at the F2a and F4b locations, respectively, targeting the top side fillet of the spring finger solder joint. Those photographs are representative of other SEM analyses performed on this connector, which indicated only what appeared to be, small fissures in the Cd (Cr) overplating layer on the fillet surface.

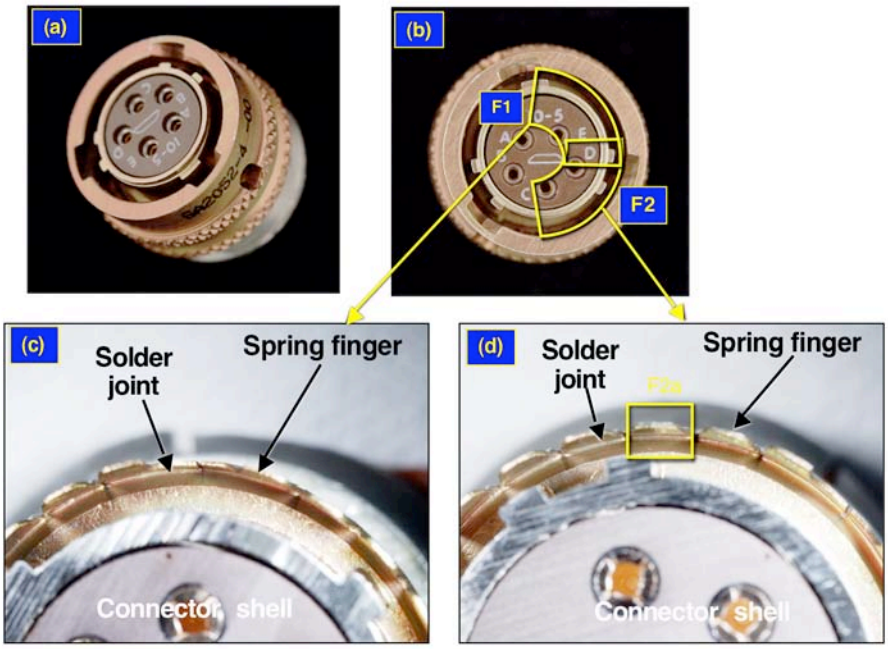

Fig. 91 (a) and (b) Low magnification stereo photographs of the SA2052-4 connector assembly designated Item #5, showing the angled view and a direct view of the contacts, respectively. In the latter image, two sectors were identified as F1 and F2. The high magnification stereo images in (c) and (d) show the top side fillet locations F1 and F2, respectively, of the spring finger solder joints.

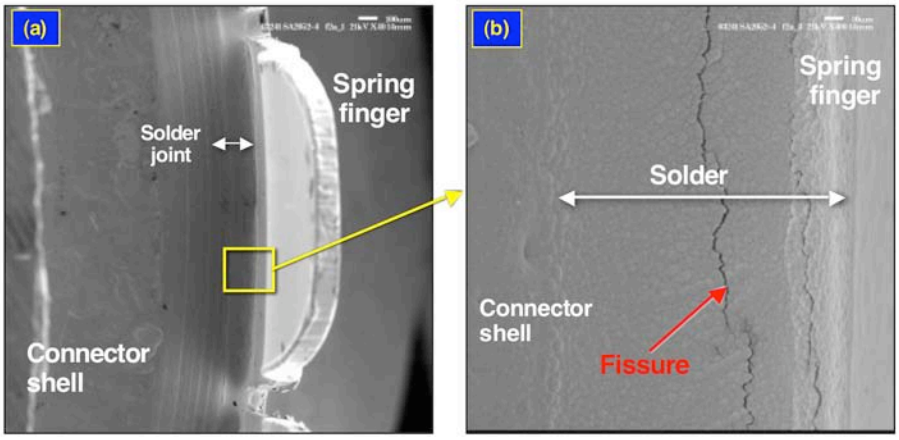

Fig. 92 (a) and (b) Low and high magnification SEM/SE photographs of the F2a location on the SA2052-4 connector assembly designated Item #5. A small fissure has been identified in the overplating layer.

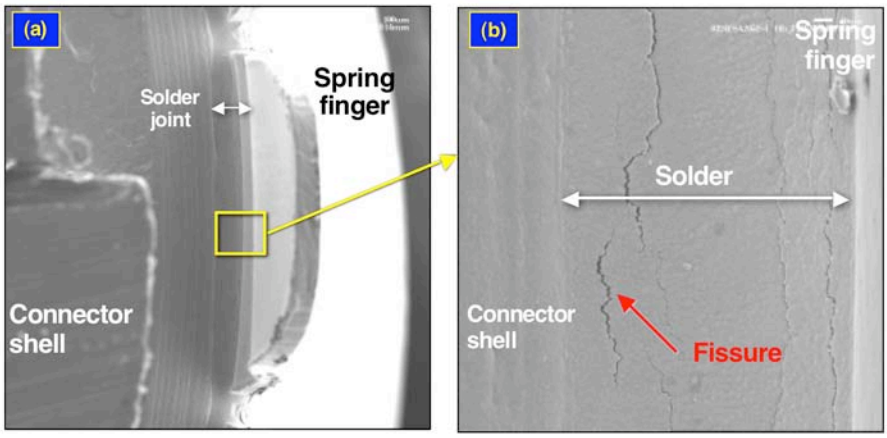

Fig. 93 (a) and (b) Low and high magnification SEM/SE photographs of the F4b location on the SA2052-4 connector assembly designated Item #5. Small fissures were identified in the overplating layer.

Metallographic cross sectional analysis was used to confirm the structural integrity of the spring finger solder joint. The optical micrograph in Fig. 94 (a) showed a low magnification view of the solder joint. There were no voids nor indications of damage to the solder joint. The fissures detected in the SEM photograph, which were reproduced in image (b) of Fig. 94, were shown in a cross section view through Fig. 94 (c). The fissures propagated from the Cd layer, through the Cu overplating layer and only a short distance into the Sn-Sb solder fillet. The images in Fig. 94 did not show evidence that the solder had been remelted after fabrication of the joint nor that there was crack damage due to flexing of the spring finger.

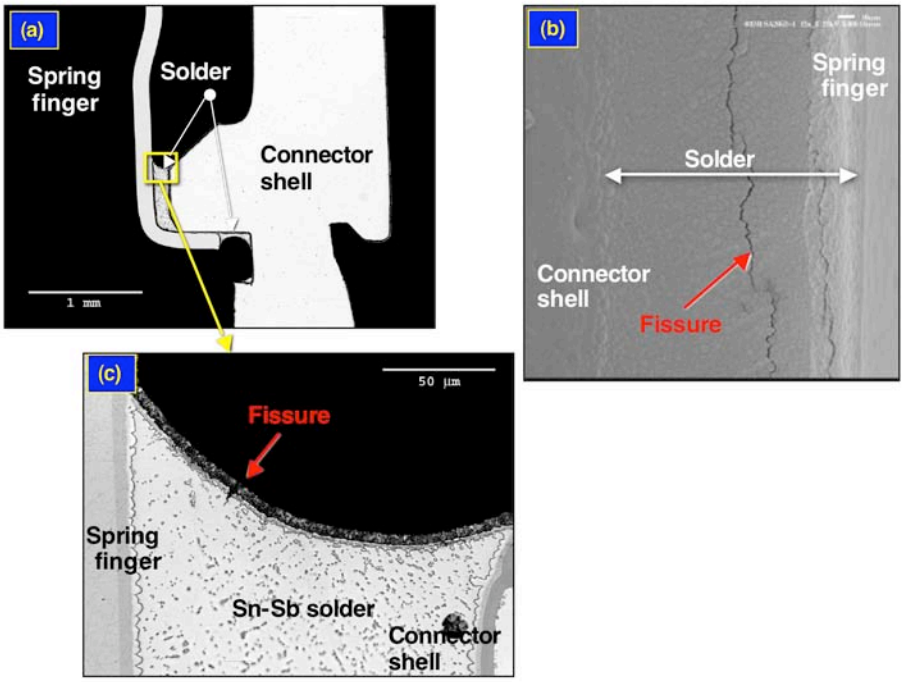

Fig. 94 (a) Low magnification optical micrograph showing the spring finger solder joint of the SA2052-4 connector designated Item #5. The location is F2a. (b) Low magnification SEM/SE photograph of the top side fillet surface at F2a, showing the small fissures. (c) High magnification optical micrograph of the top side fillet, showing the origins of the fissures.

A second region of the spring finger solder joint was similarly investigated; this region was designated F4b. The associated micrographs were provided in Fig. 95. The top side microstructure did not show signs that the Sn-Sb solder had remelted after the overplating had been applied to the assembly. Therefore, the fissures observed by the SEM photograph in Fig. 95 (b) were limited to the Cd layer. The absence of remelting of the spring finger solder joint was confirmed by the EPMA dot maps that are provided in Fig. 96. The overplating layers and, in particular, neither the Cd nor Cu layers showed indications of having been dissolved into the Sn-Sb solder.

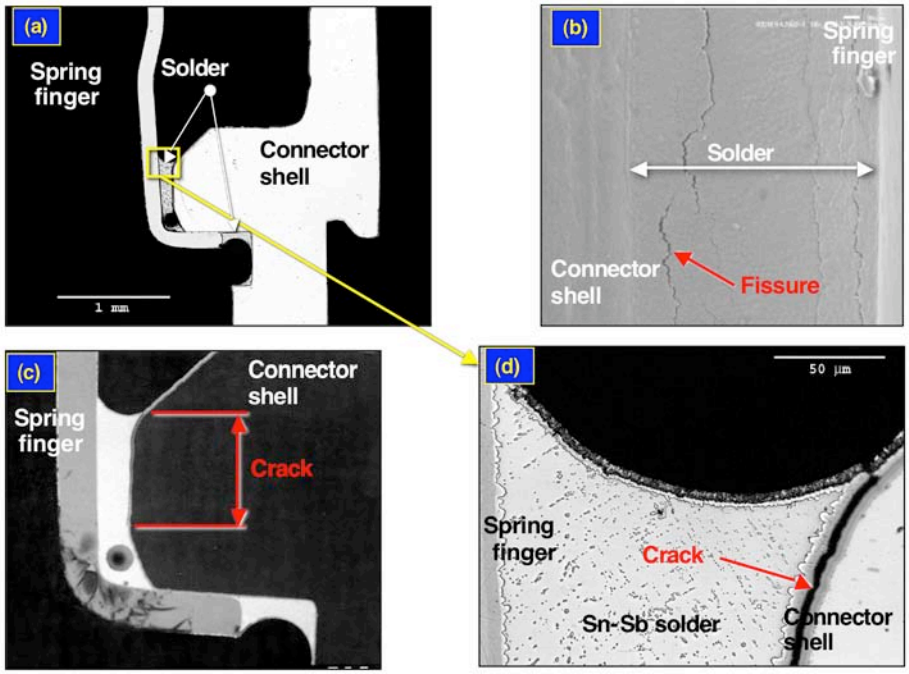

Fig. 95 (a) Low magnification optical micrograph showing the spring finger solder joint of the SA2052-4 connector designated Item #5. The location is F4b. (b) Low magnification SEM/SE photograph of the top side fillet surface at F4b. (c) High magnification optical micrograph of the top side fillet.

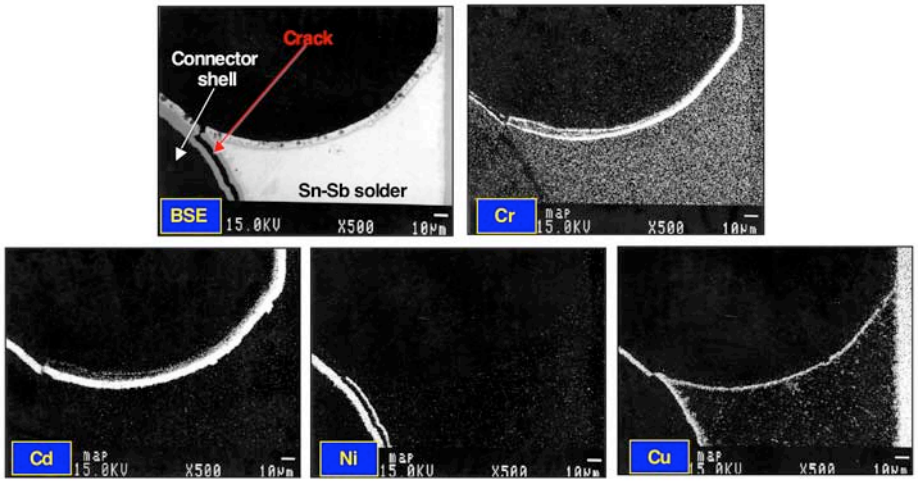

Fig. 96 Electron probe microanalysis of the top side fillet of the spring finger solder joint of the SA2052-4 connector (Item #5) at location F4b: BSE image as well as dot maps of Cr, Cd, Ni, and Cu were provided.

An unexpected feature in Fig. 95 (d) was the crack in the electroplated layer on the connector shell. The extent to which the crack extended into the spring finger solder joint was depicted in Fig. 95 (c). The morphology of the crack, together with the EPMA results in Fig. 96, showed it to have propagated entirely within the electroless Ni (P) layer. The morphology of the crack was shown in further detail by the SEM/BSE images Fig. 97, which documented the crack at the top side fillet and further down into the joint. The image in Fig. 97 (b) indicated that the crack occurred *after* the Cd (Cr) overplating layers had been deposited. Also, the fracture did not appear to be based upon a general delamination of the Ni (P) layer since the separation did not extend upwards on the connector shell past the solder fillet. This is the first instance in which this defect was observed. Typically, the mechanical overload of the spring finger solder joint was reflected by cracks along the solder/IMC interface at the spring finger side of the joint. Occasionally, the crack would be at the same interface along the connector shell side of the joint. Therefore, the crack in Fig. 97 likely indicated a weakness in the Ni (P) layer.

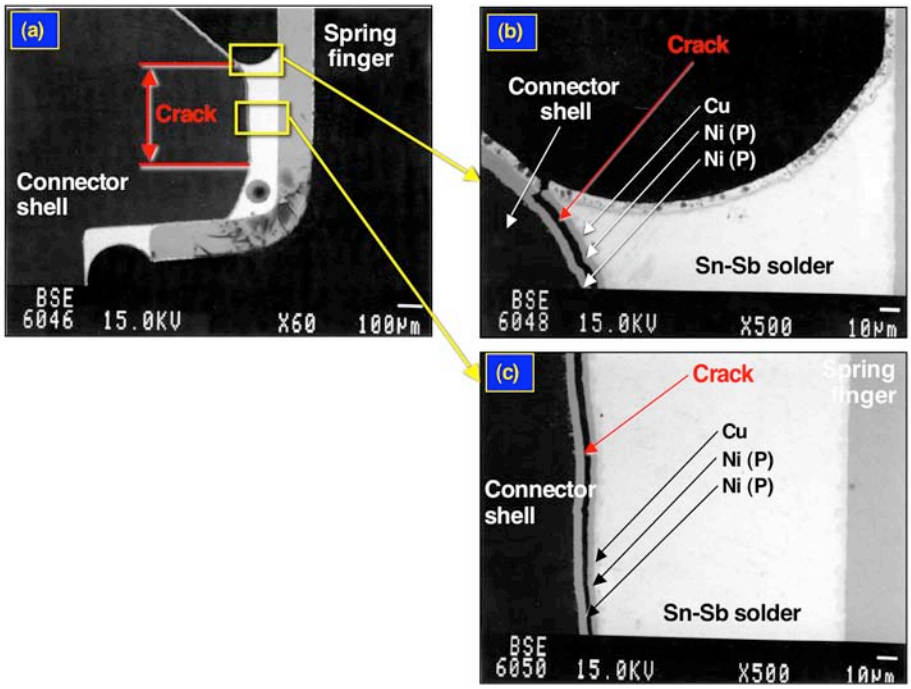

Fig. 97 (a) Low magnification SEM/BSE photograph of the spring finger solder joint of the SA2052-4 connector designated Item #5 at location F4b. Close views of the top side fillet as well as further into the solder joint were provided by the SEM images in (b) and (c), respectively.

The horizontal solder joint and bottom side fillet was similarly analyzed. The associated optical micrographs were provided in Fig. 98.

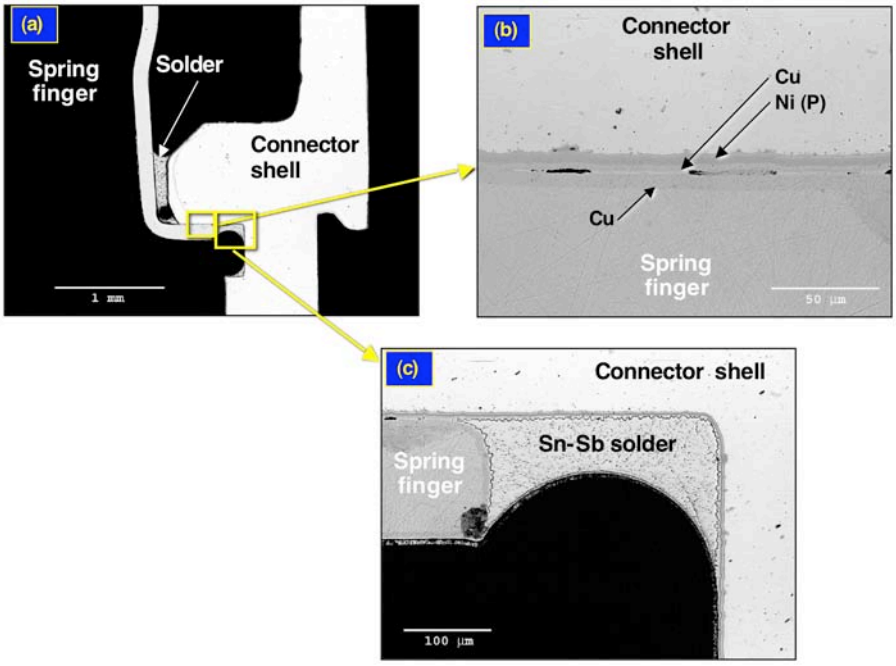

Fig. 98 (a) Low magnification optical micrograph showing the spring finger solder joint of the SA2052-4 connector designated Item #5. The location is F4b. (b) High magnification optical micrograph of the horizontal gap region. (c) High magnification optical micrograph of the bottom side fillet.

The horizontal gap was very thin in most of the cross sections made of the SA2052-4, Item #5 spring finger joints as shown in Fig. 98 (b). In fact, it was observed that IMC layer growth had actually bridged between the Cu plated layers of the connector shell and spring finger structures. No cracks were observed in the IMC layers. The IMC layer thicknesses were listed in Table 2 and were very similar to those observed on the other SA2052-4 connector assemblies. The bottom side fillet, which is shown in Fig. 98 (c), exhibited excellent integrity. The overplating layers remained "stacked" on top of the Sn-Sb solder with no indications of being dissolved into the latter due to remelting of the joint. The cracking of the Ni (P) finish, which was observed in the top side fillet as depicted in Fig. 97, was not noted in either the horizontal gap or bottom side fillet locations. Therefore, it was concluded that the aforementioned crack was a localized defect in the electroless layer.

In summary, the spring finger solder joint on the SA2052-4, Item #5 connector, did not show signs of remelting of the Sn-Sb solder after completion of the overplating process. The solder joints exhibited excellent integrity, with the exception of a localized crack in the Ni (p) plating on the connector shell. Because this was the only instance in which such a crack has been observed and the fact that similar cracking was not observed at other locations in the solder joint, this defect did not indicate a chronic problem with the electroless Ni (P) layer on this connector.

4. Summary

1. The SA1358-10 and SA2052-4 connectors are used on a wide variety of nuclear weapons and Joint Test Assembly (JTA) systems. The current emphasis on these connectors stems from their use in the MC3617 Interconnection Unit (ICU) of the W87 system. These connectors were evaluated for the following specific defects associated with the 95Sn-5Sb (wt.%) solder joint used to attach the BeCu spring fingers to the Al connector shell: (1) extended cracking within the fillet; (2) remelting of the solder joint during the follow-on assembly step (attachment of the EMR adapter ring to the connector shell and/or soldering the EMR shell to the adapter ring); and (3) spalling of the Cd (Cr) layer overplating layer from the fillet surface. Several pedigrees of connectors were evaluated, which represented fielded units as well as those assemblies that were recently constructed at Kansas City Plant.
2. **Item #1 SA1358-10.** There was substantial evidence indicating that the 95Sn-5Sb solder had melted *after* application of the Ni, Cd, and chromate conversion protective coatings (Cr), that is, during the follow-on assembly. Spalling of the Ni/Cd layer could present a corrosion concern for the connector structure. An excessively thick IMC layer developed between the Cu plating of the connector shell and the Sn-Sb solder. But, there was no evidence to suggest that the thick Cu/Sn IMC layer would pose a reliability concern for the solder joint. The contact pin solder joints exhibited excellent quality; there were no did indication of damage to the solder joints.
3. **Item #1 SA2052-4.** There was no evidence to indicate that the Sn-Sb solder had melted *after* application of the Cu (flash), Ni, Cd, and chromate conversion (Cr) protective coatings. The nodularity of the surface plating observed in the top side fillet SEM images was caused by the Ni layer deposition. There was no evidence of spalling of the Ni and Cd (Cr) layers from any of the surfaces. A thick IMC layer, which developed between the Cu plating on the connector shell and spring finger and the Sn-Sb solder, would not pose a reliability concern for the solder joint. The pin contact

solder joints exhibited excellent quality; there were no did indication of damage to the accompanying solder.

4. **Item #2 SA1358-10.** The old style SA1358-10 connector, when subjected to the new assembly process, still experienced remelting of the Sn-Sb solder that attached the spring fingers to the connector shell. Flaws that were observed on the top fillet surface by stereomicroscopic inspection or SEM, were the result of separation and cracking of the Cd (Cr) plating due to a void generated underneath it by remelting of the solder. Also, there was cracking of the top fillet solder joints, the source of which, was a mechanical load placed on the spring finger that occurred after the remelting event. Lastly, the pin contact solder joints exhibited excellent quality; there were no did indication of damage to the solder joints.
5. **Item #2 SA2052-4.** The old style SA2052-4 connector exhibited spring finger solder joints that retained excellent integrity when subjected to the new (recent) assembly process. There were no indications that the Sn-Sb solder had remelted as a result of solder process performed after the spring finger joint had been completed. Minor cracks were observed on the top side fillet that breached the Ni-Cd (Cr) overplating layer and progressed only a short distance into the underlying Sn-Sb solder. The overplating layer exhibited no indications for delamination from the spring finger or connector housing away from the solder joint.
6. **Item #4 SA1358-10.** **New design baseline.** The spring finger solder joints exhibited excellent integrity on the new design, SA1358-10 connector. There were no indications of damage to the solder, the interfaces, or to the shell and spring finger structures. All of the electroplated finishes, including the Ni (P), Cu applied to the shell; the Cu layer applied to the spring finger; and the overplating layer of Cu and Cd (Cr) exhibited excellent adhesion to the respective surfaces.
7. **Item #4 SA2052-4.** **New design baseline.** The spring finger solder joints exhibited excellent integrity on the new design, SA2052-4 connector. There were no indications of damage to the solder, the interfaces, or to the shell and spring finger structures. All of the electroplated finishes, including the Ni (P), Cu applied to the shell; the Cu layer applied to the spring finger; and the overplating layer of Cu and Cd (Cr) exhibited excellent adhesion to the respective surfaces.
8. **Item #3 SA1358-10.** The analyses confirmed that the spring finger, Sn-Sb solder joint had remelted after application of the final electroplated finish on the Item #3 SA1358-10 connector. There was no damage detected that occurred to the spring finger or the connector shell. There was some spalling of the Cd layer.
9. **Item #3 SA2052-4.** The analyses confirmed that the Sn-Sb solder joint had not remelted following the initial assembly process. There was no damage detected that

occurred to the spring finger, the connector shell, or to the electroplated layers on those structures. The solder joints and electroplated layers exhibited excellent integrity.

10. **Item #5 SA1358-10.** A recent data code, SA1358-10 connector had its spring finger solder joint be susceptible to remelting during the induction soldering process used to attach the EMR adapter ring to the connector shell. However, the extent of Sn-Sb remelting was not uniform around the circumference of the solder joint nor did it occur consistently between the top side fillet and bottom side fillet per at any one circumferential location.
11. **Item #5 SA2052-4.** The induction soldering process used to attach the EMR adapter ring to the connector shell did not cause remelting of the Sn-Sb solder joint between the connector shell and the spring fingers. There was no damage to the connector shell, spring finger, or electroplated layers that covered all fo the structures. There was a localized crack observed in the electroless Ni (P) layer on the connector shell. This separation did not appear to be a chronic defect with the connector shell.
12. These results suggested that, due to the size of the SA1358-10 connector, any of the former or current soldering processes used to attach the EMR adapter ring and/or EMR shell to the connector shell, require a level of heat energy that will always result in the remelting of the spring finger solder joint attached with either the Sn-Sb solder (or the Sn-Ag alloy, for that matter). It was more likely that the induction soldering process, which is used to attach the EMR ring onto the shell, caused the remelting event rather than the more localized heat source of the hand soldering iron used to attach the EMR shell.

5. References

[1] P. Vianco, “Evaluation of Spring Finger-to-Shell Solder Joints in the SA1358-10 Connector (MC3617, W87),” memorandum to J. Hanlon dtd. December 13, 2002 (Sandia National Laboratories, Albuquerque, NM).

[2] P. T. Vianco, K. L. Erickson, P. L. Hopkins, "Solid State Intermetallic Compound Growth Between Copper and High Temperature, Tin-Rich Solders - Part I: Experimental Analysis", *J. of Electronic Materials*, 23 (1994), p. 721.

Copy to:

J. Custer	MS0889
J. Braithwaite	MS0889
L. Andrews	MS0523
T. Ernest	MS0523
J. Baca	MS0523
P. Vianco	MS0889 (3 copies)
Central Technical Files	MS9018 (2 copies)
Technical Library	MS0899 (2 copies)

Sandia National Laboratories